MICROPARTICLE ARRAY ON GEL MICROSTRUCTURE CHIP FOR MULTIPLEXED BIOCHEMICAL ASSAYS

ZHU QINGDI

(B. Sc., Fudan University)

A THESIS SUBMITTED

FOR THE DEGREE OF DOCTOR OF PHILOSOPHY

DEPARTMENT OF BIOENGINEERING

NATIONAL UNIVERSITY OF SINGAPORE

2012

ACKNOWLEDGEMENTS

I would like to thank National University of Singapore for the provision of the opportunity to me for the pursuit of Ph.D. and the financial support of NUS Research Scholarship throughout my candidature. I also appreciate the facility and administrative support from Department of Bioengineering during my Ph.D. study. I would like to thank research grant NRF2008-POC-001-100 from National Research Foundation (Singapore) for the financial support to this work.

I want to express extreme gratitude to my supervisor, Assistant Professor Dr. Dieter Trau for his guidance and support throughout my Ph.D. study. His constructive suggestions and insightful discussions help me overcome many hurdles in my research and his patience as well as his optimism encourages me to finally complete the Ph.D. thesis. Moreover, he taught me to think critically and to solve problem independently, which can be a precious asset for my future career.

I would like to thank A/P Zhang Yong, Dr. Saif Khan, A/P Liu Wen-Tso for their valuable suggestion during my written and oral qualification exams. I am also grateful for Dr. Partha Roy to provide microfabrication facilities.

I will never forget the support and help from my lab mates. Dr. Wang Chen taught me microfabrication skills and gave me suggestions even before I joined the lab. Dr. Jiang Jie helped me with SEM experiments and also gave me suggestions for thesis writing.

Mr. Chaitanya Kantak helped me in master fabrication and also gave valuable advice for my thesis. Dr. Mak Wing Cheung and Dr. Bai Jianhao shared with me their profound knowledge in LbL and helped to revise my manuscripts. I also appreciate the help from Mr. Sebastian Beyer, Dr. Christopher Ochs, Mr. Matthew Pan Hou Wen and Mr. Zhang Ling.

My special thanks to Dr. Johnson Ng Kian-kok for his training and insightful discussion on the fabrication of gel pad arrays. I would also like to thank Dr. Shashi Ranjan for his training on the use of plasma cleaners and the help in my thesis writing. I also want to thank my friends Lin Kan, Kai Dan, Ping Yuan, Zhang Qiang, Liqun and Jinting who gave me a lot encouragement and support.

At the end of my acknowledgement, I would like to reserve deepest gratitude to my parents, my father Zhu Shuming and my mother Yan Junhui, to their love and firm support. Without their care and encouragement, it could have not been possible for me to complete this study.

TABLE OF CONTENTS

SUMMARY

Microparticle array technology has developed rapidly in recent years and has wide applications in biochemical research field such as genomics, genetic analysis, biomarker detection and cancer diagnostics. As compared to solid substrates for planar microarrays, three dimensional microparticles allow more bioprobes to be immobilized per unit of area and faster binding kinetics of the biomolecules to the bioprobe. Thus, microparticle arrays enable faster and more sensitive biochemical assays as compared to conventional planar microarrays. Currently, an important method for the arraying of microparticles is through the physical confinement in microfabricated microstructures. However, most of state-of-the-art microstructures for micropaticle array assembly are made with either expensive glass/silicon based materials or polymeric materials replicating against micromolds which are fabricated in a multi-step process in specific cleanroom facilities. This limits the possible customization of microparticle arrays in common biolabs for different bioanalysis applications. In this PhD work, novel polyacrylamide gel based microstructures are developed for the effective assembly of microparticle arrays. These microstructures are fabricated with low material cost and minimal equipment, less process steps and shorter process time, and with no need for a cleanroom and micromolds. The versatility of these microstructures is demonstrated by the integration of microparticle arrays on three types of gel microstructure chips for various multiplexed biochemical assays.

The first type of gel microstructure chip consists of gel pad array units which allow 40 serum samples to be simultaneously analysed with volume of each sample of merely 1 μl. As an example, quantitative microbead-based immunoassays for two tumor marker

proteins, hCG and PSA, are demonstrated with limits of detection lower than their cut-off concentration for cancer diagnosis. Moreover, a multiplexed immunoassay for hCG and PSA is also achieved by encoding batchwise deposited microbeads with their spatial addresses on the array. In addition, the reusability of the chip, which is rarely reported in any other microarray platform, is also demonstrated.

The second type of gel microstructure chips is designed to be integrated into a microfluidic system. Three different gel microstructures, gel pad arrays, gel well arrays and mixed microstructure arrays, have been fabricated for the assembly different types of microparticles. On-chip microfluidic single-plexed and multiplexed immunoassays for hCG and PSA in serum are demonstrated with microbeads assembled on gel pad arrays. Meanwhile, on-chip quantitative enzymatic glucose assays are also performed with microparticles assembled on gel wells arrays. Furthermore, the simultaneous immunoassays and enzymatic glucose assay are also achieved on chip, which is not reported before in any other microparticle array systems.

The third type of gel microstructure chip is designed to be integrated into a novel PEG-based capillary system. The capillary system consists of PEG micropillars fabricated by a photopolymerization reaction. The filling time and average flow rate of liquid on the capillary system is simply altered by modification with different concentrations of Tween® 20. The chip is tested by single-plexed and multiplexed microbead-based immunoassay for PSA and hCG with total assay time of 10 min and without any repeated washing steps. This is the first bioanalytical microbead array to be integrated into an autonomous capillary system for multiplexing biochemical assays.

LIST OF TABLES

LIST OF SCHEMES

LIST OF FIGURES

ABBREVIATIONS

CCD	charge-coupled device
COC	cyclic olefin copolymer
CRP	C-reactive protein
CRV	capillary retention valve
CV	coefficient of variation
DAPI	4',6-diamidino-2-phenylindole
DMD	digital micromirror device
DMPA	2,2-dimethoxy-2-phenylacetophenone
DMSO	dimethyl sulfoxide
DRIE	deep reactive ion etching
EDTA	ethylenediaminetetraacetic acid
ELISA	enzyme-linked immunosorbent assay
FBS	fetal bovine serum
FHMW	full-width at half-maximum
GOx	glucose oxidase
hCG	human chorionic gonadotropin
HRP	horseradish peroxidase
IgG	immunoglublin G
LOD	limit of detection
LOQ	limit of quantitation
NOA	Norland optical adhesive

PBS	phosphate buffered saline
PCR	polymerase chain reaction
PDMS	polydimethylsiloxane
PEG	polyethylene glycol
PEG-DA	poly (ethylene glycol) diacrylate
PSA	prostate specific antigen
RLP	removable polymer template
RT	room temperature
S.D.	standard deviation
SAM	self-assembled monolayer
SEM	scanning electron microscopy
SNP	single-nucleotide polymorphism
SPR	surface plasmon resonance
TE	Tris-EDTA
TEMED	Tetramethylethylenediamine
TNF-α	tumor necrosis factor-α
TPM	3-(Trichlorosilyl) propyl methacrylate
UV	ultraviolet
μCP	microcontact printing

Chapter 1

Introduction

Chapter 1 - Introduction

1.1 Background

Microarray technology has developed rapidly in the last two decades and it has become the leading technologies for multiplexing analysis of biomolecules. In a conventional microarray, different bioprobes are immobilized onto a planar substrate in a spatially addressable manner with each bioprobe targeting one specific biomolecule [1]. By incorporating thousands of micrometer sized bioprobe spots onto the substrate chip, a microarray enables the simultaneous multiplexed biochemical assays in a miniaturized format. Nevertheless, on a planar microarray, the binding kinetics of target biomolecules to the surface bioprobes are greatly limited by the two dimensional diffusion, which leads to a long assay time. For example, the hybridization of target DNA with the oligonucleotide probe on a planar DNA microarray could take more than 18 hrs [2].

Microparticles have been used in biochemical assays for over fifty years [3]. Owing to their three dimensional nature, microparticles allow more bioprobes to be immobilized per unit of area, while they also enable faster binding kinetics of biomolecules to bioprobes as compared to the bindispatiallinetics on a planar microarray [4]. Thus, microparticles microarray enables the faster and more sensitive biomolecule analysis than the conventional planar microarray. For example, Ng et al. [5] developed an oligonucleotide microbead array which was able to detect target DNA in merely 10 min. Due to these advantages, microparticle arrays have found wide applications in

biochemical research fields such as genomics [6, 7], genetic analysis [8, 9], biomarker detection [10-12] and cancer diagnostics [13, 14].

The majority of the state-of-the-art microparticle arrays utilize the orderly assembled biofunctionalized microparticles on certain solid substrates [15-17]. Currently, most of the microparticle arrays are assembled on the solid substrate either with the assistance of external forces, such as magnetic forces [18-20], electric forces [21, 22] and electrostatic forces [23-25], or with the confinement in certain physical microstrucutures [9, 12, 16, 17, 26]. The external forces assistant assembly, as it requires pre-patterned microcomponents on the substrate (micromagnets, microelectrodes and patterns of charged molecules), usually involves fabrication process in cleanroom facilities with expensive equipment which are not accessible for most biolabs. Furthermore, external forces assistant assembly is incapable to pattern non-magnetic and non-charged microparticles which could also limit its application. In contrast, the physical confinement method is applicable to most microparticles regardless of their chemical or physical properties. Silicon/glass microstructures were the first to be utilized for physical confinement of microparticles [15, 26, 27]. However, the expensive substrate material as well as the complicated microfabrication process could be a limitation. Recently, inexpensive polymeric materials, such as PDMS, cyclic olefin copolymer (COC) and optical epoxy resin, have been more frequently employed for the fabrication of microstructures for microparticle assembly [17, 28-30]. The fabrication of these polymer microstructures is based on molding [17, 30] or embossing [28] against certain micromolds and is less complicated than the fabrication of silicon/glass microstructures as these molds are usually reusable. Despite that, if polymeric microstructures can be fabricated even without a micromold which is usually microfabricated on silicon or metal substrate in a cleanroom, the entire

fabrication process for microparticle arrays could be further simplified and the microparticle array could be potentially more customizable to most researchers.

Another important issue for microparticle arrays, when being applied for bioanalysis, is the delivery of different bio-reagents to the array during the biochemical assays. Microfluidics, with its minute volume, fast mass transfer rate and automated flow control, is a good candidate for reagent delivery [31]. Thus, microparticle arrays have been integrated into microfluidics for rapid, sensitive and multiplexed biochemical assays [32-34]. For most microfluidic microparticle arrays, the delivery of the reagent requires external pumping elements such as syringe pumps or peristaltic pumps. Although these pumps can automatically and precisely control the flow rate, they are usually bulky in size and are connected with external power sources. This could limit the application of microparticle arrays in on-site point-of-care tests. The idea of passive pumping, which integrates the self-pumping element inside the microfluidic system, could be a solution to this limitation. Although various passive pumping methods have been developed [35-37], none of them has been employed for integration with microparticle arrays for bioanalysis. Therefore, it will be promising to develop microfluidic devices with integration of microparticle arrays as well as passive pumping elements for multiplexed point-of-care test.

On the other hand, while existing microparticle arrays focus mainly on the multiplexed analysis of different biomolecules of one category (e.g. different proteins [10], DNAs [38] or small metabolites [39]) by one type of biochemical assays (e.g. immunoassay, DNA hybridization assay or enzymatic assay), few has been reported for the multiplexed detection of different categories of biomolecules. In fact, the multiplexed detection of different categories of biomolecules is desired for specific biomedical

applications. For example, the diagnosis of pancreatic insulinoma is based on the measurement of serum glucose level as well as the serum insulin level with two assays, the enzymatic glucose assay as well as the immunoassay for insulin [40]. Another example is the diagnosis of colorectal cancer by measuring the serum level of carcinoembryonic antigen (CEA) and the serum free DNA which also require two assays, an immunoassay for CEA and a PCR based assay for free DNA [41]. In these two cases, if an array can be fabricated incorporating microparticles biofunctionalized with bioprobes for specific protein, DNA and glucose, different categories of biomolecules could be measured with merely one assay and the time required for diagnostics will be greatly shortened. Thus, there is a need to fabricate arrays of microparticles with different bioprobes to simultaneously perform different biochemical assays for the detection of different categories of biomolecules.

To summarize, most of the current methods for the fabrication of polymeric microstructures for physical confinement of microparticles require micromolds which are fabricated in specific cleanroom facilities with expensive equipment. The fabrication cost and time could be greatly reduced if microparticles could be assembled on polymeric microstructures which are fabricated with mold-free methods and with minimal equipment required. Furthermore, currently, no bioanalytical microparticle array has been integrated into an external-pump-free microfluidic system to be optimized for point-of-care tests and no efforts has been made to enable the multiplexed detection of different categories of biomolecules with a single microparticle array for potential biochemical applications.

Therefore, there is a need to develop mold-free fabricated polymeric microstructures for the assembly of microparticle arrays which can subsequently (1) be used for

multiplexed biochemical assay for biomolecules either from the same category or from different categories (2) be integrated into a passive pumping element embedded microfluidic system for multiplexed point-of-care tests.

1.2 Objectives and specific aims

The main objective of this work is to develop a microparticle array platform based on the mold-free fabricated gel microstructure chips, to subsequently apply this microparticle array for the multiplexed biochemical assays for different categories of biomolecules and to integrate the microparticle array into an external-pump-free microfluidic system.

To accomplish the main objective, there are four specific aims to be completed:

Specific Aim 1: To develop mold-free fabricated polyacrylamide gel microstructures with low background fluorescence for the assembly of microparticle arrays.

Specific Aim 2: To integrate the microparticle arrays assembled on gel based microstructures into a microchip for quantitative, multiplexed and high-throughput immunoassays.

Specific Aim 3: To integrate the microparticle arrays assembled on gel based microstructures into a microfluidic system for the simultaneous multiplexed immunoassay and enzymatic assay for the detection of proteins and glucose.

Specific Aim 4: To integrate the microparticle arrays assembled on gel based microstructures into an autonomous capillary microfluidic system for multiplexed immunoassays.

1.3 The scope

This thesis work includes the development of polyacrylamide gel microstructures for the assembly of biofunctionalized micropaticle arrays and the integration of these microparticle arrays into chip-based platforms for the applications in miniaturized multiplexed biochemical assays, especially in immunoassay, enzymatic assay and hybridization assay. With very low material cost and minimal equipment required, with short process time and no cleanroom work involved, the fabrication of gel microstructures can be easily adapted for most biolabs. Therefore, it could be useful for researchers to rapidly fabricate and assemble microparticle arrays for various bioanalysis applications.

In the first part of the work, a gel pad array chip has been developed to hold multiple microbead arrays for high throughput immunoassays for serum samples. The performance of the chip is tested with both single-plexed and multiplexed microbead based fluorescence immunoassays for tumor marker proteins. Moreover, the stability of microbeads on the gel pad array during the assay is also investigated. Another special feature, the reusability of the chip, which is rarely reported in other microparticle array platforms, is also validated. Lastly, the one-assay integration of DNA hybridization assay and immunoassay is also demonstrated.

In the second part of the work, microparticle array assembled on gel microstructure chip is integrated into microfluidics for microfluidic quantitative immunoassays and enzymatic assay. The simultaneous detection of two tumor markers and glucose is achieved by the first time in the literature, the integration of immunoassays and enzymatic assay in a microparticle microarray platform.

In the third part of the work, a chip with novel PEG-based capillary microfluidic system is fabricated in a simple fabrication process with minimal equipment required. A simple surfactant surface modification method is employed to alternating the filling time and average flow rate of liquid in the capillary system. By integrating gel pad arrays into this capillary system chip, we demonstrate the first multiplexed immunoassay with a microbead array in a passive pumping element embedded microfluidic system. With only 10 min assay time and no external pump or energy source required, the integrated chip could be potentially contributed to the multiplexed point-of-care diagnostics.

Chapter 2
Literature Review

Chapter 2 - Literature Review

2.1 Introduction

Microparticles have been used in biochemical assays for over fifty years [3]. The advantages utilizing the microparticles rather than conventional two dimensional solid substrate for biochemical assays lie in their high surface to volume ratio which allows more bioprobes to be immobilized and the three dimensional diffusion which results in faster reaction/binding kinetics between the target biomolecules and bioprobes [4, 42, 43]. The assembly of microparticles into a microarray format not only embraces all the above advantages but also enables multiple biomolecules to be detected and analyzed [44]. Therefore, the microparticle array has been widely used in various kinds of biochemical assays such as in immunoassays [10, 29, 45-47], DNA hybridization assays [5, 6, 9, 38, 48] and enzymatic assays [49].

The two major formats of microparticle arrays are suspension microparticle microarray and on-substrate microparticle microarray. Suspension microparticle array technique, which was developed by Luminex Corporation, employs color-encoded microparticles suspended in liquid for the biochemical assays [50]. The microparticles encoded with different ratio of two dyes are attached with different bioprobes and are mixed together in solution, thus forming a suspension microarray [51]. Besides the suspension microparticle arrays, the majority of the other microparticle arrays are assembled on certain substrates. In this chapter, we emphasize mainly on the current methods for the fabrication of on-substrate microparticle arrays and their applications in bioanalysis. The following review will cover (1) the state-of-the-art methods for the assembly of micropartcle arrays; (2) microparticle encoding methods for multiplexed biochemical

assays and (3) the application of microparticle arrays in biochemical assays. In addition, recent progress in the development of capillary pump systems for biochemical assays will also be reviewed.

2.2 Methods for the assembly of microparticle array

One challenge for the fabrication of microparticle arrays is the manipulation and assembly of minute and highly mobile microparticles into an ordered pattern/array. In recent years, various methods have been developed for the assembly of microparticles with the most notable ones including magnetic force assisted self-assembly, electric field assisted self-assembly, electrostatic force assisted self-assembly, optical manipulation and physical confinement.

2.2.1 Magnetic force assisted self-assembly

The utilization of paramagnetic microparticles in the biochemical assays can be retrospected to over 30 years ago [52]. To assemble a paramagnetic microparticle array, magnetic force should be applied to manipulate and pattern the microparticles onto the substrate. The generation of the magnetic force could be from external macroscopic magnets, integrated microscopic magnets or integrated micro-electromagnets [53]. For example, Fan et al. [54] demonstrated the patterning of magnetic microparticles in eight separate microchannels by using an external bulk magnet. The patterned biofunctionalized microparticles were used as a bioarray for the simultaneous detection

of multiple target oligonucleotides. Alternatively, Smistrup et al. [18] integrated magnetized permalloy into the microfluidic chip for the attraction of magnetic microparticles. With multiple permalloy micro-magnets, microparticles arrays can be fabricated on the side wall of the microchannel and be used for the multiplexed biochemical assay. Another approach, pioneered by Choi et al. [55], was the integration of electromagnets for the capture and pattern of magnetic microparticles. The advantage using electromagnets instead of permanent magnets is the flexibility to control the magnetic force by changing the current in the conductor coil thus allowing the capture and releasing of the microparticles. While all the above works only demonstrated the assembly of clusters of microparticles, Xu et al. [19] recently fabricated permalloy disk and line arrays which allows the assembly of single paramagnetic microparticle arrays. The limitations of the magnetic force assisted microparticle array assembly are (1) Single microparticle array cannot be fabricated by using bulky external macroscopic magnets. (2) Complicated fabrication processes are usually required for the integration of microscopic magnets and micro-electromagnets.

2.2.2 Electric field assisted self-assembly

Charged microparticles can be captured and manipulated under certain electric field due to the electrostatic attraction between the electrode and the microparticles [56, 57]. By integrating microfabricated microelectrode arrays onto the substrate, microparticles can be assembled in an ordered array both in dry conditions [22, 58] and in solution phase [59]. The advantage to array charged microparticles in dry conditions lies in the high stability of immobilized microparticles after the retrieval of the electric field as these microparticles will not move randomly through Brownian motion [22]. In

contrast, the retrieval of electric field in solution phase usually leads to the random movement of microparticles [56]. Barbee et al. [21] solved this problem by patterning protein-coated microbeads directly on gold microelectrodes which have high non-specific affinity to the proteins. The resulting stably arrayed microparticles in solution phase allowed the immediate integration with biochemical assays. While the electric field assisted assembly possesses the superiority of much shorter assembly time (tens of seconds) over other microparticle assembly methods, it also has obvious limitations such as the complicated fabrication process for microelectrode arrays and the restricted application for only charged microparticles.

2.2.3 Electrostatic force assisted self-assembly

Another method for the assembly of charged microparticle arrays is the electrostatic force assisted assembly. In a pioneer research, Aizenberg et al. [23] employed micropatterned anionic or cationic self-assembly monolayers (SAMs) for the assembly of polystyrene microparticles arrays. Sivagnanam et al. [24] extended this approach by assembly of protein-coated microparticles on patterned SAMs with the opposite charge. Arrays of single or multiple microparticles were fabricated by controlling the size of the SAM patterns and the arrayed microparticles were directly used for the biochemical assays [33]. Besides the charged SAMs, polyelectrolytes were also frequently employed for the patterning of charged regions for microparticle assembly [25, 60, 61]. However, the patterning of both SAMs and polyelectrolytes requires complicated photolithography procedures in cleanroom such as the fabrication of masters for the stamp of microcontact printing (μCP) [23] and the fabrication of

templates for the patterning of silanes [62]. This limits the utilization of electrostatic assisted self-assembly methods in common biochemistry labs.

2.2.4 Optical manipulation

The manipulation of microparticles with optical force was first demonstrated by Ashkin in 1971 [63]. In this study, single microparticle was selectively accelerated and captured by applying a radiation pressure using laser beam. This was later developed into the “optical tweezer” technique for the manipulation of particles [64] as well as cells [65] and atoms [66]. Although the early generation of optical tweezers achieved accurate manipulations of microparticles, they were limited to the capture of one microparticle at one time and were not suitable for the assembly of an array of microparticles. To manipulate multiple microparticles at one time, Tam et al. [67] developed an optical tweezer array using fiber optic bundles to split laser beam for the simultaneous manipulation of more than one hundred microparticles. Another approach reported by Merenda et al. [68] employed micromirror array to split the laser and thus allowing multiple microparticles to be arrayed. This approach was further advanced by using a programmable digital micromirror device (DMD) which is able to pattern hundreds to thousands of spatially addressable microparticles [69]. The advantage of optical manipulation method lies in its capability to directly pattern microparticles without the need for the fabrication of any physical templates or chemical micropatterns. However, the inability for the simultaneous assembly of large number of microparticles as compared to other methods (hundreds versus millions) and the requirement of expensive laser light source could hinder the application of optical manipulation methods in the fabrication of microparticle arrays.

2.2.5 Physical confinement

Physical confinement method, which employs certain physical microstructures to constrain the microparticles, is a more straightforward approach for the fabrication of microparticle arrays. Compared to the external force (e.g. magnetic force and electric field) assisted assembly of microparticle array, the physical confinement method only relies on the geometry and the size of the microstructure for the patterning of either single or multiple microparticle arrays [16]. Thus, it is not restricted for the assembly of specifically modified microparticles (e.g. magnetic or charged micropaticles) but for microparticles made with different materials and of various geometries. Silicon/glass and polymer are the two categories of most frequently used materials for the fabrication of microstrcutures for microparticle array assembly.

2.2.5.1 Silicon and glass microstructures

Silicon and glass based materials are the basis for the semiconductor industry and numerous standardized fabrication protocols are available for the fabrication of microstructures on these substrates. Thus, it is not surprising that the fabrication of microparticle array was initially achieved on silicon and glass based microstructures. Professor David Walt's research group reported first high density microparticle array assembled on end-etched glass optic fiber bundles in 1998 [70] (**Figure 2.1a**). The distal faces of every optical fiber core can be etched out by hydrofluoric acid [71] or hydrochloric acid [10] thus forming microwells which are separated from each other by the inert cladding layers. A high density array of microparticles was then successfully fabricated on these microwells [15]. The assembled microparticles arrays

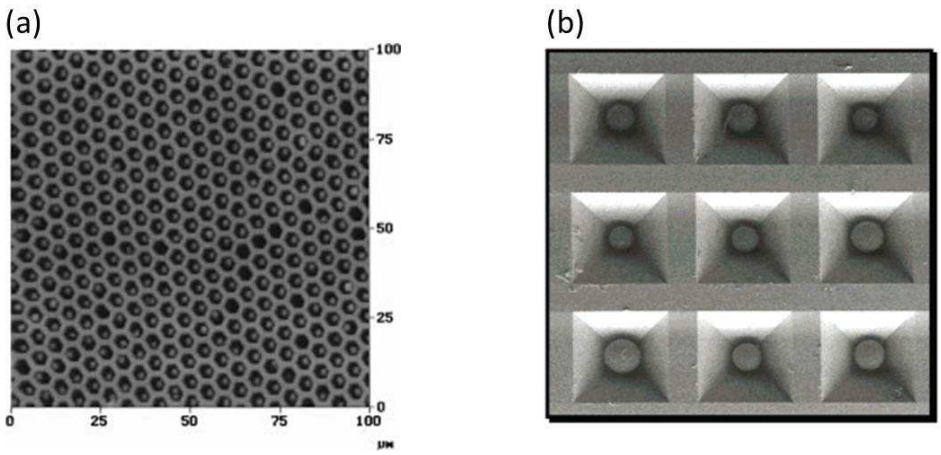

Figure 2.1 Microparticle arrays assembled on glass/silicon based microstructures. (a) Microbead array assembled in microwells on an end-etched optical fiber (From [70]). (b) Microbead array assembled on microwells etched on a silicon wafer (From [72]).

has been widely used in various applications such as immunosensing [73], DNA hybridization assays [74], aptamer based assay [75] and artificial olfaction [76]. This technique was also commercialized by Illumina, Inc [77]. Besides the optical fiber array technique, Illumina also commercialized the technique to assemble microparticle on microwells etched on a silicon wafer which was named as BeadArray™ platform [7]. Professor John McDevitt's research group also employed etched silicon microwells for the assembly of biofunctionalized microbeads [26, 72] (**Figure 2.1b**). Different from optical fiber array platform and BeadArray™ platform, microparticles were immobilized in through-etched microwells which allowed the reagents to pass though freely. This enabled the direct integration of the microparticle array into microfluidic systems for biochemical assays [9, 78, 79]. However, there are two drawbacks for this system: (1) only relatively big microparticles (>100 μm [9, 72, 78, 80]) can be assembled due to the size of microcavities (upper diameter >200 μm) which limited the maximum number of microparticles per unit of area; (2) microparticles were transferred into each microwell manually with a micro-manipulator in a one particle one time manner [26, 81] which is not applicable for the

fabrication of high-density microparticle array for high multiplexing biochemical assays. For the above microparticle arrays assembled on silicon and glass based microstructures, the limitation lies in their requirement for expensive substrate materials (silicon wafers, glass wafers or glass optic fibers) as well as multi-step fabrication process in specialized cleanroom facilities with well-trained technicians.

2.2.5.2 Polymer microstructures

Polymer is another widely used substrate material for the fabrication of microstructures for microparticle assembly. Compared to the silicon and glass based materials, polymeric materials are less costly and more flexible for casting, molding and patterning. Most of the current polymer microstructures for microparticle assembly are fabricated by molding against certain templates. Zhou et al. [12] fabricated PDMS based microchambers integrated with microfluidic channels by soft-lithographical replica molding method against silicon masters for the assembly of tens of antibody-coated microbeads for microfluidic immunosensing [82], DNA detection [83] and RNA detection [34]. Lim et al. [17] advanced the technique by the assembly of more than ten thousands of microbeads on novel dome-shaped PDMS microstructures which is molded against a specially made master (**Figure 2.2a**). PDMS itself was also used as a template for the molding of epoxy resin based microcavities for microparticle assembly [29]. While the molding of PDMS based microstructures still requires microfabricated silicon or glass masters, microstructures can also be fabricated with microfabrication-free methods such as breath figure method [84]. Lu [85] et al. used breath figure method to fabricate micropores on silica-polystyrene hybrid polymer films with condensed water droplets as template. Different

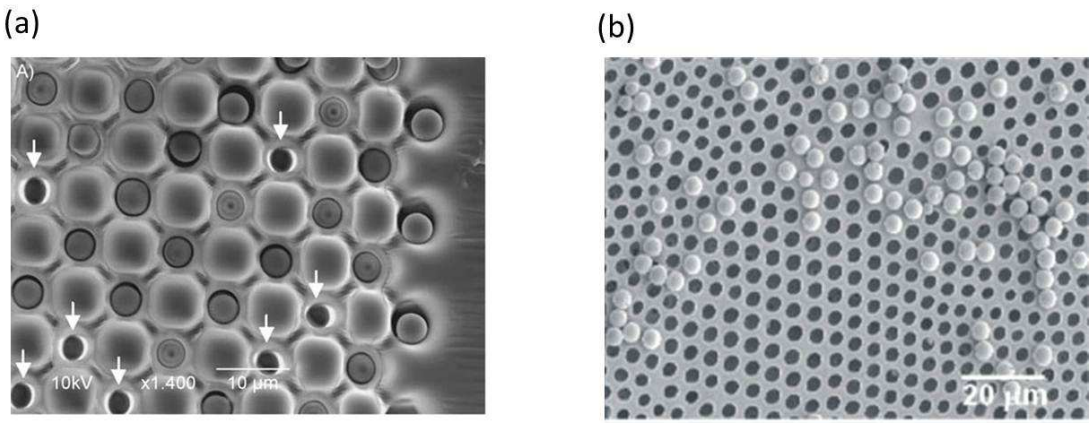

Figure 2.2 Microparticle array assembled on polymer based microstructures. (a) Microbead array assembled on a PDMS based microstructure made by replica molding (From [17]). (b) Microparticle array assembled on polystyrene/silica porous film made by breath figure method (From [85]).

sized micropores can be generated by controlling the ratio between silica and polystyrene in polymer solution, thus fitting for microparticles with different sizes (**Figure 2.2b**).

As an alternative method to mold/template assistant molding, Jason et al. [86] reported the fabrication of a microwell array by direct hot-embossing of a silicon master against cyclic olefin copolymer (COC) substrate. The embossing process only took seconds time and the resulting microwells provided good immobilization stability of antibody-coated polymeric microbeads [28]. Ng et al. [5] developed photo-patterned polyacrylamide gel pad arrays which were subsequently employed for the assembly of oligonucleotide coated microbeads with 100% immobilization stability. Different from the conventional photolithography methods for photoresist patterning, the fabrication of these gel based microstructures is a one-step process and requires no cleanroom facilities. Both of the above two approaches enable rapid fabrication of polymeric microstructures without the need for expensive sophisticated equipment and could thus

provide simple and effective solutions for the fabrication of robust biofunctionalized microparticle arrays for common biochemistry labs.

2.2.6 Miscellaneous methods

Methods for the fabrication of microparticles arrays, which cannot be categorized into the above five methods, were also developed by multiple research groups. Lee et al. [87] fabricated a microparticle array on a photo-curable adhesive layer which was microcontact printed with removable polymer template (RLP) in advance. After triggering the adhesion between the microparticles and the adhesive layer by UV exposure, RLP was removed by a water/ethanol (80/20) solution, leaving an array of microparticles which only sit on the non-patterned region on the adhesive layer. Yan et al. [88] used μCP method to directly printing arrays of microparticles onto the poly(vinyl alcohol) film. By solvent swelling or mechanical stretching of the PDMS μCP stamps, microparticle arrays with different patterns and intra-particle distances can be fabricated [89, 90]. Lilliehorn et al. [91] reported the acoustic manipulation of single microparticle for array assembly using ultrasonic transducers. The resulting biofunctionalized microparticle array was proved to be robust in microfluidic binding assays [92]. Another interesting method was introduced recently by Palla-Papavlu et al. [93] who employed a physical phenomenon called “laser induced forward transfer” for the selective transfer of microparticle onto the target substrate. The microparticles were transferred from the donor substrate to the target substrate by the propelling energy generated during the laser induced decomposition of sacrificial layer on the

donor substrate. Arrays of clusters of microparticles can thus be assembled by control the laser radiation position on the donor substrate.

A summary of the current method for the assembly of microparticle arrays is demonstrated in **Table 2.1**.

2.3 Microparticle encoding methods

Microparticle encoding methods were initially developed for applications in combinatorial chemistry for the screening of particular synthesized chemicals from a microparticle based combinatorial library [94]. As applied in bioanalytical microparticle arrays, proper encoding methods allow the distinguishment of microparticles functionalized with different bioprobes which enable the correlation of the output signals with the correspondence biochemical interactions/reactions [95]. Several encoding methods are currently adopted for microparticle arrays used for multiplexed biochemical assays, with three of them most frequently used: color encoding method, barcode encoding method and spatial encoding method.

2.3.1 Color encoding

A most prevailing microparticle encoding method is the color encoding method which employed spectrally distinct microparticles prepared by embedding chromophores, fluorophores or semiconductive nanocrystals onto the particle surface or into the particle matrix [96, 97]. A most straightforward way for color encoding is to dope

Table 2.1 Summary of the current methods for microparticle array assembly

Methods to assembly of microparticle arrays	Microparticle	Substrate	Extra Equipment for assembly	Throughput	Cleanroom work	References
Magnetic force assisted self-assembly	paramagnetic	Silicon/glass patterned with micromagnets	DC power supply for micro-electromagnets	high (>100,000)	Yes	[18,19,53-55]
Electric field assisted self-assembly	charged	Silicon/glass patterned with micro-electrodes	DC Power Supply	high (>100,000)	Yes	[22, 56-59]
Electrostatic force aasisted self-assembly	charged	Silicon/glass patterned with charged SAMs or polyelectrolytes	No need	high (>100,000)	Yes	[23-25, 33, 60, 61]
Optical manipulation	No restriction	No restriction	Optical Tweezer	low (~ 100)	No	[63-69]
Physical confinement	No restriction	Silicon/glass or polymer microstructures	No need	high (>100,000)	Yes (Silicon/Glass); No (Polymer)	[7, 15, 26, 70, 72, 77]

different microparticles with different fluorescent dyes. Egner et al. [98] demonstrated the labelling of different microparticles with six spectrally distinct fluorescence dyes which can be easily distinguished by a fluorescence microscope. The problem with the "one dye one bead" approach is the limited number of codes which can be generated as restricted by the availability of different spectrally distinct dyes. Luminex Corporation reported an improved approach by doping microparticles with different ratios of two organic dyes to generate 100 different types of microparticles which can be later

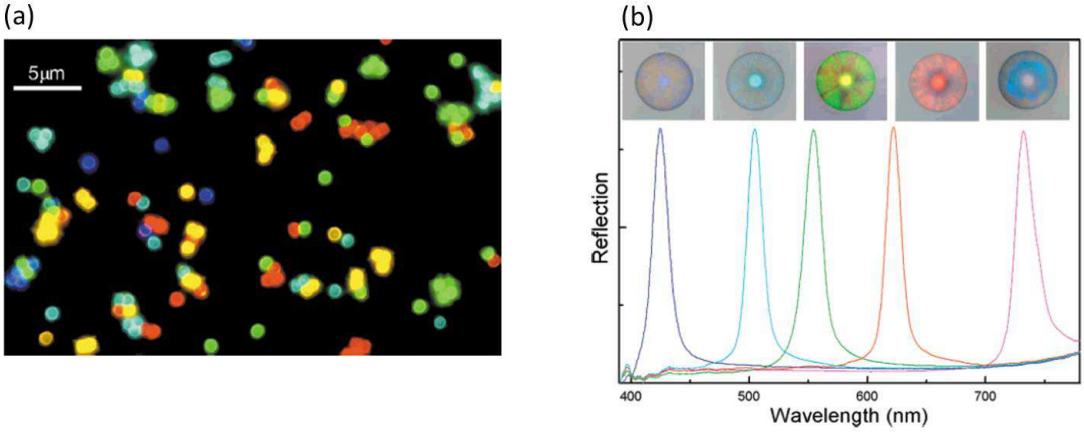

Figure 2.3 Microparticles encoded by color. (a) Microparticles encoded with quantum dots (From [99]). (b) Microparticles encoded with silica colloidal crystal (From [100]).

decoded by a customized flow cytometer [38]. In this case, the microparticles are not only discriminated by their colors but also by the emission intensity in certain wavelength. Furthermore, with the same approach, the number of different types of microparticles can be potentially increased if three or more dyes are doped [47]. However, the organic dyes usually suffer from photobleaching problem and the emission of organic dyes require multi-wavelength excitation light source which could add complexity for the optical detection system.

As an alternative to organic dyes, inorganic semiconductor nanocrystals, named "quantum dots", were also employed for the encoding of micorparticles. Compared to organic dyes, quantum dots embrace several advantages such as the non-bleaching nature, the single-wavelength excitation for multi-wavelength emission, tunable emission wavelength and narrower emission peak [101]. Han et al. [99] doped microparticles with different intensity and color of quantum dots for color encoding (**Figure 2.3a**). Theoretically, six different colored quantum dots at 10 different intensities levels could create one million types of encoded microparticles. A slight concern for quantum dots is the high cytotoxicity of cadmium and selenium which may require extra safety measures. Besides quantum dots, photonic crystals were also used for the spectral encoding of microparticles [102]. Cunin et al. [103] reported the first research using photonic crystal microparticles as the microcarrier for biochemical assays. By adjusting the pore size of silicon photonic crystals during the microfabrication process, microparticles with different visible spectra can be obtained. Hereafter, the process for making these encoding photonic crystal microparticles was simplified by Zhao et al. by assembly microbeads with silica nanoparticles [100] (**Figure 2.3b**). The robustness of this approach is the direct integration of the spectral code with the microparticles during the fabrication process, thus eliminating the need for any doping or embedding of dyes or nanocrystals. The advantages using these photonic crystals for color encoding lie in their extremely narrow emission peak (ca. 11 nm full-width at half-maximum, FWHM [103]) as well as their colormetric visibility which can be distinguished without fluorescence excitation. A more advanced method was developed by Tang et al. [104] who employed both photonic crystal particles and quantum dots for color encoding. The number of codes that can be generated was multiplied by encoding the microparticles with the binary combination

of the fluorescence spectra of quantum dots and the reflective spectra of photonic crystals. Nevertheless, the major limitation of the current color encoding methods is the lack of readout equipment powerful enough to resolve more than 100 different combinations of colors and intensities which is the maximum number reported until today by Lunimex Corporation [38].

2.3.2 Barcode encoding

Another widely used approach for the encoding of microparticles for multiplexed biochemical assays is the barcode encoding approach [105]. Nicewarner-Peña et al. [106] reported the fabrication of microrods with metal stripes. As each metal material has its distinct reflective spectrum, the combination of these metal stripes served as one dimensional barcode for the encoding of microrods. Theoretically, unlimited numbers of barcoded microrods can be fabricated by alternating the number of metals employed and the order and the width of each metal strip. With an alternative approach, Dejneka et al. [107] developed glass microparticles striped with different rare earth for barcoding. The different fluorescent patterns of the rare earth on each microparticle can be identified by using a simple fluorescence microscope and both one dimensional and two dimensional barcodes can be fabricated [108]. However, the general applications of the above two methods for micropartiles barcode encoding are limited by the expensive materials (gold, silver, platinum and rare earth) used, the very specialized and complicated multistep fabrication process involved and the powerful readout system required for resolving the spectral pattern [107, 109]. SmartBead Technologies fabricated aluminium microrods with different patterns of one-dimensional etched holes for barcode encoding [110]. The identity of each microrod

was recognized by the length and position of etched holes, which requires no spectral resolving devices for decoding. However, the aluminium material may not be ideal for the attachment of bioprobes. Biocatis [111] recently developed silicon based microparticles with two dimensional etched holes as barcodes. With the well-known surface chemistry of silicon, it is more feasible to attach bioprobes (e.g. antibodies) to the microparticle surface for multiplexed biochemical assays. Besides the metal and silicon, polymeric SU-8 photoresist was also employed for the fabrication of barcoded microparticles [112, 113]. With proper surface functionalization [114], SU-8 could be an inexpensive material to generate biofunctionalized barcoded micropaticles for biochemical assays [113].

Another innovative method to generate barcode on microparticles is through the spatial selective photobleachng of different regions on the surface of fluorescent microparticles to directly “write” graphic barcodes [115]. Infinite number of codes can be generated as virtually all types of barcodes can be written on the microparticle surface with this method. However, the requirement of expensive laser scanning confocal microscope as well as the time-consuming “one-paticle-one-time” fabrication process could limit the general application of this method.

While all the approaches mentioned above are either involved with complicated microfabrication in cleanroom or limited by the time-consuming fabrication process, Professor Doyle’s research group developed a one-step approach for the rapid fabrication of two dimensional barcoded microparticles, which is name as “Continuous-flow Lithography” [116]. The dot-codes as well as the rest part of the microparticles were synthesized in milliseconds time by illuminating microfluidic flow of poly(ethylene glycol) diacrylate prepolymer solution with the UV source through a

soft-mask [117]. In theory, this system has the power to fabricate more than one million different types of barcoded microparticles and these encoded microparticles can be aligned in a microchannel and subsequently be screened and recognized in high throughput by a high-speed imaging system [118]. Moreover, the capability of simultaneous incorporation of barcodes and bioprobes in synthesis process is not applicable for any other barcoded microparticle fabrication methods. However, the relatively large particle size (~100 μm) and the small pore size of the PEG gel [119, 120] could slow down the diffusion of big-sized biomolecules (e.g. DNAs and proteins) towards bioprobes, thus affecting the reaction kinetics and extending the assay time (> 1.5 hrs [121]).

2.3.3 Spatial encoding

Spatial encoding method is widely used in conventional planar microarrays where different bioprobes are discriminated by their addressable position on the substrate [2, 122]. The prerequisite to encode microparticles with spatial positions is the great stability of immobilized microparticles which will not move during the encoding as well as the biochemical assay process. Goodey et al. [26] demonstrated the arrangement of five types of microparticles which were attached with different complexones (metal chelating reagents) for the detection of three types of metal ions. Microparticles were transferred into micro-cavities etched on a silicon chip and the identity of each microparticle was encoded by their spatial position on the micro-cavity array. This approach was further employed for the encoding of microparticles functionalized with enzymes [81], oligonucleotides [9], aptamers [79] or antibodies [72] for multiplexed biochemical assays. The similar spatial encoding approach was

also employed by Zhou et al. [12] to address antibody microparticles in a one-dimensional array for multiplexed immunoassay. However, in these early works, the manual “one-by-one” assembly of individual microparticle made the encoding process tedious. As a result, the number of microparticles can be assembled was limited and the multiplexing power as well as the redundancy of the data points was also compromised. As an improvement, Ng et al. [5] demonstrated the spatial encoding of

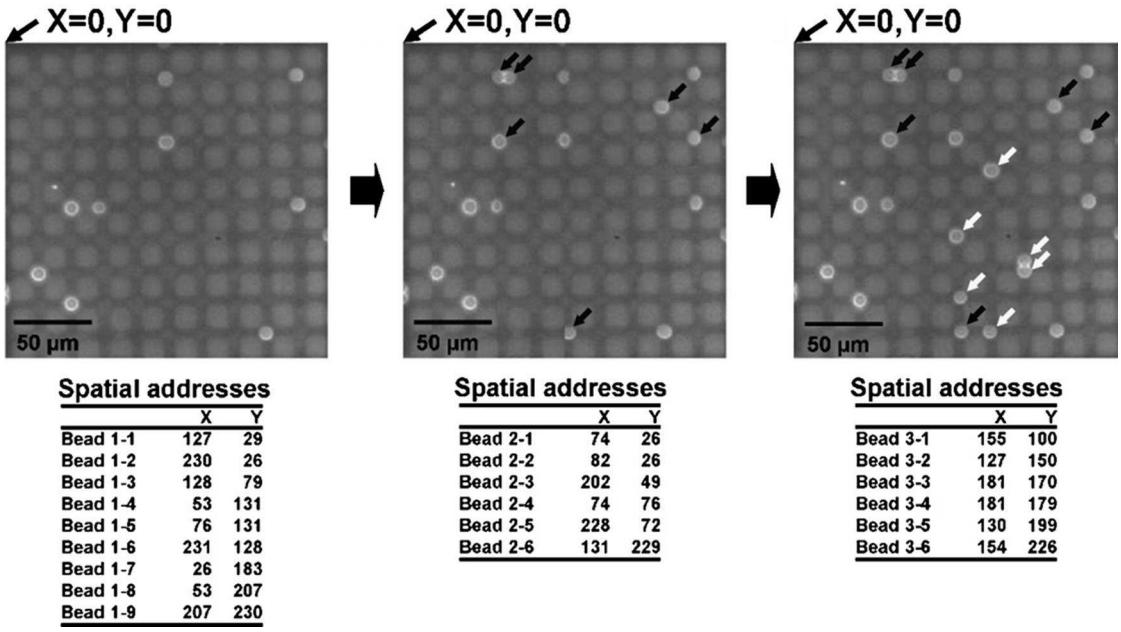

Figure 2.4 Spatial encoding of microbeads by sequential deposition (From [5]).

microparticles by analyzing images captured after random deposition of each batch of microparticles on a gel pad array (**Figure 2.**). The unique sticky property of the gel enabled the stable immobilization of microparticles which remained in their spatial position during the encoding/decoding process. The different types of microparticles can thus be assembled on gel pad array by simple pipetting and the redundancy of each batch of microparticles was greatly increased. By adjusting the density of microparticle in solution, this approach allows much more types of microparticles to be immobilized and encoded than the previous approaches. Recently, Barbee et al. [59] developed

another chip-based platform for efficient immobilization and encoding of microparticles. With the assistance of an external electric field, different types of microparticles can be sequentially deposited onto the microelectrode surface with each deposition being done in merely tens of seconds, and the microparticles can then be encoded with their spatial positions by imaging. The encoding of twenty batches of microparticles was demonstrated with ten deposition process and two fluorescence encoding dyes. There are three most notable advantages of spatial encoding method over other methods: (1) spatial encoding does not require fabrication of specialized microparticles or the modification of the microparticles with colors or barcodes, and therefore the choice of microparticles can be much more flexible to fit for the optimization of biochemical assays; (2) spatial encoding is a more efficient method as the encoding process is simultaneously done with the assembly of microparticle array while for other encoding methods, the pre-encoding and array fabrication should be done stepwise; (3) decoding of microparticles do not require any complicated spectral or barcode resolving equipment.

2.3.4 Miscellaneous encoding methods

Other miscellaneous methods were also developed for the encoding of microparticles. Benecky et al. [123] developed multiplexed immunoassay using different sized microspheres. A customized particle flow analyzer, which was able to distinguish 0.1 μm difference in particle diameter, was employed for size based decoding for four types of microparticles. However, the fabrication of different types of microspheres with well-controlled sizes is very challenging and the available “size codes” could thus be limited. In another research work, Evans et al. [112] fabricated shape-encoded SU-8

microparticles, named as “FloCode”, which can be decoded by flow cytometry. Multiplexed fluorescence DNA hybridization assays were demonstrated with these encoded microparticles. Kastl et al. [124] also fabricated different shaped “graticles” with grated surface for SPR detection. Label free multiplexed detection for both DNAs and proteins was achieved by measuring the SPR signals arisen from shape encoded graticles [125]. Nevertheless, the involvement of cleanroom and expensive equipment for shaped microparticle fabrication could limit the application of shape encoding method.

While the encoding of microparticles was done either before or during the microarray fabrication process for all the above methods, Illumina, Inc. developed a method to encode microparticles after the assembly of the microarray [126]. Microparticles with different surface oligonucleotide probes were sequentially hybridized and denatured with target DNAs which were label with fluorescence dyes (either type of two dyes) or were not labelled. Thus, in every hybridization step, each microparticle can obtained a code from three possible codes (0 for unlabelled target, 1 for dye A labelled target, 2 for dye B labelled target.). With eight sequential steps, theoretically 6561 (3^8) different eight-digit ternary codes can be generated, and as an example, 1520 types of these codes were used for encoding the microparticles with different oligonucleotide probes. Although this method achieved highest multiplexing power among the current microparticle arrays, its application is limited to only DNA hybridization assays.

A summary of the current microparticle encoding methods is demonstrated in **Table 2.2**

Table 2.2 Summary of the current microparticle encoding methods

Encoding method	Color encoding	Barcode Encoding	Spatial Encoding
Principle	Encoding microparticles with their different spectral properties (color, spectrum, or intensity).	Encoding microparticles with their different barcode (1D or 2D barcodes).	Encoding each batch of microparticles with their random spatial addresses on the substrate.
Multiplexing Capability	mid (100 -1000); limited by the spectral-resovling power of the decoding system.	theoretically unlimited.	theoretically unlimited.
Cost of the readout and decoding system	High	Moderate	Low
Microparticle modification and fabrication	Dye doping or nanocrystal fabrication. Complicated process.	Define physical or graphical barcode by microfabrication, continuous lithography or laser bleeching. Complicated process.	No need of pre-modification of the microparticles or the fabrication of specific microparticles.
Microparticle array fabrication time	Short	Short	Moderate to long (batchwise process)

2.4 Microparticle array for biochemical assays

Microparticle allows more bioprobes to be immobilized per unit of area and enables the three dimensional diffusion of target analytes towards the bioprobes, thus microparticle is regarded as an important solid support for biochemical assays [127]. The integration of microparticles into microarray embraces the advantages of fast kinetics as well as the multiplexing capability, and various biochemical assays have been done on microparticle array platforms. In the next session, the recent application of microparticle arrays on biochemical assays, especially DNA hybridization assays and immunoassays, will be reviewed.

2.4.1 DNA hybridization assays

The attachment of nucleic acids or oligonucleotides onto microparticles' surface was originally used for the application of DNA/RNA separating and purification [128] and solid phase sequencing [129]. With the development of solid-phase DNA assay and microarray technology, microparticle arrays have been utilized intensively for multiplexed DNA hybridization assays. Luminex Corporation and Illumina Inc. are two of the most successful companies who developed commercialized microparticle arrays for DNA hybridization assays.

Luminex Corporation developed a suspension microparticle array platform with flow cytometry based detection [50]. With this platform, as the reporter fluorescence dye has different excitation and emission wavelength with the encoding fluorescence dyes, the encoding as well as the quantitation can be done simultaneously using two-laser excitation. It has been widely utilized for multiplexed DNA hybridization assays [38]. As an example, Yang et al. [130] reported the expression profiling of 20 genes from *Arabidopsis thaliana* using Luminex suspension microbead array system. The total hybridization assay time was only ~1 hr which was much shorter than the time required for conventional Affymetrix cDNA microarrays (~16 hrs [131]). Besides the expression profiling, the Luminex suspension microparticle-based DNA microarray was also employed for the detection of single nucleotide polymorphisms (SNPs) [132], the detection of genetic disease [133] and microbial detection [134]. The advantage of the Luminex platform is its high flexibility as the microparticles were commercially available and can be attached with desired oligonucleotide probes by the customer themselves. However, the limitation for Luminex suspension microparticle DNA microarray platform is the low multiplexing capability which only allows the

simultaneous detection of 100 different target DNA/RNAs which could be not enough for genome level analysis.

Illumina Inc. developed two platforms for the microparticle-based multiplexed DNA hybridization assays, named Sentrix Array Matrix and Sentrix Beadchip [8]. The Sentrix Assay Matrix integrated etched fiber optical bundles into 96-well plates while Sentrix Beadchip utilized etched microwell chip on a silicon substrate. Both platforms allow the microparticles to be stably immobilized and encoded after the array assembly as discussed in session **2.3.4** and the fluorescence detection were also employed. These platforms have been applied for gene expression profiling [135], SNP detection [6] and epigenetic profiling [136]. Compared to Luminex suspension microparticle array, Illumina platforms have higher multiplexing (>1000 [135]). However, the Illumina microparticle arrays are less flexible to be customized by customer themselves.

Although these two companies have developed matured microparticle array technology for high-throughput multiplexed DNA analysis, the cost of the specialized instruments is high. Thus, other cost-effective microparticle array platforms have been developed for low to mid multiplexing DNA hybridization assays which also found their application in scientific research. As an example, Ali et al. [9] developed microbead array assembled on etched silicon microwells chips which was integrated into a flow chamber system for automatic delivery of DNA samples. The hybridization assay time was only 10 min which is much less than the time needed for the commercial systems. As an alternative, Wen et al. [34] reported the integration of microbead array into microfluidic device for the multiple gene expression detection. Each microparticle was separated from each other in microfluidic chambers. The hybridization time with this microfluidic microparticle array was only 20 min while

the sample volume was reduced to 2 μl. The same platform has been altered for the detection of single nucleotide mismatch [137] and cancer gene detection [138]. Another cost-effective platform was reported by Ng et al. who employed simple-fabricated gel pad array chip for the assembly of microparticle array for the multiplexed discrimination of bacteria species [5] as well as the diagnosis of genetic disease [139]. While the cost of the chip was very low, the DNA hybridization assays can be done within 10 min on this platform.

2.4.2 Immunoassays

The first microparticle-based biochemical assay was the latex agglutination test which was based on the agglutination of antibody-coated latex microparticles in the presence of the antigens and it was the primitive format of the modern immunoassays [3]. Once being integrated into microarray format, microparticle-based immunoassay enables the multiplexed detection of target antigens as well as fast reaction time, thus possessing superiority over conventional enzyme-linked immunosorbant assay (ELISA) which is currently the immunoassay gold standard. Various microparticle array platforms have been developed for immunoassays.

A widely used microparticle array platform for immunoassay is the Luminex xMAP suspension platform which employed 100 different dual-color coded microparticles for multiplexed immunoassays [50]. The immunoassay could be done in conventional 96-well plate while the decoding of microparticles is through flow cytometer with two laser source, one to simultaneously excite the two encoding dyes, one to excite the reporting dye conjugated to the detection antibodies. As different antibodies can be conjugated to the microparticles, this platform has been used for the quantitative

detection of various panels of analytes such as cytokines [140], tumor markers [14], antibodies [141] and toxins [142]. Nevertheless, for such a commercialized system, the expensive dedicated flow cytometer could not be cost-effective for low to mid multiplexed immunoassays and the 100 multiplexing capability is not enough for proteomic research.

Another commercialized microparticle array platform for immunoassay is the "Veracode" platform developed by Illumina Inc. [77]. This platform employs cylindrical glass microparticles encoded with holographic barcodes for multiplexing immunoassay. An automated workstation serves to suck the microparticle solution from a 96-well plate after the sandwich fluorescence immunoassay reaction and to align the microparticles into a groove plate for fluorescence detection. The decoding and detection are through the scanning of each microparticle with two laser beams, one for the barcode recognition, one for the reporter dye excitation. Theoretically unlimited number of codes can be generated with 24-bit of barcodes and the multiplexing capability could be very high in this platform.

For most non-commercialized platforms, the multiplexed immunoassays were usually done with encoded antibody-coated microparticles immobilized in certain microstrcutures, such as the etched wells on optical fiber bundles [10] or on silicon wafer [59, 80], hot-embossed wells on polymer substrate [28] and into the microchambers in a microfluidic system [12]. Another strategy is the use of different channels to separate antibody-coated microbeads as described by Sivagnanam et al. [33]. One special microarray made with clusters of antibody-coated microbeads immobilized in alginate gel matrix was recently introduced by Li et al. [11]. The pore size of the alginate gel is small enough to trap 1 μm microparticles inside while it is

also bigger enough for the free diffusion of antigens and detection antibodies. With this microarray, LODs in the range of pg/ml for 6 different protein analytes were achieved with the assay time of 3 hrs. Similar strategy was also employed by Ikami et al. [143] who fabricated antibody-coated microparticle cluster arrays inside flow channels by spatially controlled photopolymerization of polymer solutions containing microparticles. Multiplexed detection of three protein markers with LODs at sub-nanogram per microliter was achieved with the total assay time <10 min. This microparticle-based multiplexed and high throughput (simultaneously ~24 assays) immunoassay platform could be very promising for point-of-care diagnostics.

While all the above platforms directly relate the signal intensities of microparticles with the concentration of analytes for quantitative immunoassay, Rissin et al. [46] developed microparticle-based novel "Digital Immunoassay" platform which relates the concentration of analyte with the ratio of fluorescent microparticles to all microparticles arrayed on etched optical fiber wells. This platform works based on the principle that when the target analyte concentration is extremely low so that the number of analyte molecules is less or comparable to the number of the antibody-coated microparticles, the percentage of microparticles that can capture one analyte molecule follows Possion distribution [144]. After a sandwich immunoassay and the attachment of a secondary enzyme-conjugated antibody, the percentage of microparticles bound with at least one analyte molecule can be visualized by converting a non-fluorescent substrate into fluorescent signals in each microwell through enzymatic reactions. The great advantage of this method is the capability to detect sub-femtomolar of antigens (theoretically, one molecule) which is not possible for other microparticle-based immunoassays or conventional ELISA method. This platform was applied for the analysis of serum prostate specific antigen (PSA) level for

prostate cancer recurrence monitoring [13] and was later integrated into a polymeric disc device which allowed the simultaneous analysis of 24 samples [145]. Despite the obvious advantage of this microparticle array platform, its inability for multiplexed immunoassay could be a limitation and thus it requires further optimization.

2.5 Autonomous microfluidic capillary system

In conventional microfluidic biochemical assay systems, external pumps such as peristaltic pumps and syringe pumps are employed to drive the flow through the microchannels. These external pumps serve to control the flow rate thus providing both appropriate flow conditions for the assay and consistent flow conditions for the reproducibility of the results. However, external pumps are usually bulky and require electric power sources which increasing the complexity of the analysis system.

Several passive pumping techniques have been developed to replace the external pumps in microfluidics, such as pumping by absorbance of air in pre-vacuumed PDMS microchannels [35, 146], pumping by chemically generated oxygen in sealed chamber [37] and pumping by autonomous microfluidic capillary system [36]. Among all these techniques, the autonomous microfluidic capillary system could be the most widely used method for external-pump-free delivery of liquid in microchannels. The following section will review the principle of the microfluidic capillary system as well as its state-of-the-art applications in biochemical assays, especially in immunoassays.

2.5.1 Working principle of microfluidic capillary system

An autonomous microfluidic capillary system employs wettable microchannels as well as geometries in microchannels to guide the fluid through capillary actions. It is originated from the conventional lateral flow test which employs a porous membrane as well as filter papers to provide the capillary pressure to drive the fluid. **Figure 2.5** demonstrates a typical microfluidic capillary system fabricated in silicon [147] which contains loading elements, capillary retention valve (CRV), flow resistance and the capillary pump. In such a microfluidic capillary system, the flow rate of the fluid was determined by the following equation [36]:

$$Q = \frac{1}{\eta}\frac{\Delta P_c}{R_F} \qquad \textbf{Equation 2.1}$$

Where Q is the flow rate, ΔP_c is the difference of capillary pressure between the two flow fronts (advancing and receding fronts), R_F is the flow resistance of the channel and η is the viscosity of the flow. For liquid in a closed rectangular microchannel, P_c can be calculated by [148]:

$$P_c = -\gamma\left(\frac{\cos\alpha_b + \cos\alpha_t}{d} + \frac{\cos\alpha_l + \cos\alpha_r}{w}\right) \qquad \textbf{Equation 2.2}$$

Where γ is the surface tension of the liquid, $\alpha_{b,t,l,r}$ are the contact angles of liquid on the bottom, top, left and right surfaces of the channel, d and w are depth and width of the microchannel.

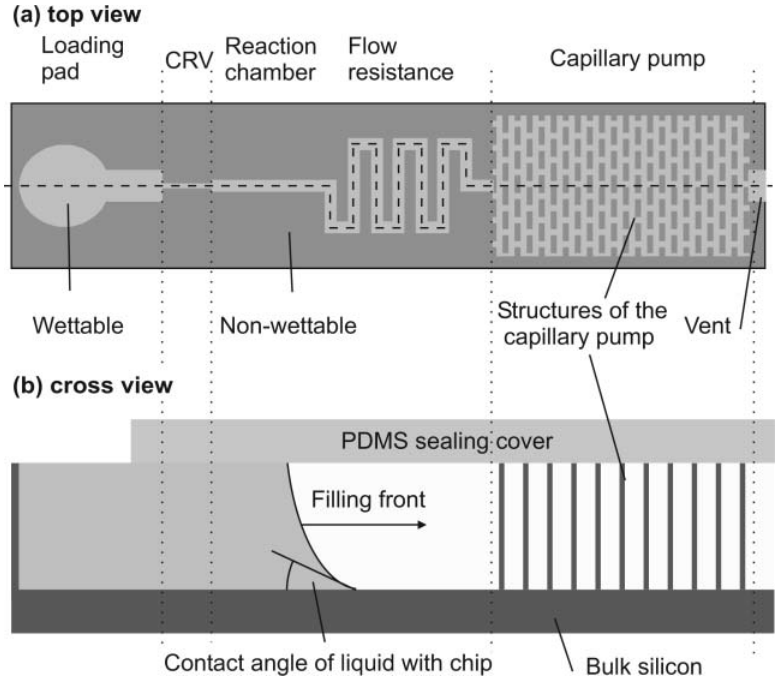

Figure 2.5 A typical microfluidic capillary system. (a) Top view. (b) Cross view (From [147]).

The R_F of the capillary system is usually accumulated with the length of the channel. For a rectangular microchannel, R_F can be approximated by the equations below as described by Delamarche et al. [147, 148]:

When $w < d$:

$$R_F = \left[\frac{1}{12} \frac{(d+w)^2}{d^2} \left(1 - \frac{1}{8} \frac{w}{d} \right) \frac{dwr_H^2}{L} \right]^{-1} \qquad \textbf{Equation 2.3}$$

When $w > d$:

$$R_F = \left[\frac{1}{12} \left(1 + \frac{5d}{6w} \right) \frac{dwr_H^2}{L} \right]^{-1} \qquad \textbf{Equation 2.4}$$

Where d and w are depth and width of the microchannel, r_H is the hydraulic radius of the microchannel which equals to $dw/(d+w)$, L is the length of the microchannel.

In a typical capillary system as shown in **Figure 2.5**, when liquid is added into the loading pad, which is open to air, the capillary pressure of the microchannel enables the gradual introduction of liquid into the microchannel. The downstream capillary pump element contains microstructures to provide suitable capillary pressure as well as to provide enough volume for reagents, while the flow resistance of the system is mainly determined by the thin and long microchannel in the middle. The CRV region has the highest capillary pressure in the entire system and it thus can act as a valve to prevent the drying out of the liquid in the downstream reaction chamber [36]. The flow rate in such a capillary system can be programed by: (1) alternation of the geometry of the microstructure in the capillary pump (change of capillary pressure); (2) alternation of the wettability of the microchannel surfaces (change of capillary pressure); (3) alternation of the length of the flow resistor. (1) and (3) can be achieved simply by changing the design of the microfluidic system while (2) can be achieved by altering the material as well as the surface modification method of microchannels.

2.5.2 Fabrication of microfluidic capillary system

As mentioned above, the liquid flow rate in a capillary system is determined by both the geometry of the microstructures in microchannels and the wettability of the channel surface. Thus, the two key processes during the fabrication of the microfluidic capillary system are the microfabrication of microstructures and the surface modification.

The microfabrication process of microstructures for capillary systems is entirely compatible with conventional microfabrication process. A research group at IBM

Research Lab - Zurich fabricated capillary systems on silicon wafers using standard photolithography and deep reactive ion etching (DRIE) to generate microchannels and microstructures [36, 147, 149-151]. The advantage for silicon substrate is obvious as the dimension of the microstructures can be precisely controlled and the silicon surface is compatible with various surface modification process. However, the tedious fabrication steps (8 steps [150]) could be a major concern. Alternatively, Åmic AB, a Swedish bio-company, fabricated a capillary pump system with a cyclo-olefin copolymer (COC) substrate by either injection molding [152] or hot embossing [153] which both involve only one-step fabrication processes. The simplified fabrication process enabled the company to massively produce the capillary pump chips. Another prevailing microfabrication method, soft-lithography, was also employed for the fabrication of capillary system as it requires no expensive equipment and is thus more applicable to common biolabs. Several research groups reported the fabrication of capillary system with PDMS using soft-lithography [154-156].

As the capillary system employs hydrophilic surfaces to generate capillary pressures, it is required for the stable hydrophilic modification of the microstructure surfaces, especially for hydrophobic surfaces. Moreover, when being applied for the biochemical assays, the capillary system should also be surface modified with biocompatible materials which should also not generate strong interfering background signals after the assays. Juncker et al. [36] modified the silicon chip based capillary system sequentially with gold and thiolated poly(ethylene glycol) to render a hydrophilic and protein repellent surface for the application in immunoassay. This method was later simplified by direct immersing of the silicon chip into poly(ethylene oxide) solution (Pluronic® F108) which has the similar properties as PEG [149]. Åmic AB employed a silane-dextran chemistry to modify the COC based capillary system

which turned the surface contact angle of COC from 90° to 30° [152]. The coupled dextran molecules not only provided a stable hydrophilic surface (contact angle stable for 2 months) but also enabled the coupling with capture antibodies through Schiff base reaction for immunoassays. For PDMS based capillary system, the most popular surface modification method is oxygen plasma treatment [155]. However, the plasma treated PDMS recovers its hydrophobicity quickly in ambient conditions [157] and cannot maintain long term stable hydrophilicity. As an improvement, Lillehoj et al. [154] coated PEG onto plasma treated PDMS by simple heating, resulting in a stable and hydrophilic surface on PDMS based capillary system. With a different approach, Thorslund et al. [158] coated a heparin layer onto the PDMS to generate a hydrophilic and bioactive surface. The heparin moieties on the surface can be further linked with avidin to be coupled to biotinylated reagents for bioassays [156]. Despite the availability of these surface modification methods and the simple soft-lithographical molding process, PDMS itself is not an ideal material for the fabrication of capillary systems due to its intrinsic hydrophobic property. As a substitute material to PDMS, Norland Optical Adhesives (NOA) has been used for the fabrication of capillary systems [159-161]. NOA based microstructures can be fabricated by UV curing against a PDMS coated silicon mold (to prevent the adhesion between NOA and silicon surface) or a PDMS mold. The cured NOA has a native hydrophilic surface (contact angle ~67° [159]) and its surface can be further treated with oxygen plasma to generate even more hydrophilic surface (contact angle ~40° [159]) with long term stability. Thus, capillary system fabricated in NOA could require no further surface modification process [161] for the generation of capillary pressure which could greatly reduce the entire production time.

2.5.3 Capillary system for biochemical assays

The most prominent advantage of a capillary system over a conventional microfluidic system for biochemical assays is the autonomous delivery of samples and reagents with programmable flow rate of liquid without the need of bulky pumps and energy sources. Thus, the capillary system is more suitable for point-of-care assay applications which require a simple set-up with minimal manual assay steps.

So far, the most important application of capillary system is for the autonomous immunoassays as enlightened by conventional lateral flow test [162]. In a pioneer research, Juncker et al. [36] fabricated a silicon based capillary system for the immunoassay of C-reactive protein (CRP). The immunoassay was done with sequential introduction of reagents with a total reagent volume of only 3 μl and an assay time of 25 min. A similar capillary system was later integrated with micromosaic immunoassay for the detection of tumor necrosis factor-α (TNF-α) with a sensitivity of 20 pg/ml [163]. This silicon capillary system was further advanced by integrating all the immunoassay reagents (capture and detection antibodies) and blood filtering element into the system which enabled a one-step immunoassay for the detection of cardiac marker with merely 5 μl of the whole blood sample (**Figure 2.6**) [149]. Besides the silicon based capillary system, Åmic AB developed COC based "4castchip®" for the one-step lateral flow immunoassay of CRP [152]. The chip consists of a sample zone, a detection zone and a wicking zone which resemble to the sample pad, the detection line and the suction pad in a lateral flow test strip. All these three zones contained thousands of hydrophilically modified micropillars for the delivery of the sample fluid. While all the above capillary systems only allowed the detection of one

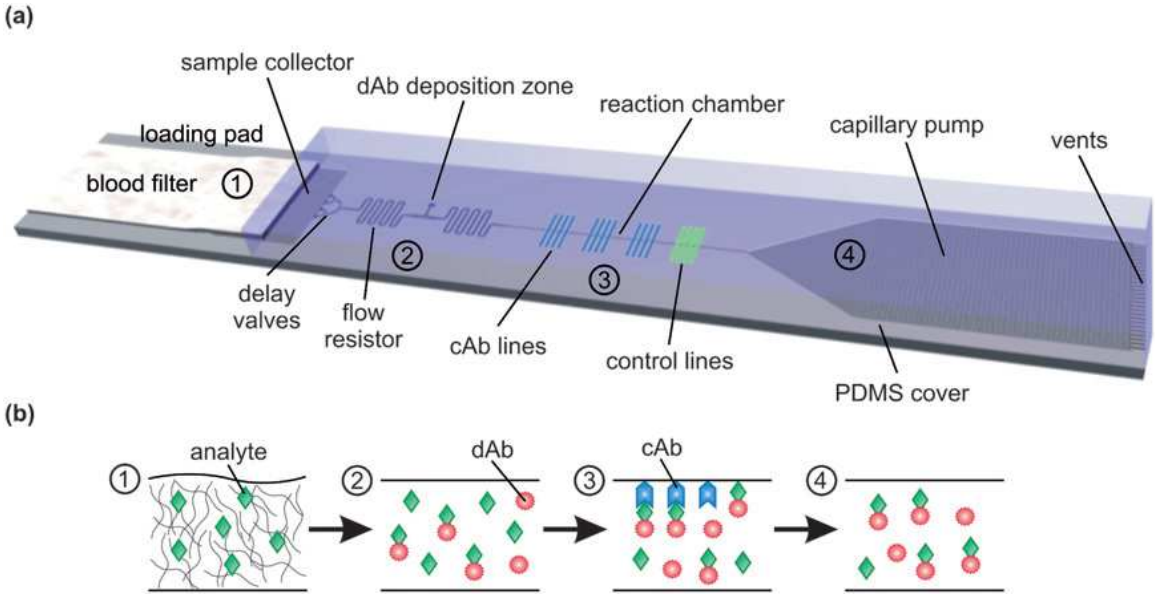

Figure 2.6 A capillary system chip for one-step lateral flow immunoassay. (a) The design of the chip. (b) The position and interaction of analytes with detection and capture antibodies (dAb and cAb) along different part of the chip (From [149]).

antigen, Wang et al. [161] developed a NOA 63 and glass hybrid chip which can simultaneous detect 11 different proteins from the whole blood in a one-step immunoassay. The site specific immobilization of 11 different antibodies was achieved through the hybridization binding between the surface patterned oligonucleotides to the antibodies conjugated with complementary oligonucleotides [164]. The capillary pressure was generated by the hydrophilic surface of glass and NOA 63 as well as the downstream filter papers.

In addition to the immunoassay, capillary systems were also utilized to other biochemical assays. Hitzbleck et al. [165] recently reported the detection of DNA target from PCR product within a capillary system which was integrated with external heating element for the melting of the DNA and hybridization of target DNA with the oligonucleotide probe. The reaction time was controlled by a capillary soft valve which can be manually pressed to allow the reaction mixture to flow through to the

downstream detection zone by capillary pressure. Dudek et al. [153] developed a capillary system to measure human plasma fibrinogen based on the Åmic 4castchip®. Once the plasma was introduced, the thrombin coated onto the chip converted the fibrinogen into fibrin and thus causing the clogging of the plasma and the stop of the flow. In principle, the distance of the plasma travelled on the chip, which is related to the clogging time, is inversely proportional to the concentration of fibrinogen. This chip allowed the measurement of fibrinogen in the physiological concentration range in human serum.

Chapter 3

Gel pad array chip for microbead-based immunoassay

Chapter 3 - Gel pad array chip for microbead-based immunoassay

3.1 Introduction

Microbead microarray technology has developed rapidly over the recent years and was utilized intensively in the bioanalysis field with applications such as genotyping [5, 8, 166], biomarker detection [10, 47, 167] and pathogen detection [168, 169]. Compared to a conventional microarray based on microspots of bioprobes immobilized on a planar surface, the microbeads allow more bioprobes to be immobilized per unit of area, while they also accelerate the binding kinetics of the biomolecules to the bioprobes [4]. Thus, the incorporation of microparticles into microarrays enables faster and more sensitive biomolecule detection than conventional planar microarrays.

Except the suspension microbead microarray which uses microbeads suspended in a liquid [38, 50], the majority of state-of-the-art microbead microarrays requires immobilization and assembly of microbeads onto certain substrates. However, the high mobility of the minute microbeads makes the immobilization of microbeads challenging. One of the widely used methods for stable microbead immobilization is the physical confinement method [9, 16, 26, 28-30, 70]. The physical confinement method, which employs certain microstructures to constrain the microbeads, is a straightforward approach to assemble microbeads as the immobilization is not dependent on the surface chemistry of the microbeads and no external manipulation, such as magnetic force or an electric field, is required. The fabrication methods for

these microstructures depend on the substrate material used. With the well-developed fabrication methods from the semiconductor industry, a number of research groups fabricated silicon based microstructures for the assembly of microbead arrays [16, 21, 26, 170]. While the standard semiconductor fabrication processes provide precise control on the shape and dimension of silicon based microstructures, these fabrication processes, which usually involve photolithography and etching, are laborious and require specialized cleanroom facilities, expensive equipment as well as intensively trained professionals. An alternative to silicon based substrates is fiber optic bundles [15]. Well-ordered micrometer-sized wells can be etched out on the distal end of a fiber optical bundle [70], thus providing cavities for microbead immobilization. However, a slight concern of the customized optical fiber bundles as well as silicon substrate is the high cost of material. Recently, several groups reported the fabrication of microstructures for microbead assembly with polymeric materials such as cyclic olefin copolymer (COC) [28, 145], optical epoxy resin [29] and PDMS [17, 30]. These polymeric microstructures provide stable immobilization for microbeads while greatly reducing the fabrication cost.

Another polymeric microstructure for the assembly of microbead arrays is the gel based microstructure which was reported recently [5]. As reported, polyacrylamide gel based micropad arrays (gel pad arrays) was used for the assembly of polystyrene microbead arrays. These gel micropads was fabricated by the UV photopolymerization of polyacrylamide prepolymer though a photomask [171]. Neither cleanroom facilities nor expensive and sophisticated equipment is needed for fabrication. Furthermore, the fabrication of gel pad arrays requires no pre-fabricated molds or masters as compared to the fabrication processes for other polymeric microstructures used in microbead array assembly, such as hot embossing [28], injection molding [145] and soft-

lithography [30]. Nevertheless, current application for the microbead array assembled on gel pad array is only limited to the semi-quantitative DNA based analysis [5, 139]. The potential application of the gel pad array for the assembly of biofunctionalized microbead for sensitive and quantitative bioassays, specifically, immunoassays, is not explored yet. One obstacle towards employing gel pad array in microbeads-based quantitative immunoassay could be the autofluorescence of the polyacrylamide gel polymerized using methylene blue as the photoinitiator [172], which could decrease the sensitivity of the assay.

In this chapter, a novel gel pad array chip is developed which was employed for sensitive and quantitative microbeads based immunoassays to detect protein markers from 1 μl of serum sample. In detail, firstly, the great reduction of autofluorescence of gel pad array is demonstrated by using non-fluorescent 2,2-dimethoxy-2-phenylaceto-phenone (DMPA) instead of strongly fluorescent methylene blue as the photoinitiator for the photopolymerization of polyacrylamide gel. Secondly, novel PEG based micropillar rings are integrated to the chip to serve as hydrophilic microbarriers for the containment of multiple samples. Next, on-chip immunoassays for two model protein markers, prostate specific antigen (PSA) and human chorionic gonadotropin (hCG), are demonstrated. The reproducibility of the on-chip immunoassay, the stability of microbeads on the gel pad array and the reusability of the chip are also discussed. Subsequently, we demonstrate the on–chip multiplexed immunoassay for simultaneous detection of two protein markers by using spatially encoded microbeads. Lastly, the preliminary result is presented for the simultaneous on-chip detection of protein and DNA.

3.2 Materials and methods

3.2.1 Materials and reagents

Microscopic glass slides were purchased from Corning. Polymer spacers were purchased from Specac. Sodalime glass chrome masks were all purchased from Infinite Graphic. NAP™ 5 columns were purchased from GE Healthcare. Streptavidin-coated polystyrene microbeads (~10 μm in diameter) were purchased from Bangs Laboratory. Acrylamide/Bis-acrylamide solution (40%, 19:1), Poly(ethylene glycol) diacrylate (PEG-DA, Mw 575 Da), bovine serum albumin (BSA), N,N,N',N'-Tetramethylethylenediamine (TEMED), 3-(Trichlorosilyl) propyl methacrylate (TPM), Tween® 20, (+)-Biotin N-hydroxysuccinimide ester (biotin-NHS), 2,2-dimethoxy-2-phenylaceto-phenone (DMPA), toluene, heptane, methylene blue and recombinant hCG were purchased from Sigma-Aldrich. Repel silane (Dimethyldichlorosilane, 2% solution in octamethylcyclotetrasiloxane) was purchased from GE healthcare. Ethanol was purchased from Fisher Chemicals. Dimethyl Sulfoxide (DMSO) was purchased from MP Biomedicals. PBS was purchased from 1st Base. Alexa Fluor 594 NHS ester and fetal bovine serum (FBS) were purchased from Invitrogen. PSA, monoclonal anti-PSA clone 5 antibody, monoclonal anti-PSA clone 7 antibody, monoclonal anti-β-hCG clone 1 antibody and polyclonal goat anti-whole hCG antibody were purchased from Arista Biologicals. Biotinylated oligonucleotide (seq. 5' biotin-TCACATTTTGGATAATCCCAACC) and Texas Red labelled oligonucleotide (seq. 5' Texas Red-GGTTGGGATTATCCAAAATGTGA) were purchased from Proligo, Sigma. Deionized water was produced by Arium® 611 UV system (Sartorius AG, Go).

3.2.2 The fabrication of gel pad array chip

3.2.2.1 The chip design

The gel pad array chips were fabricated on a microscopic glass slide with the dimension of 75 mm (L) x 25 mm (W) x 1 mm (H). The design of the masks was done in AutoCAD software (Autodesk). The design of the masks allowed the fabrication of 40 polyacrylamide gel pad array units (**Figure 3.1a**) and 40 PEG based micropillar rings (**Figure 3.1b**). The distance between two gel pad array units and two micropillar rings were all set to be 4.5 mm so as to be identical with the distance between the two wells on a conventional 384-wells plate, thus making the chip compatible with commercialized multi-channel micropipettes. Feature for each gel pad array unit contains 17 x 17 square gel pads (20 μm x 20 μm) with 10 μm gap (**Figure 3.1a**). Feature for each micropillar ring contains polar array of 20 circles (200 μm in diameter) with the total diameter of the array of 2 mm (**Figure 3.1b**). The entire features on the mask design cover an area of approximately 40.5 mm x 13.5 mm which fits well onto a microscopic glass slide.

3.2.2.2 Fabrication Process

The fabrication process of the gel pad array chip consists of three steps:

(1) Surface modification of the glass slides.

The glass slides were sequentially cleaned with ethanol, detergent and deionized water. They were then treated with 30% H_2O_2 for 30 min. These glass slides were subsequently treated with 5 mM TPM solution (4:1 heptane and chloroform [120]) for 30 min. The silanized glass slides were cleaned with ethanol and deionized water before being stored in a clean microscopic slide storage box.

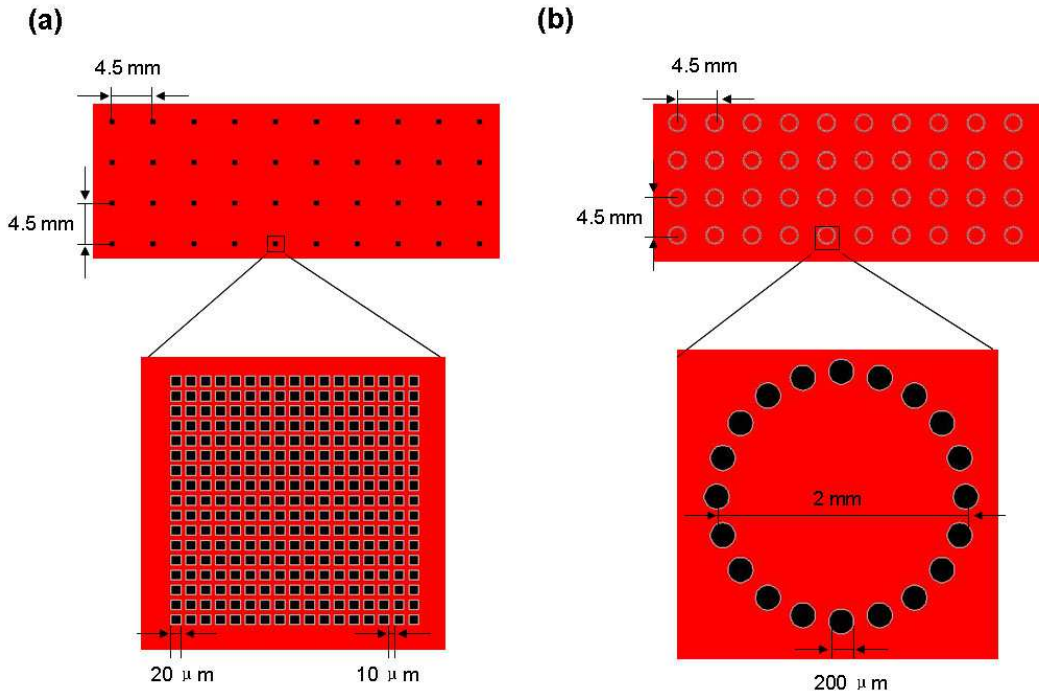

Figure 3.1 The mask design for gel pad array chip. Red area is chrome coated and black area is kept clear. (a) The design for polyacrylamide gel pad array units. Top: an array of gel pad array units. Bottom: a single gel pad array unit; (b) The design for PEG based micropillar-rings array. Top: an array of micropillar-ring. Bottom: a single micropillar-ring.

(2) Fabrication of polyacrylamide gel pad array units through photopolymerization.

The mask with features of gel pad array units was pre-treated with Repel Silane for 15 min to prevent the attachment of polyacrylamide gel. Next, a 10% acrylamide/bisacrylamide precursor solution doped with 0.02% (w/v) DMPA and 1.2% (v/v) TEMED was transferred into the gap between the photomask and a TPM treated glass slides through capillary action. The height of the gap is defined by a pair of 12 μm mylar spacers. The solution was then UV exposed under a fluorescence microscope equipped with a mercury lamp, a 4X magnification lens and a DAPI filter (350 nm excitation). The power of the UV light was ~150 mW/cm^2. Each gel pad array unit was exposed for 1 min which made the total fabrication time of ~40 min. The

glass slide with patterned gel pad array was then detached from the mask and washed with ethanol and deionized water.

(3) Fabrication of PEG micropillar-ring array through photopolymerization.

The mask with features of micropillar-ring array was pre-treated with Repel Silane for 15 min to prevent the attachment of PEG. The mask was then aligned to the glass slide with gel pad array under microscope to make sure each array unit was in the center of each micropillar ring. A pair of 150 μm Teflon spacers was used to define the height of the gap between mask and the glass slide. The mask-spacers-slide apparatus was then clamped from the side to prevent movement. Subsequently, pure PEG-DA pre-dissolved with 1.5% (w/v) DMPA was transferred into the gap by capillary action. The apparatus was then put into a UV crosslinker (365 nm excitation; power of ~4 mW/cm^2) and exposed for 6 s. The glass slide with both gel pad array and micropillar ring array was then detached from the mask, washed with ethanol and deionized water. The fabricated gel pad array chip was stored in a clean petri-dish and sealed with parafilm.

The schematic fabrication process was shown in **Scheme 3.1**. The silanization and photopolymerization chemistry are shown in **Scheme 3.2**. The fabricated gel pad array chip is shown in **Figure 3.2**. It contains 40 gel pad array units segregated by the PEG micropillar rings. The current chip is designed for the sample volume of 1 μl and the sample volume can be altered by change the size of the micropillar ring by masks with different designs.

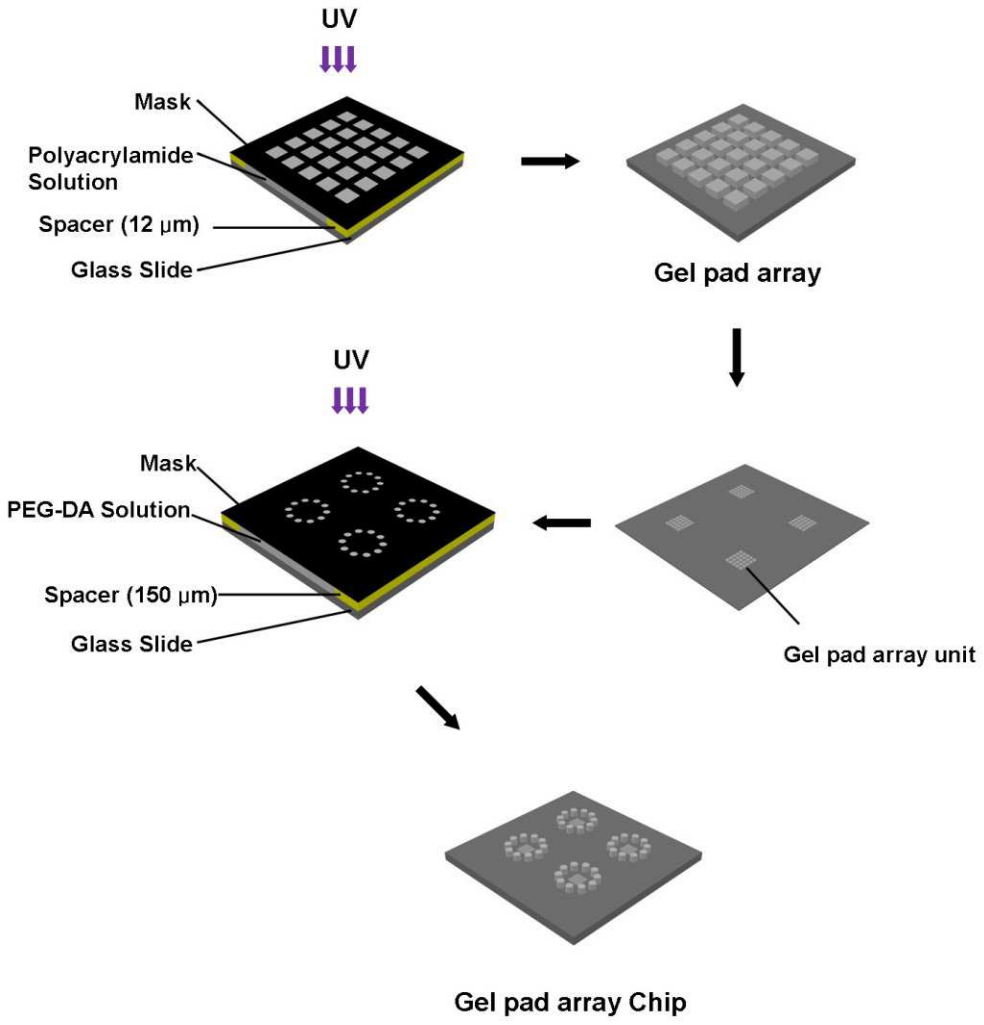

Scheme 3.1 Schematic diagram of the fabrication process of gel pad array chip.

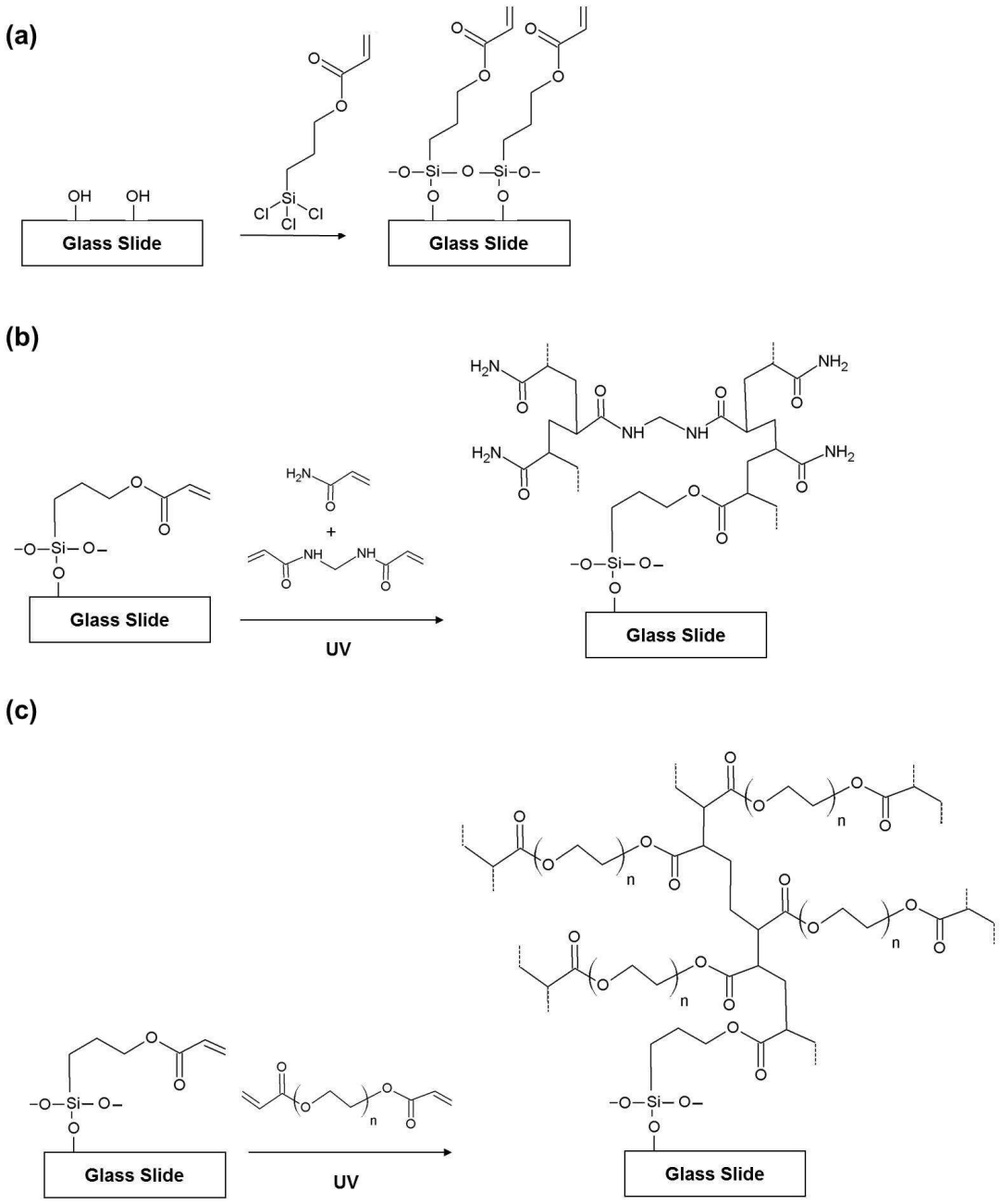

Scheme 3.2 The silanization and photopolymerization chemistry. (a) The surface silanization of glass slide with TPM. (b) The photopolymerization of acrylamide prepolymer on the TPM treated glass slide. (c) The photopolymerization of PEG-DA on the TPM treated glass slide.

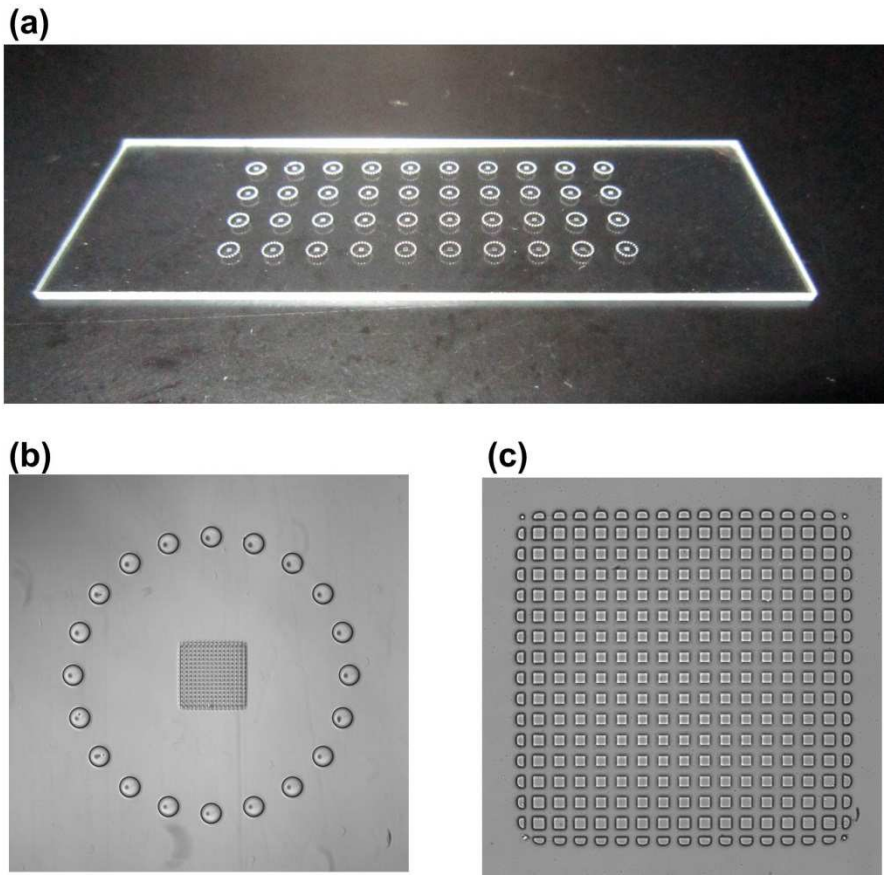

Figure 3.2 Gel pad array chip. (a) Overview. (b) A gel pad array unit with PEG micropillar ring around. (c) The gel pad array unit.

3.2.3 Preparation of antibody conjugates

Monoclonal anti-PSA clone 5 antibody and monoclonal anti-β-hCG clone 1 antibody were used as capture antibodies and were conjugated with biotin. The biotinylation was done using a modified method from a previous protocol [173]. A 10 mg/ml biotin-NHS solution (in anhydrous DMSO) was added to the antibody solution (in PBS, with 0.2-0.5 mg of antibody and a concentration > 1 mg/ml) with 10:1 molar ratio of biotin-NHS to antibody. The mixture was gently shaked at RT for 2 hrs. The biotinylated antibody was separated and purified by using NAP™ 25 columns. The concentration of the biotinylated antibody was determined by using a UV2450 spectrophotometer (Shimadzu). The biotinylated antibody solution was aliquoted and stored in -20 °C.

Monoclonal anti-PSA clone 7 antibody and polyclonal goat anti-whole hCG antibody were used as detection antibody and were conjugated with Alexa Fluor 594. A 1 mg/ml Alexa Fluor 594-NHS solution (in anhydrous DMSO) was added to the antibody solution (in PBS, with 0.2-0.5 mg of antibody and concentration >1 mg/ml) with 10:1 molar ratio of dye to antibody. The mixture was gently shaked in a dark chamber at RT for 2 hrs. The Alexa Fluor 594 conjugated antibody was separated and purified by using NAP™ 25 columns. The absorbance of the Alexa Fluor 594 antibody was measured by using a UV2450 spectrophotometer (Shimadzu). The concentration of the antibody-dye conjugate was estimated based on the equation below as suggested by the manufacturer:

$$\text{Antibody concentration (M)} = \frac{[A_{280} - A_{590} \times 0.56]}{203,000} \times \text{dilution factor} \qquad \textbf{Equation 3.1}$$

3.2.4 Preparation of biofunctionalized microbeads

Streptavdin-coated microbeads (~18000 beads/μl) were washed twice with PBS-B-T (1X PBS, 1% BSA, 0.05% Tween® 20) and re-suspended in the same volume of PBS-B-T as the stock solution. The microbeads solution was then mixed with equal volume of biotinylated antibody solution with the final antibody concentration of 0.1 mg/ml. The mixture was incubated at RT for 2 hrs. The microbeads were then washed with PBS-B-T for 5 times before being re-suspended in PBS and stored at 4°C.

Oligonucleotide-coated microbeads were prepared as below. Streptavdin-coated microbeads (~18000 beads/μl) were washed twice with TE buffer (10 mM Tris, 1 mM EDTA, pH 8.0) and re-suspended in the same volume of TE buffer as the stock

solution. The microbeads solution was then mixed with an equal volume of biotinylated oligonucleotide with the final oligonucleotide concentration of 10 μM. The mixture was incubated at RT for 2 hrs. The microbeads were then washed with TE buffer for 5 times before being re-suspended in TE buffer and stored at 4 °C.

3.2.5 Contact angle measurement

The surface hydrophilicity of TPM treated glass slides and polymerized PEG film was characterized by using contact angle measurement. The polymerized PEG film (150 μm thick) was fabricated in the same way as the fabrication for PEG micropillar-ring array mentioned in section **3.2.2** except that a Repel Silane treated glass slide rather than a mask was used. The contact angle was measured using the static sessile drop method with a goniometer (VCA Optima surface analysis system, AST Products Inc.). Droplet volume of 0.5 μl and a stabilizing time of 10s were used for all the measurements.

3.2.6 On-chip microbead-based immunoassay

The on-chip microbead-based immunoassay was done in the format of a fluorescence sandwich immunoassay (**Scheme 3.3**).

For the single-plexed immunoassay for hCG and PSA, the density of the antibody-coated microbeads in the solution was first adjusted to ~500 beads/μl. 0.1 μl of microbeads solution was applied to each gel pad array unit. The deposition of

microbeads was achieved by evaporating away all the liquid at room temperature in ~2 min to affiliate the settlement of microbeads between gel pads. The chip was then washed with PBS from the side for 10 s to remove any microbeads which settled outside the gel pads array. After the chip was dried under nitrogen gas, 1 μl of each FBS sample with target analyte (PSA or hCG) was applied onto each gel pad array unit using a single-channel or multi-channel micropipette. The chip was then incubated at RT for 30 min in a home-made wet chamber (100% humidity). Subsequently, the chip was taken out of the wet chamber and rinsed with PBS-T (1X PBS, 0.05 % Tween® 20) for 10 s to remove majority of the sample. Next, the chip was put into a clean petri-dish filled with 20 ml of PBS-T and was rotated at 60 rpm for 10 min to completely remove the non-binding analyte. The chip was then rinsed with PBS and nitrogen gas dried. 1 μl of detection antibody in PBS was then applied onto the each gel pad array unit and was allowed to be incubated with the microbeads for 30 min in the wet chamber. The step to remove excess amount detection antibody is identical to the step for the removal of unbinding analyte. After the immunoassay, the chip was imaged by using a fluorescence microscope.

For the multiplexed immunoassay for the simultaneous detection of hCG and PSA, the density of the antibody-coated microbeads in the solution was first adjusted to ~200 beads/μl. Two batches of microbeads, anti-hCG and anti-PSA microbeads were sequentially arrayed onto the gel pad array employing the same deposition procedure for single-plexed assay. After deposition of first batch of microbeads, each array unit was imaged under microscope so as to record the spatial position for every microbead on hydrated gel pad array. The following immunoassay procedures were similar to that of the single-plexed immunoassay except that FBS samples were spiked with both

analytes (PSA and hCG) and the detection antibody solution contained Alexa Fluor labelled antibody for both analytes.

The summary of the on-chip immunoassay procedures was shown in **Table 3.1**.

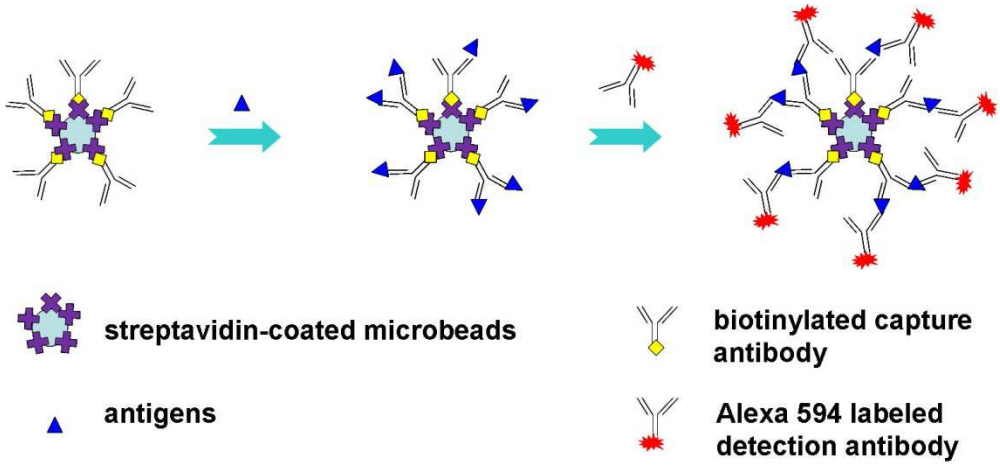

Scheme 3.3 Schematic diagram for fluorescence sandwich immunoassay.

Table 3.1 Immunoassy procedures on gel pad array chip

Procedures	**Time**	
	On-chip (Single-plexed)	**On-chip (Multiplexed)**
Immobilization of microbeads	2-3 min	2-3 min/batch
Imaging and spatial encoding	N/A	5 min/batch
Sample incubation	30 min	30 min
Washing	10 min	10 min
Detection antibody incubation	30 min	30 min
Washing	10 min	10 min
Total assay time	< 1.5 hrs	< 2 hrs (2 batches) < 3 hrs (10 batches)

3.2.7 Imaging and data analysis

All bright field and fluorescence images were taken by a CCD camera (Retiga 4000R, Qimaging) mounted on a BX41 Olympus fluorescence microscope (Olympus) equipped with a Texas Red filter (560 nm excitation, 595 nm dichroic mirror and 630 nm emission, Chroma Technology) and a mercury arc excitation source. The exposure time for immunofluorescence was kept at 4 s unless otherwise noted. The fluorescence intensity was measured by analyzing the pixel values of microparticles with Image J software (National Institutes of Health). The SEM images were recorded with a Supra 40 instrument (Carl Zeiss).

3.3 Results and Discussion

3.3.1 The gel pad array chip

3.3.1.1 Choice of the photoinitiator

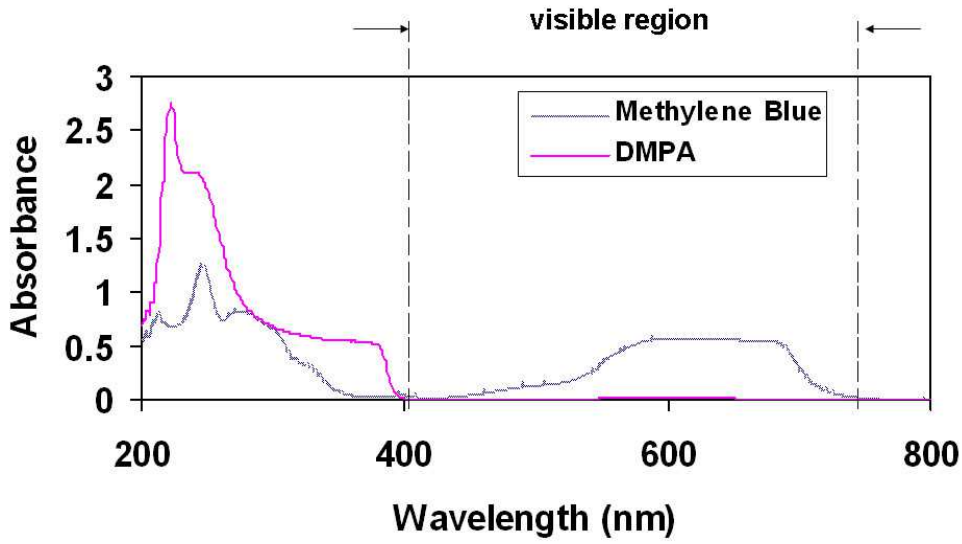

Figure 3.3 Spectra of methylene blue and DMPA. Concentration of methylene blue is 0.1 mM in water and concentration of DMPA is 0.1 M in ethanol.

The polyacrylamide gel pad arrays reported previously [5, 139] were all fabricated using methylene blue as the photoinitiator. One problem for methylene blue is its strong absorbance in the visible region. As shown in **Figure 3.3**, methylene blue has strong absorption from 500 nm to 700 nm while it also has slight absorption in the other region of the visible spectrum. The absorbance spectrum of methylene blue covers the excitation wavelength for almost all major fluorescence dyes for the labelling of bioprobes, for example, Cy3 (550 nm), Cy5 (650 nm), Cy 5.5 (675 nm), fluorescein (494 nm), Texas Red (590 nm), Alexa Fluor 488 (495 nm), Alexa Fluor 546 (556 nm), Alexa Fluor 594 (590 nm) and Alexa Fluor 647 (650 nm). Thus, the residue of methylene blue after the polymerization reaction could cause background fluorescence of the gel, which will limit the application of gel pad array chip for

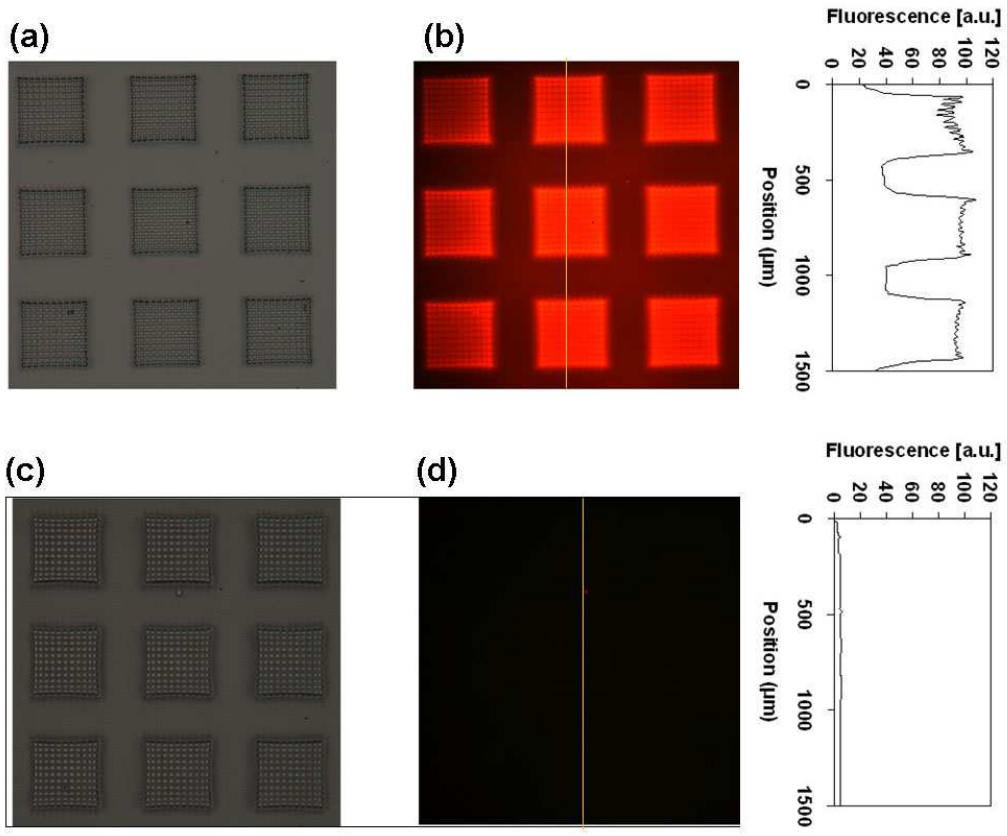

Figure 3.4 Comparison of the gel pad array made with different photoinitiator. (a) Array made with methylene blue. (b) Fluorescence image of (a). (c) Array made with DMPA. (d) Fluorescence image of (c). Both fluorescence images were taken with the same fluorescence microscope with same exposure time (4s). Fluorescence intensity on the yellow lines is shown in the right diagram.

sensitive and quantitative biochemical assays. Therefore, it is demanded to utilize a low autofluorescent photoinitiator to replace the methylene blue for the photopolymerization of polyacrylamide.

DMPA is a colorless photoinitiator which was reported to be used for the efficient photopolymerization of acrylamide [174, 175]. Unlike methylene blue, DMPA has almost zero absorption in the visible region as shown in **Figure 3.3**, thus making it an ideal non-fluorescent photoinitiator. The gel pad array made with DMPA showed much lower autofluorescence compared with the gel pad array made with methylene

blue as demonstrated in **Figure 3.4**. No change of the morphology of the gel pads was observed (**Figure 3.4c**). Based on these results, DMPA was used as the photoinitiator all over this work to substitute methylene blue.

3.3.1.2 PEG micropillar ring array

For high throughput microarray analysis, the microarray on the substrate should be separated by certain micro-barriers to form sub-arrays so as to simultaneously deal with multiple samples. A most commonly used substrate for sub-array fabrication is the conventional multi-well plate [10, 176-178]. Microwells on the plate serve as identical reaction chambers for the sample on each sub-array, thus ensuring reproducibility for biochemical assays. The sample volume for this kind of sub-arrays is usually >20 μl as determined by the volume of each well. The sample volume could be further reduced by fabricating miniaturized hydrophobic/hydrophilic micro-barriers for each sub-array. Current methods to define miniaturized barriers including photolithographical patterning of hydrophobic/hydrophilic SAMs [179], adhesion of teflon multi-hole tapes [180] and wax-pattern imprinting [181]. These methods define hydrophilic regions which are segregated by the hydrophobic regions on the substrate material to trap the sample liquid. Typically, 1 μl of sample volume is enough to perform a multiplexed biochemical assay on each sub-array.

To integrate certain microbarriers to separate each gel pad array unit on the glass chip, we employed a new approach using PEG-DA for the photo-patterning of hydrophilic microbarriers. There are several advantages for the use of PEG-DA as the patterning material:

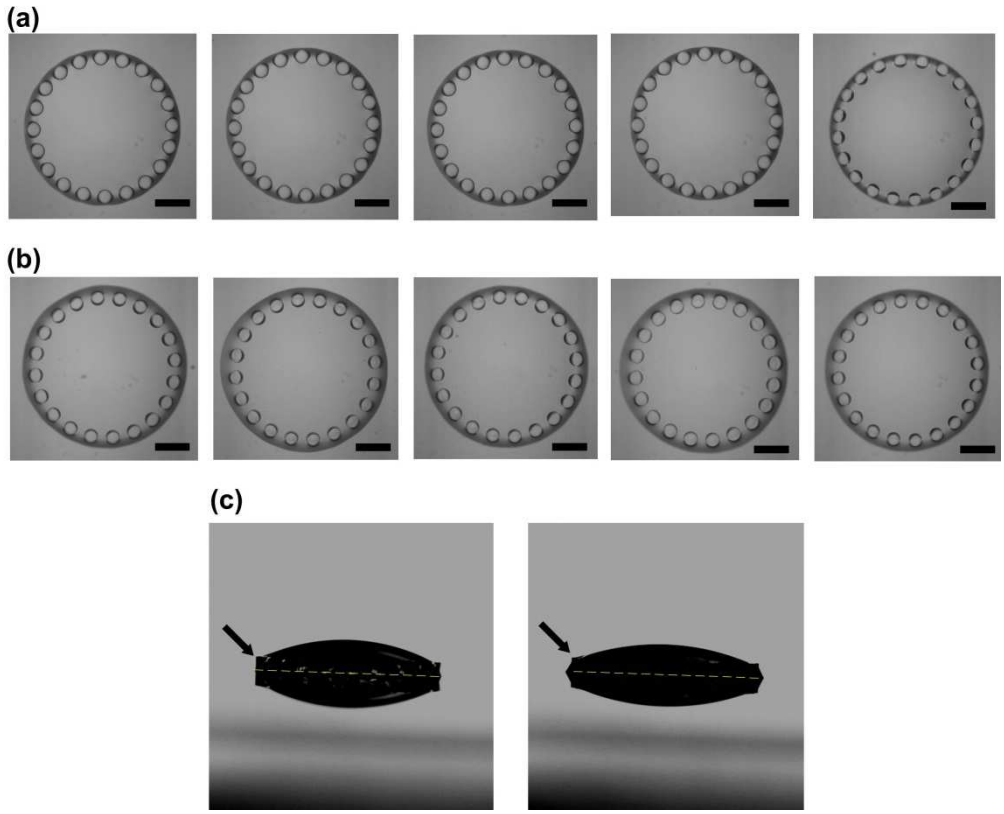

Figure 3.5 Entrapment of liquid inside PEG micropillar rings. (a) 1 μl of PBS buffer trapped in five different micropillar rings on the chip. (b) 1 μl of FBS trapped in five different micropillar rings on the chip. Scale bars represent 500 μm. (c) The side view of trapped liquid. Left: PBS. Right: FBS. The arrows indicate the edge of the PEG micropillars rings. Dashed lines indicate the glass surface.

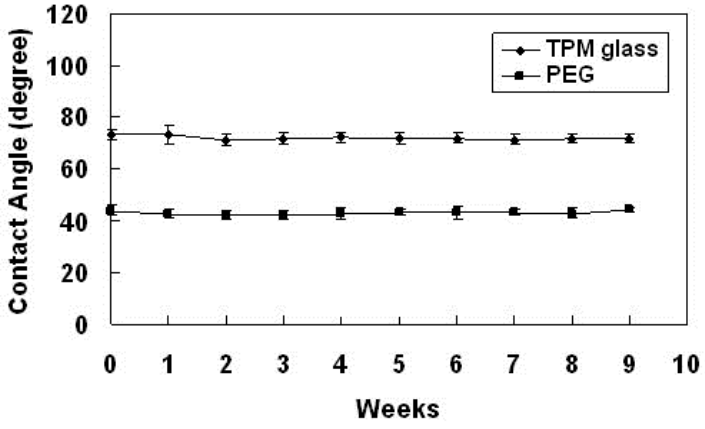

Figure 3.6 Surface contact angle of TPM treated glass slide and PEG surface over 2 months' time. Each error bars represent one standard deviation of 15 measurements on three glass slides or PEG surfaces.

(1) The photo-patterning of PEG-DA is a well-established technique [182] which requires less optimization of the formulation.

(2) The photo-patterning of PEG-DA is a rapid process which only requires seconds' time.

(3) No extra surface modification process is required for the glass slides as PEG-DA can be covalently photo-crosslinked with TPM coated surfaces.

(4) The crosslinked PEG has small pore size (~1 nm [119]) which can prevent the antigens as well as antibodies to diffuse in.

(5) PEG is a protein-resistant material [183, 184] which can minimize the unspecific surface absorption of either antigens or antibodies during the immunoassay process.

In addition to these advantages, polymerized PEG surface (contact angle of ~40º) is more hydrophilic than TPM treated glass surface (contact angle of ~70º), which makes it possible to trap sample liquid and other aqueous reagents within the area as defined by PEG micropillar rings. As shown in **Figure 3.5**, both PBS buffer and FBS can be trapped inside the PEG based micropillar rings. The trapped FBS spreads a little further than the PBS as the FBS has the lower surface tension than PBS. For both PBS and FBS, the shapes of the liquid inside different micropillar rings are almost identical. Therefore, the segregated and identically shaped sample liquid and reagent liquid ensured the consistency of the experimental conditions for biochemical assay on each gel pad array unit. Moreover, both PEG surface and TPM treated glass surface are stable as indicated in **Figure 3.6** by the surface contact angle measurements over 2 months' time. The good surface stability ensures the long-time storage of the chip without change of the assay performance.

3.3.1.3 Microbeads immobilization on the gel pad array

In conventional planar microarrays, the bioprobes were spotted or printed onto the substrate [1] with their position defined by programing the x-y stages on the microarrayer. These arrayers are usually bulky and expensive. For our gel pad array chip, nevertheless, the deposition of the microbeads can be done by simple pipetting. Usually 0.1 μl of microbeads solution is enough to cover one gel pad array unit (~500 μm x 500 μm) and 4 μl of microbeads solution is enough for each chip.

The process of assembling microbeads on a gel pad array is shown in **Figure 3.7**. After the solution was applied to gel pad array, microbeads randomly settled down in different positions such as in the cross-point of four gel pads, on the micro-trench between two gel pads or on the surface of gel pads (**Figure 3.7a** left). With the gradual evaporation of the solution, the liquid level dropped and the surface tension forced the microbeads to move from metastable positions, the micro-trench and surface of the gel pad, to the stable positions, the cross-points, as shown in **Figure 3.7a** (middle). Finally, after the solution was completely evaporated, most of the microbeads settle in the cross-points as shown **Figure 3.7a** (right). An interesting phenomena is the deformation of the gel pads by the microbeads after the evaporation of the liquid as shown in both microscopic image (**Figure 3.7a** right) and SEM images (**Figure 3.7b**). The deformation of the gel pads indicated the strong interaction between the polyacrylamide gel and the biofunctionalized polystyrene microbeads, thus, the mechanism for the microbeads immobilization on the gel pad array could be a combination of physical entrapment and physical adhesion.

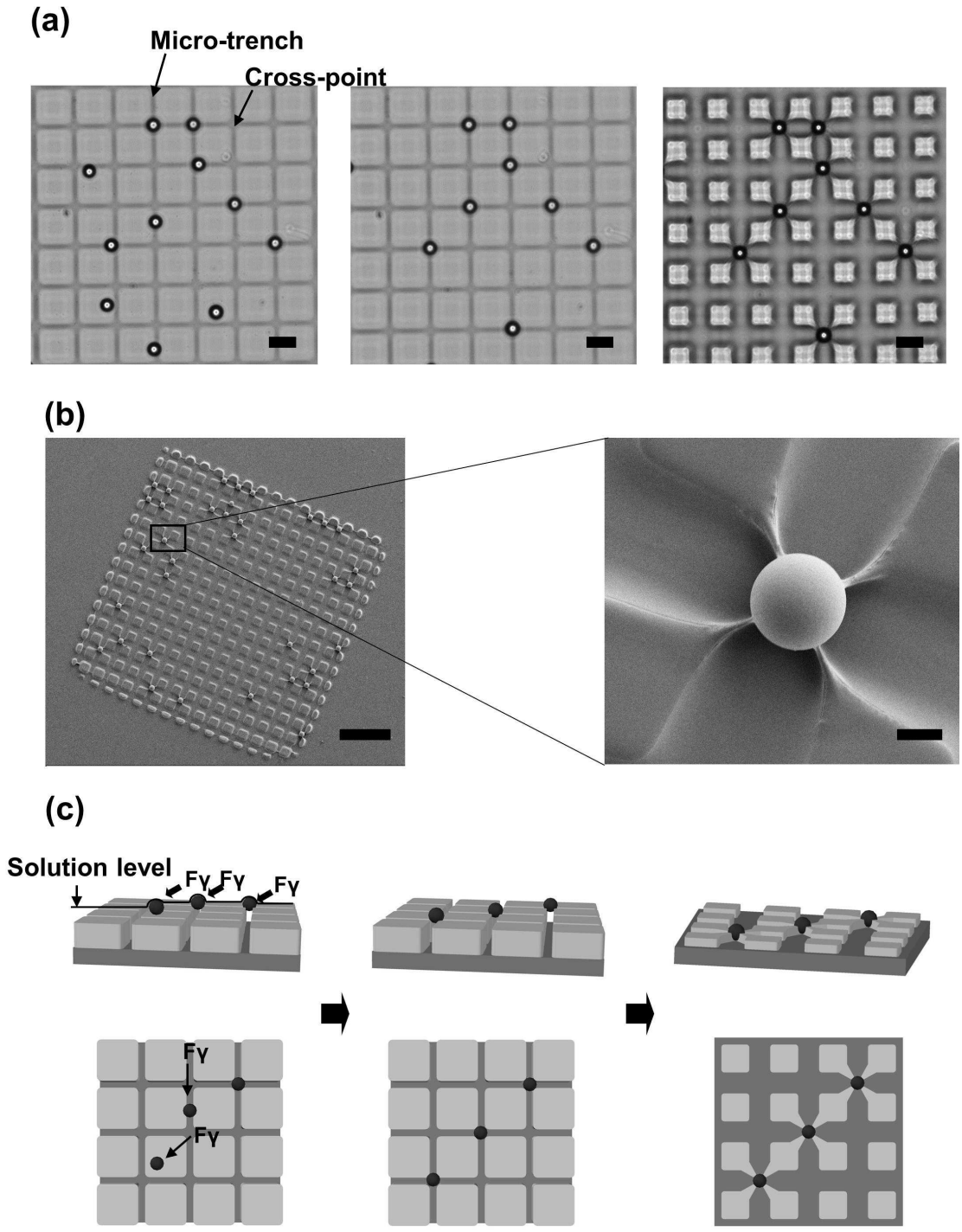

Figure 3.7 Immobilization of microbeads onto the gel pad array. (a) Left: random settlement of microbeads; middle: settlement of microbeads in cross-points; right: after complete evaporation of solution. Scale bars represent 20 μm. (b) SEM images of dried gel pad array unit with microbeads. Scale bars represent 100 μm for the left image and 5 μm for the right image. (c) Schematic diagram for microbead immobilization on the gel pad array.

3.3.2 On-chip single-plexed immunoassay for hCG and PSA

3.3.2.1 hCG and PSA

Human chorionic gonadotropin (hCG) and prostate specific antigen (PSA), two of important protein tumor markers [185], were chosen as target analytes in this study.

hCG is a 36.7 kDa glycoprotein with 2 subunits, an α subunits with 92 amino acids and a β subunits with 145 amino acids [186]. It is produced in high concentration by placental trophoblasts during the pregnancy periods [187]. Thus, hCG has been widely used as the major protein marker for the test of pregnancy. hCG levels can also been elevated in men and in non-pregnant women with tumor. The elevated serum hCG level can be an indicator of trophoblast cancer and ovary cancer in non-pregnant women, while it also can be an indicator of testicular cancer in men [187]. As the cut-off serum hCG level is very low (5 - 10 IU/l, or 0.5 – 1 ng/ml [188]), immunoassays with high sensitivity are required to measure the hCG for the diagnosis of cancers [188]. The commonly used detection devices for hCG are the lateral flow pregnancy test strips which are of low cost and easy to use. However, these lateral flow test strips usually have limit of detections (LODs) in the range of 25 – 100 IU/l [189] which are not low enough for the application in cancer diagnosis. The immunoassay gold standard ELISA, is a much more sensitive method for the detection of hCG [190]. However, ELISA is usually laborious and require relatively big amount of sample (~100 μl) and big quantity of antibody (0.1 μg/ microplate well).

PSA is a 34 kDa glycoprotein which is specifically produced from the prostate gland and has protease activity [191]. The function of PSA in healthy men is to liquefy the semen in the seminal coagulum thus giving sperm freedom to swim [192]. PSA is

widely used for the diagnosis of prostate cancer as its level elevates in the serum of patient [193]. The widely used cut-off PSA level is 4 ng/ml and patients with serum PSA >4 ng/ml are considered suspicious for prostate cancer [194, 195]. The current gold standard for the measurement of PSA is also ELISA [196] which also suffered from the limitations as discussed before.

3.3.2.2 Quantitative immunoassay for hCG and PSA in serum

The performance of the on-chip immunoassay was first evaluated by on-chip microbead-based quantitative immunoassays for hCG and PSA. All the samples were prepared by spiking either hCG or PSA in non-diluted FBS to mimic the condition in real human serum. The calibration curves were generated by measuring the average fluorescence intensity of microbeads after the on-chip assay for serial dilutions of hCG (0.0625, 0.125, 0.25, 0.5, 1, 2 and 4 ng/ml) and PSA (0.125, 0.25, 0.5, 1, 2, 4 and 8 ng/ml). Blank FBS samples were used as zero concentration samples. The calibration curves for hCG and PSA is shown in **Figure 3.8**. Each error bar indicates one standard deviation of three individual experiments for sample with the same analyte concentration. As shown in the calibration curves, for both hCG and PSA, the fluorescence intensity is proportional to the concentration of the analyte. Good linearity of the calibration curves are obtained for both hCG (R^2 = 0.9993, sensitivity = 9.5011 a.u./ng · ml^{-1}) and PSA (R^2 = 0.9991, sensitivity = 5.0661 a.u./ng · $ml^{-1)}$. The assay LODs were determined to be 42 pg/ml (1.1 pM or 0.38 IU/l) for hCG and136 pg/ml (4 pM) for PSA as calculated by adding 3 S.D. to the measured mean value of the blank measurement. The assay LOQs were determined to be 82 pg/ml (2.2 pM or

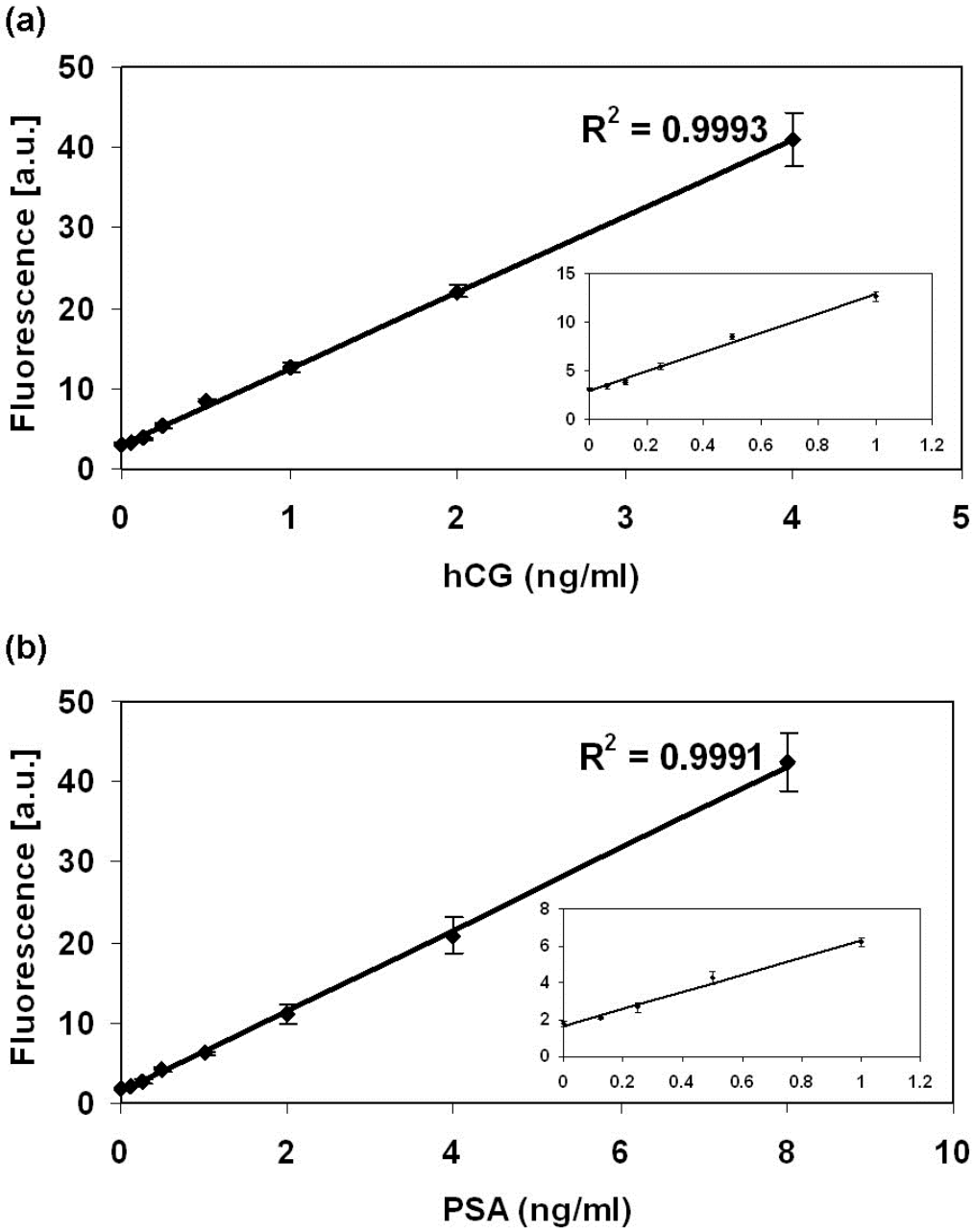

Figure 3.8 On-chip immunoassay calibration curve for (a) hCG and (b) PSA in FBS.

0.75 IU/l) for hCG and 194 pg/ml (5.7 pM) for PSA as calculated by adding 6 S.D. to the measured mean value of the blank measurement. As the cut-off values of hCG and PSA for cancer diagnosis are 5-10 IU/l (0.55 - 1 ng/ml [188]) and 4 ng/ml [194] respectively, the LODs of our on-chip assay for both tumor marker is at least one order lower than the cut-off value. Compared with the conventional ELISA method for hCG

[197, 198] and PSA [196, 199, 200], our microbead-based on-chip immunoassays have comparable LODs as well as sensitivities while require much less sample (1 μl vs. 50 – 100 μl), much less consumption of detection antibody (1 μl vs. 100 μl) and much less capture antibody (antibody on surface of less than 100 microbeads vs. antibody on the 96 or 384 well plate). Considering the sample volume of 1 μl, the on-chip immunoassay is actually capable for the detection of merely 1.1 amol (10^{-18} mol) of hCG and 4 amol of PSA.

3.3.2.3 Reproducibility of on-chip immunoassay

The reproducibility of the on-chip microbead-based immunoassay was evaluated by the intra- and inter-assay coefficient of variation (CV). The CVs were calculated by dividing the mean of 8 measurements by the variation of these 8 measurements. Each measurement was the average fluorescence intensity of all the microbeads on one gel pad array unit. For intra-CV, the same sample was applied to 8 gel pad array units on the same chip while for inter-CV the sample was applied to 8 gel pad array units on 8 different chips. The 1 ng/ml of hCG and 4 ng/ml PSA were used in the evaluation of CVs as these two concentrations are the cut-off concentrations for cancer diagnosis.

The results of the reproducibility test are shown in **Figure 3.9**. The intra-assay CVs for hCG and PSA were 4.8% and 6.5% while the inter-assay CVs for hCG and PSA were 8.8% and 12.0%. The low intra- and inter-assay CVs indicated the good reproducibility of the on-chip immunoassay which could contributes to the consistent shape and size of the samples defined by the PEG micropillar-rings. These CVs are comparable to that of the ELISA methods [196-200] as well as the state-of-the-art microbead-based immunoassay systems [10, 14, 47].

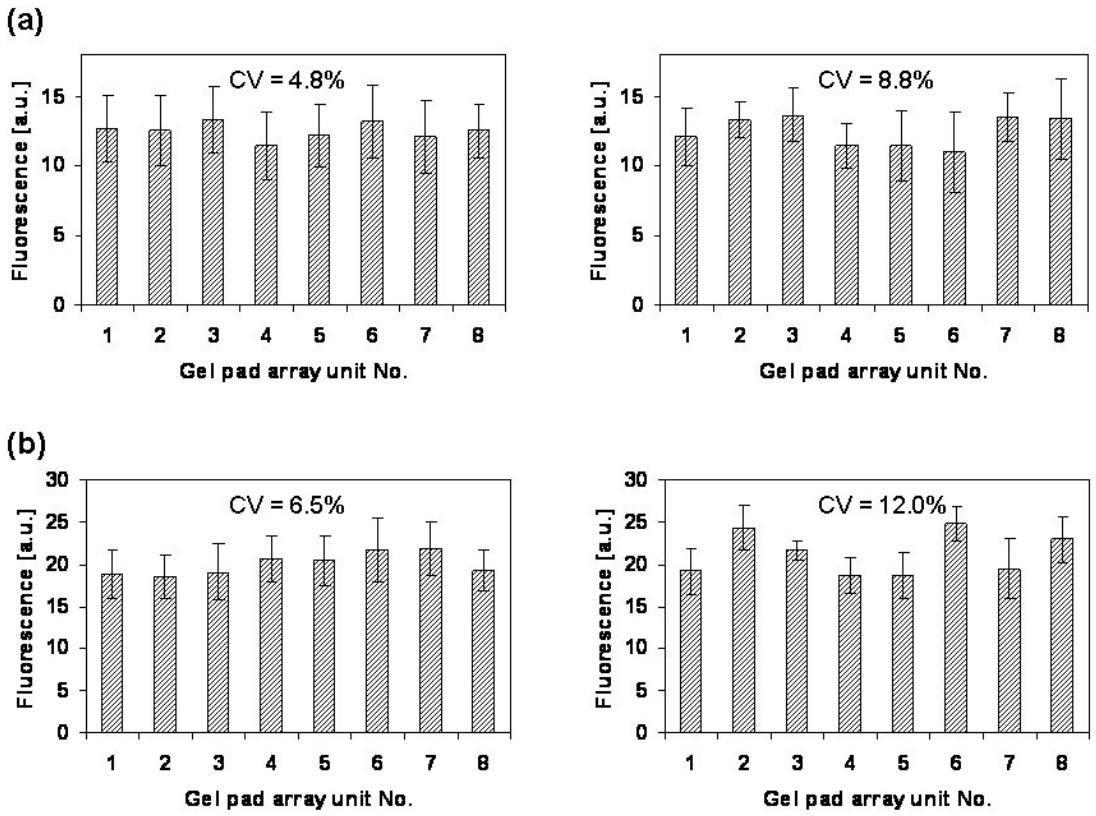

Figure 3.9 The reproducibility of the on-chip immunoassay. (a) The intra- (left) and inter-assay (right) CV for immunoassays for 1 ng/ml hCG. (b) The intra- (left) and inter-assay (right) CV for immunoassays for 4 ng/ml PSA. Error bars represent 1 S.D. for average fluorescence intensity of microbeads on each gel pad array unit.

3.3.3.4 On-chip stability of antibody-coated microbeads

The gel pad array has been proved to provide stable immobilization of oligonucleotide coated microbeads [5]. However, whether the stable immobilization is applicable to antibody-coated microbeads remains unknown. The stability of antibody-coated microbeads on the gel pad array during the assay could be very important if the chip is going to be used for multiplexed microbead-based immunoassay using spatial encoding method (discussed in later section). The on-chip stability of microbeads was calculated by counting the number of microbeads on each gel pad array unit before and after the assay. Each type of antibody-coated microbeads deposited on 24 gel pad array

Table 3.2 Stability of antibody-coated microbeads on gel pad array unit

Bead Type	**No. of microbeads**		
	Before Assay	**After Assay**	**Stability (%)**
anti-hCG beads	930	928	99.8
anti-PSA beads	648	643	99.2

units was counted before and after the assay. As shown in **Table 3.2**, more than 99% of microbeads remained on the gel pad array after the immunoassay. The result indicates that the interaction between the polyacrylamide gel and the protein-coated polystyrene microbeads is strong enough to sustain the microbead after the multiple washing steps during the immunoassay procedures. Moreover, the position of each microbead remains unchanged after the assay. One sample is shown in **Figure 3.10** with anti-hCG microbeads. The unchanged position of each microbead actually can be used as an addressable code which allows the spatial encoding of microbeads for multiplexed analysis.

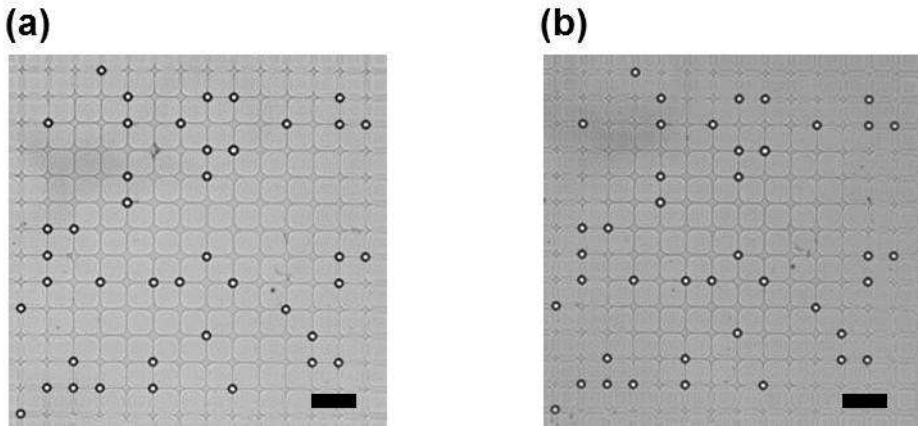

Figure 3.10 Microbeads on a gel pad array (a) before and (b) after the immunoassay. Microbeads shown here are anti-hCG microbeads. Scale bars represent 50 μm.

3.3.3 On-chip multiplexed immunoassay for hCG and PSA

3.3.3.1 Spatial encoding of microbeads on gel pad array

As discussed in **Chapter 2**, the spatial encoding method uses the spatial position of each microbeads for the encoding/decoding process [5, 59], thus eliminating the need for color encoding or barcode encoding which involve either complicated fabrication process for microbeads or the expensive or highly specific equipment for readout. The prerequisite for spatial encoding is the stable immobilization and patterning of microbeads which do not change their spatially encoded addresses during the bioassay process. As mentioned previously, the antibody-coated microbeads showed great stability on gel pad array during the on-chip immunoassay process. Thus, the simple and straightforward spatial encoding method will be an ideal encoding method for our microbead-based multiplexed immunoassay.

By using microbeads with low density in the solution, we demonstrated the spatial encoding of 10 batches of protein (streptavidin) coated microbeads in **Figure 3.11**. As can be seen, no microbead loss or change of position was observed during the entire deposition and encoding process. Although the density of microbeads was reduced to ~100 beads/μl, there were still enough beads in each batch (0.1 μl) to provide the redundancy (> 5 beads) to give statistically significant results. Theoretically, more than 400 batches (40 gel pad array units x 10 batches) of different microbeads can be encoded on each chip, thus providing significant multiplexing capability. The recognition of each batches of microbeads is also possible to be automated by using image recognition software [201].

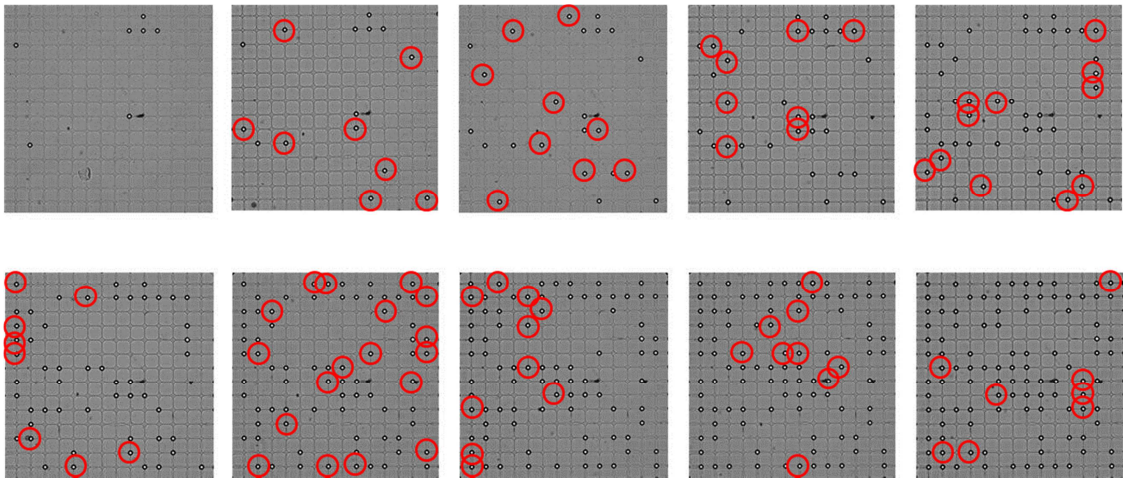

Figure 3.11 Spatial encoding of 10 batches of protein (streptavidin) coated microbeads.

3.3.3.2 Multiplexed immunoassay for hCG and PSA

Multiplexed immunoassay was performed using both anti-hCG and anti-PSA microbeads. As shown in **Figure 3.12a and b**, the two batches of microbeads were sequentially deposited onto the gel pad array unit with images taken after each deposition step for spatial encoding. After the assay for the sample spiked with cut-off concentrations of hCG and PSA, while no microbeads loss was observed, all the microbeads showed strong fluorescence (**Figure 3.12c**). Furthermore, thanks to the spatial encoding method, the fluorescence signals from both types of microbeads were detected using merely one Texas Red emission and detection filter set. This could enable the readout of a microbead microarray for multiplexed protein analysis using a simple, one-filtered fluorescence microscope which is affordable to most biochemistry labs.

The cross-reactivity of the hCG and PSA immunoassay was also examined by performing immunoassay with FBS samples spiked with different combinations of the two analytes. **Figure 3.13a** demonstrates the results from the immunoassays with

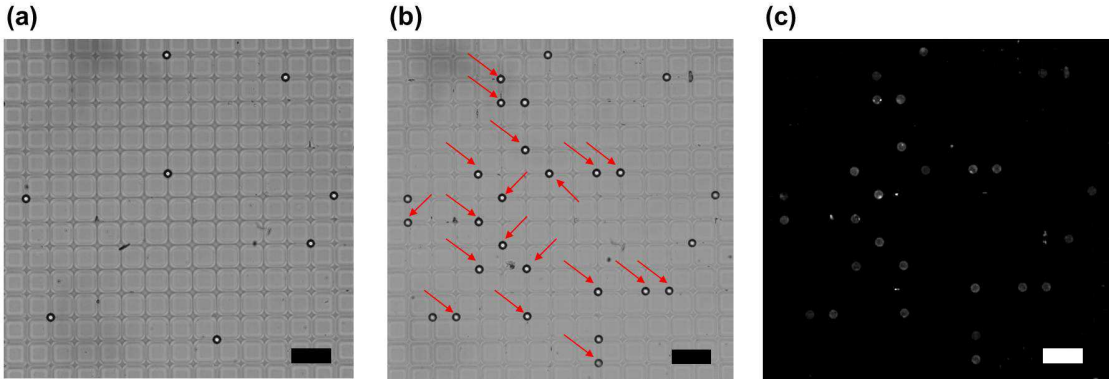

Figure 3.12 Multiplexed immunoassay for hCG and PSA. (a) Deposition of anti-hCG microbeads. (b) Deposition of anti-PSA microbeads which are arrowed out. (c) The fluorescence image after the assay. The sample contained 1 ng/ml of hCG and 4 ng/ml of PSA. Scale bars represent 50 μm.

spiked with fixed cut-off concentration of hCG (1 ng/ml) and 4X serial dilution of PSA (0, 0.5, 2, 8 ng/ml) while **Figure 3.13b** demonstrates the results from the immunoassays with samples spiked with fixed cut-off concentration of PSA (4 ng/ml) and 4X serial dilution of hCG (0, 0.25, 1, 4 ng/ml). Each error bar represents one standard deviation of three individual experiments for the same sample. As shown in the **Figure 3.13**, the linearity of signals for PSA (R^2 = 0.9996) and hCG (R^2 = 0.9995) was not distorted in the presence of the other analyte in the sample. Moreover, the signals from the cut-off concentration of PSA and hCG remained consistent in the presence of the other analyte. These results indicate the high specificity of the antibodies used in this study which minimized the cross-reaction between the two analytes. Thus, our on-chip multiplexed immunoassay system could be used for the measurement of hCG and PSA in human serum samples for cancer diagnosis. By integrating antibody pairs for other protein disease markers, our on-chip immunoassay could be promising for the serodiagnosis of various diseases. Compared to the multiplexed protein microarray fabricated on 96-well plate [10, 178], the advantages of our chip are the less sample volume (1 μl vs. 100 μl) as well as the simpler method to

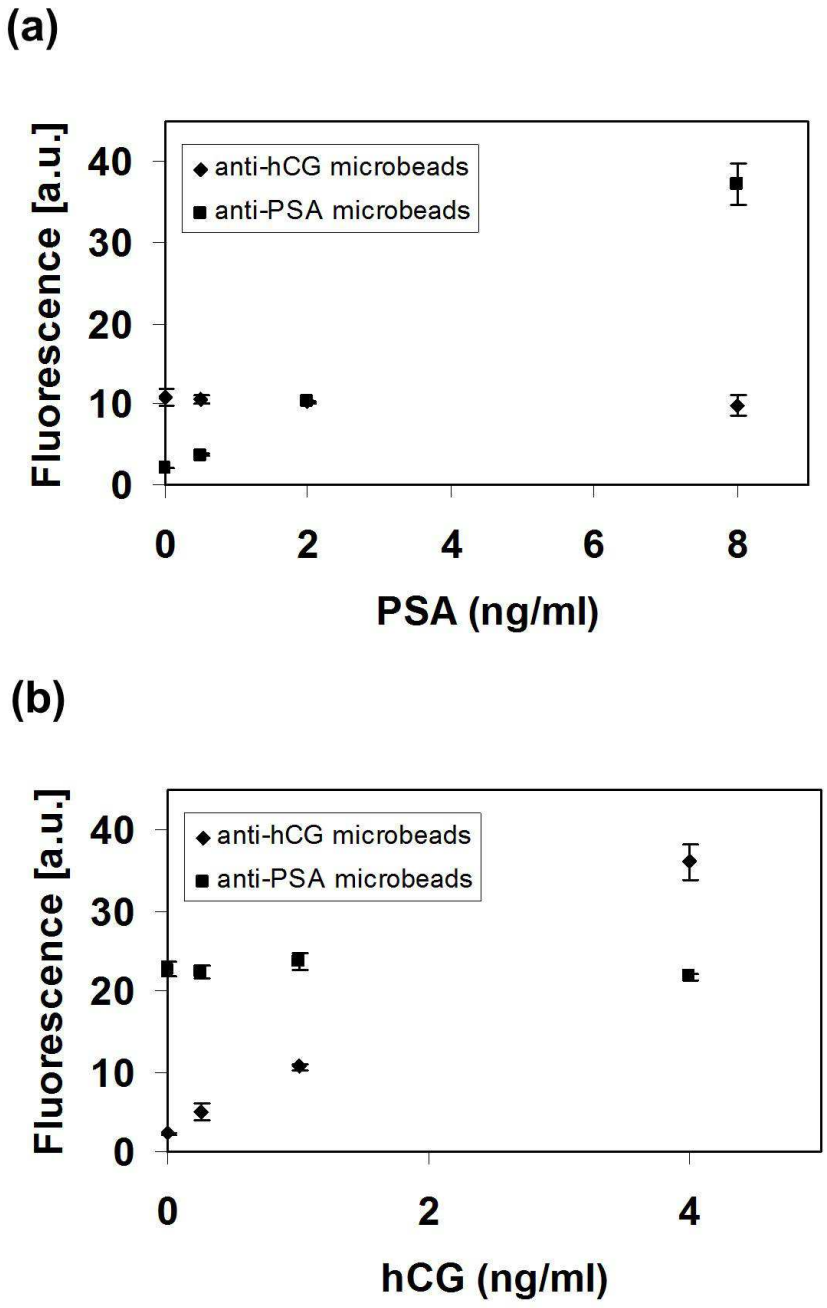

Figure 3.13 Testing the cross-reactivity of hCG and PSA by multiplexed immunoassay. (a) Immunoassay for samples with 1 ng/ml of hCG and serial dilution of PSA. (b) Immunoassay for samples with 4 ng/ml of PSA and serial dilution of hCG.

assemble the array (micropipette vs. microarray spotter). Recently, several groups reported the used of multi-microwell planar protein microarray chips which required small sample volume (1 µl to 1.5 µl) comparable to this study for each assay [180, 202,

203]. However, unlike our gel pad array chips which allow detection of multiple analytes in one array unit, all of these studies are only restricted to the detection of one analyte in each microwell.

3.3.4 Reusability of the gel pad array chip

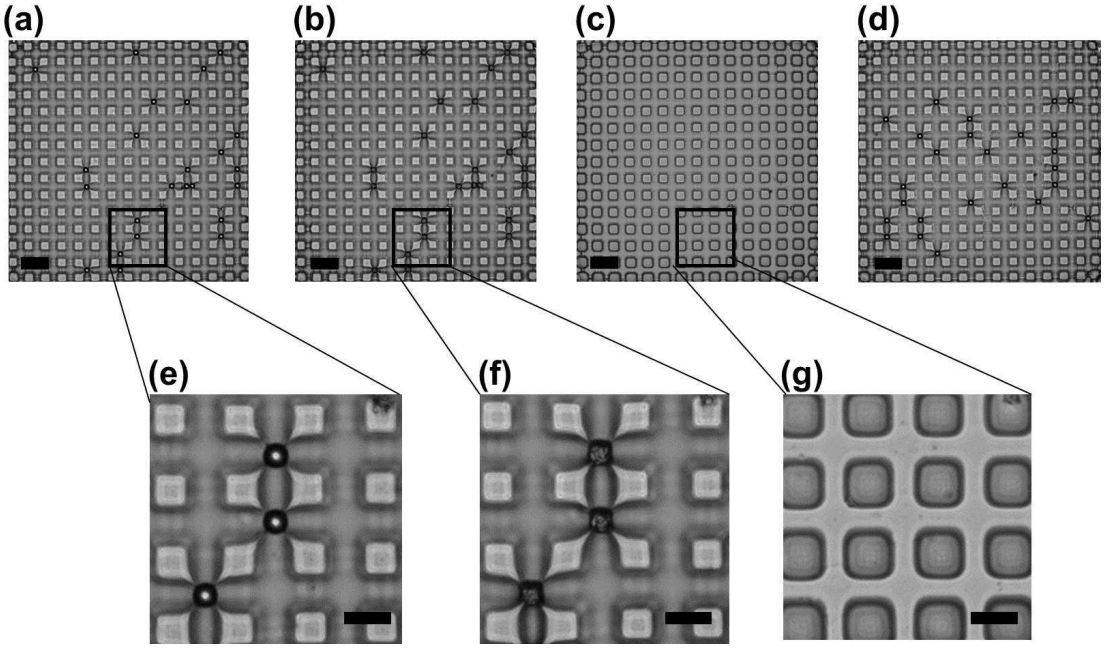

Figure 3.14 Reuse of the chip by removing polystyrene microbeads. (a) Microbeads on a gel pad array. (b) After immersed in toluene for 10 min. (c) After subsequent sonication for 10 min. (d) Reload the gel pad array with a new batch of microbeads. (e), (f) and (g) are the enlarged pictures of (a), (b) and (c). Scale bars represent 50 μm for (a), (b), (c) and (d), 20 μm for (d), (e) and (f).

Besides the fact that the gel pad array chips were fabricated with simple procedures and very low material cost (< S$ 0.2/chip), the chip can be further reused by removing the old microbeads and subsequently applied with a new batch of microbeads. As the gel pad array provides stable immobilization of microbeads, it is difficult to remove all the microbeads through simple rinsing or sonication. To reuse the gel pad array, we

removed the microbeads by swelling and dissolving microbeads in toluene with the affiliation of sonication. As shown in **Figure 3.14**, antibody-coated polystyrene microbeads can be swelled by toluene (**Figure 3.14f**) and can be completely removed after 10 min of sonication in toluene (**Figure 3.14g**). A new batch of microbeads can then be applied for the reuse of the chip (**Figure 3.14d**). The deformation of the gel pads by the microbeads can still be observed after the reuse of the chip which indicates the strong interaction between the microbeads and the polyacrylamide gel is not weakened after sonication in toluene.

The reusability of the chip was also tested by generating the calibration curves for hCG in FBS sample on the same reused chip. The chip was reused for two times to generate three calibration curves for hCG. The three calibration curves are shown in **Figure 3.15** with each error bar representing one standard deviation of three individual experiments for the samples with the same concentration. The linearity of the calibration curves are not compromised by the reuse of the chip as indicated by the R^2 value (R^2 value: 1^{st} use = 0.9993, 2^{nd} use = 0.9938, 3^{rd} use = 0.9992.). The CV of the sensitivity of the three calibration was 4.4% (Sensitivity: 1^{st} use = 9.5011 a.u./ng $\cdot$ ml^{-1}, 2^{nd} use = 8.9103 a.u./ng $\cdot$ ml^{-1}; 3^{rd} use = 8.7358 a.u./ng $\cdot$ ml^{-1}) which indicated a small variation between the immunoassay sensitivity on the reused chip. The stability of the microbeads was also tested by counting the anti-hCG microbeads on the gel pad array unit before and after the assay in the each reuse of the chip. As shown in **Table 3.3**, more than 98% of the microbeads remained stable on the gel pad array in a third time immunoassay on the same chip. All these results prove that the gel pad array chips can be robustly reused for the quantitative and sensitive microbead-based immunoassay, which is rarely reported in other planar or microbead microarray platforms. The reusability of the chip can further reduces the chip material cost for each immunoassay

(< S$ 0.2 per chip with < S$ 0.005 per assay on each array unit and with < S$ 0.002 per assay if with two reuse.). Thus, our chip could potentially be used for the low-cost disease diagnosis in developing countries.

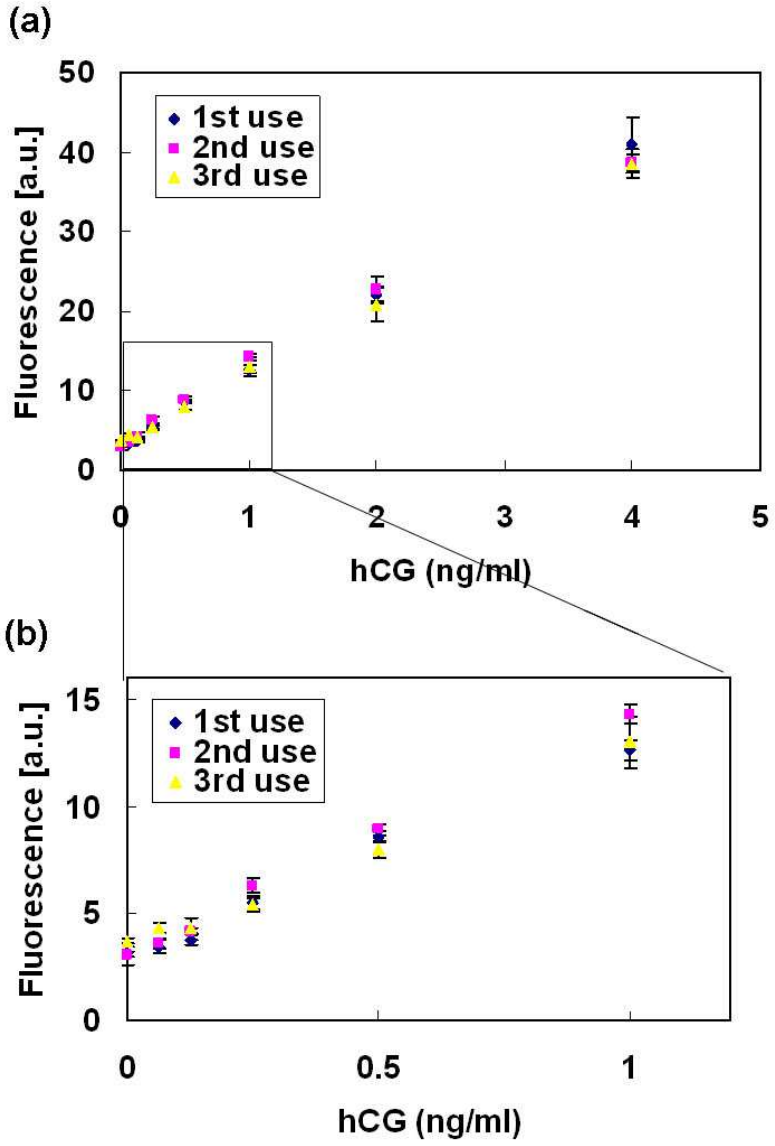

Figure 3.15 Calibration of hCG on the reused chip. (a) The calibration curve obtained from the same chip with two times reuse. (b) The calibration curve for low concentration of hCG (0 – 1 ng/ml).

Table 3.3 Stability of anti-hCG microbeads on the reused chip

	No. of microbeads		
	Before Assay	**After Assay**	**Stability (%)**
1st use	930	928	99.8%
2nd use	795	787	99.0%
3rd use	972	958	98.6%

3.3.5 Simultaneous detection of protein and DNA: Preliminary results

DNA hybridization assay and immunoassay are both binding based assays which rely on the specific binding of bioprobes (oligonucleotides and antibodies) with target analytes (oligonucleotide and antigens). As the gel pad array provides stable immobilization for both oligonucleotide [5] and antibody coated microbeads, it is possible to combine the hybridization assay with immunoassay for simultaneous detection of protein and DNA using spatially encoded microbeads.

One possible challenge towards the integration of hybridization assay and immunoassay is the different buffer systems. For DNA hybridization, SSC buffer and formamide are usually used while, for immunoassay, PBS buffer is most commonly used. In this study, we chose the PBS buffer as it has been proved in several studies to be compatible with DNA hybridization assay [204-207]. The hybridization assay was tested using oligonucleotide probe conjugated microbeads (seq. 5' biotin-TCACATTTTGGATAATCCCAACC) to detect the a serial dilution (100 pM – 1 μM) of target oligonucleotide (seq. 5' Texas Red-GGTTGGGATTATCCAAAATGTGA, a part of the cDNA sequence from the RNA-dependent RNA polymerase gene in SARS coronavirus [208]) in PBS as shown in **Figure 3.16**. The incubation time was 30 min.

Each error bar represents one standard deviation of three individual experiments for samples with the same target oligonucleotide concentration. The results indicated a proportional relationship between the intensity of the microbeads to the concentration of the target analyte. This further proves the compatibility of PBS buffer to the quantitative hybridization assay.

As a proof of concept, we performed a simultaneous immunoassay for hCG and hybridization assay for target DNA. 100 ng/ml of hCG and 100 nM of target oligonucleotide were spiked in PBS as the sample. The assay procedures were similar to that of the on-chip immunoassay despite that PBS was chosen instead of FBS. As shown in **Figure 3.17**, while there was no bead loss or change of position during the assay as expected, both anti-hCG and oligonucleotide microbeads showed fluorescence after the assay. It is also noticeable that, by using fluorescence label with similar excitation and emission spectrum (Alexa Fluor 594 and Texas Red), the simultaneous detection of the two kinds of biomolecules can also be done through one-filter set fluorescence microscope. Compared with a recent report [125] for the simultaneous detection of DNA and protein using biofunctionalized microparticle with SPR detection method, our chip based approach is simpler and with much less sample consumed although the SPR approach had the advantage of label-free detection. One potential application of our on-chip simultaneous immunoassay and hybridization assay could be the combination of genomic analysis [6] with proteomic analysis [122, 209] using microbeads conjugated with different oligonucleotide and antibody probes.

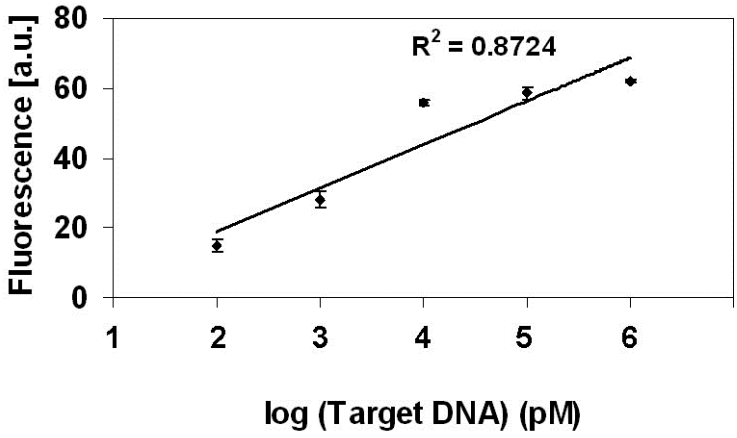

Figure 3.16 On-chip hybridization assay calibration curve.

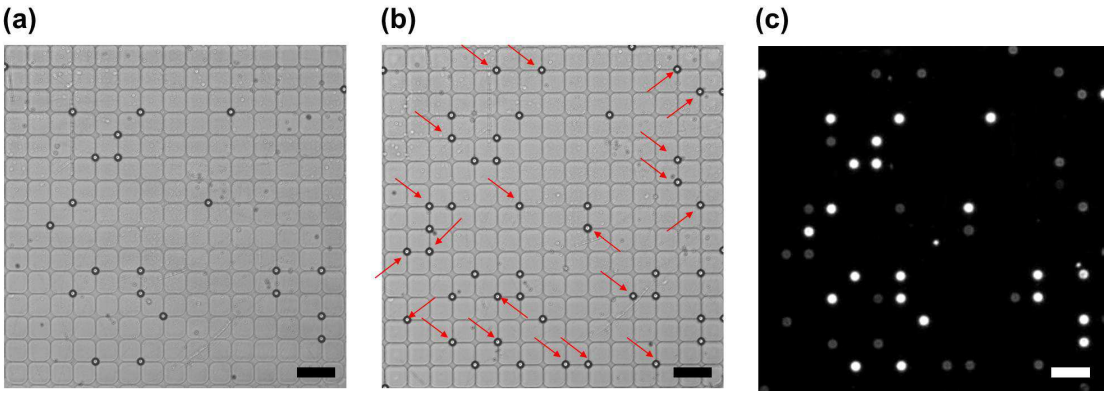

Figure 3.17 Simultaneous immunoassay and hybridization assay for hCG and target DNA. (a) Deposition of anti-hCG microbeads. (b) Deposition of oligonucleotide microbeads which are arrowed out. (c) The fluorescence image after the assay. Scale bars represent 50 μm.

3.4 Conclusion

In this chapter, we presented a novel gel pad array chip for microbeads-based immunoassays. The previous protocol for gel pad array fabrication was first optimized by substituting the strongly fluorescent methylene blue with non-fluorescent DMPA as the photoinitiator, thus greatly reducing the background autofluorescence of the polyacrylamide gel. In addition, we integrated novel PEG micropillar rings into the chip to provide hydrophilic barriers to segregate both FBS samples and other reagents.

The optimized gel pad array chip has 40 gel pad array units and allows the biochemical assay to be performed with merely 1 μl of sample on each array unit. On-chip quantitative immunoassays for hCG and PSA in serum samples were performed with the LODs determined to be 42 pg/ml for hCG and 136 pg/ml for PSA. Both LODs are lower than the cut-off level for hCG (1 ng/ml) and PSA (4 ng/ml) as serum tumor markers for cancer diagnosis. The on-chip immunoassays also showed good reproducibility as demonstrated by the small intra- and inter-CVs which are less than 12%. Moreover, more than 99% of the antibody-coated microbeads remained their position during the assay process. The great stability of the microbeads allowed the multiplexed immunoassay for both hCG and PSA to be performed on-chip using spatial encoding strategy. As up to 10 batches of microbeads can be sequentially deposited onto each gel pad array, the multiplexed ability of the chip could be potentially increased by immobilization of more batches of microbeads with different antibodies. The reusability, which was rarely reported in other microarray systems, was also demonstrated. The microbeads on the reused chip still remained high stability (> 98%) and the sensitivity of the on-chip immunoassay was not compromised during the reusing process. Lastly, as a proof of concept, we demonstrated the on-chip multiplexed detection of two different types of biomolecules, protein and DNA, which could further expand the application of our chip. As our chips were fabricated at low material cost without the requirement for any cleanroom facilities and expensive equipment, it could either be used as a platform for the DIY of microbead array in common biolabs or be potentially used as a low cost disease diagnosis tool in developing countries.

Chapter 4

Microfluidic microparticle array on gel microstructure chip for biochemical assays

Chapter 4 - Microfluidic microparticle array on gel microstructure chip for biochemical assays

4.1 Introduction

The recent development of microfluidic analysis system, also known as micro-total-analysis-system (μTAS), provides new platforms for biochemical assays [210-212]. Owing to the fast mass transfer rate in miniaturized microchannels, microfluidic systems enable the biochemical assays to be done with much less sample volume and much shorter time as compared to the conventional bioanalytical methods [213, 214]. One of the major formats of microfluidic biochemical assay is the heterogeneous assay which integrates certain solid substrate in microchannels for the immobilization of bioprobes. The immobilized bioprobes, such as oligonucleotides [215], antibodies [152, 216] and enzymes [217], can either capture or react with the target biomolecules in the microfluidic channels and subsequently produce signals for the quantitation.

Microparticle has been widely used as a solid substrate in microfluidic biochemical assays [9, 31, 218, 219]. There are several advantages to utilized microparticles instead of other planar solid substrates for microfluidic biochemical assays: (1) microparticles allow more bioprobes to be immobilized per unit area, thus increasing either the binding capacity or reactivity with the target biomolecules and resulting in the enhancement of the quantitation signals; (2) the minute biofunctionalized microparticles can be directly incorporated into miniaturized microfluidic systems by simple injection [17] or pipetting [28] without any specialized micropatterning [220]

or delivering techniques [149] which are required to fabricate planar biofunctionalized substrates to be integrated a microfluidic system; (3) microparticles with various surface chemistries can be separately attached with different bioprobes and can be simply incorporated to the microfluidic system later on [59, 218] whereas it is more challenging to integrated planar substrates with different surface chemistries and different bioprobes into one microfluidic systems. Due to these obvious advantages, microparticle has been integrated into microfluidics for various kinds of biochemical assays with three most notable ones, the immunoassays [27, 29, 59, 221-223] , DNA hybridization assays [9, 218, 224, 225] and enzymatic assays [39, 226]. Moreover, multiplexed microfluidic assays were also achieved by using biofunctionalized microparticles which are either encoded or are immobilized in different microchannels [32, 33]. Nevertheless, while most of current microfluidic microparticle-based assays are able to detect multiple biomolecules of one category (e.g. different proteins, DNAs or small metabolites), few have been demonstrated for the detection of different categories of biomolecules (e.g. proteins and small metabolites).

In **Chapter 3**, as a proof-of-concept, we demonstrated the multiplexed microbead-based assay for two categories of biomolecules, protein and DNA, on the gel pad array chip. While the integration of immunoassay and DNA hybridization assay, which are both binding based assays, could be achieved simply using microbeads with different surface bioprobes, the integration of binding kinetic based assay and reaction kinetic based assay (e.g. enzymatic assays) could be more challenging due to the intrinsically different assay mechanisms. In this chapter, the final aim is to develop the microfluidic microparticle-based assay which integrates both binding kinetic based immunoassay and reaction kinetic based enzymatic assay for the detection of different categories of biomolecules. To achieve this, the stability of different biofunctionalized

microparticles under microfluidic flow conditions is first tested. Subsequently, the microfluidic microbead-based immunoassays for serum samples are developed by integrating the existing gel pad array platform. Multiplexed microfluidic immunoassays are also demonstrated by using spatially encoded microbeads. Furthermore, PEG based microparticles, which contain glucose oxidase (GOx) and horseradish peroxidase (HRP), are fabricated for the enzymatic assay for glucose. A novel gel well array is developed to affiliate the immobilization of enzyme-containing microparticles. Next, the microfluidic enzymatic glucose assay is performed with both PBS and FBS samples. Lastly, by immobilizing both antibody-coated microbeads and enzyme-containing microparticles on a novel mixed gel microstructure chip, we demonstrate the simultaneous detection of proteins and glucose by integrating both microfluidic immunoassay and enzymatic assay. To the best of our knowledge, this is the first report for the integration of binding kinetic based biochemical assay and reaction kinetic based biochemical assay into one microfluidic microparticle array platform.

4.2 Materials and methods

4.2.1 Materials and reagents

Microscopic glass slides were purchased from Corning. Polydimethylsiloxane (PDMS) prepolymer (Sylgard 184) was purchased from Dow Corning. All the hard and soft masks were purchased from Infinite Graphic. Silicon wafers were purchased from University Wafer. SU-8 50 negative photoresist and SU-8 developer were purchased from Microchem. The 10 μm streptavidin-coated polystyrene microbeads were

purchased from Bangs Laboratory. Alexa Fluor 594 NHS ester and fetal bovine serum (FBS) were purchased from Invitrogen. Prostate specific antigen (PSA, from human seminal fluid), monoclonal anti-PSA clone 5 antibody, monoclonal anti-PSA clone 7 antibody, monoclonal anti-β-hCG clone 1 antibody and polyclonal goat anti-whole hCG antibody were purchased from Arista Biologicals. Recombinant hCG, acrylamide/Bis-acrylamide solution (40%, 19:1), Poly(ethylene glycol) diacrylate (PEG-DA, Mw 575 Da), glucose oxidase (GOx, from *Aspergillus niger*, type X-S, 158900 U/g solids), horseradish peroxidase (HRP, from horseradish, type II, 188000 U/g solids), trichloro(1*H*,1*H*,2*H*,2*H*-perfluorooctyl) silane, bovine serum albumin (BSA), N,N,N',N'-Tetramethylethylenediamine (TEMED), Ampliflu Red, Tween® 20, 3-(Trichlorosilyl) propyl methacrylate (TPM), (+)-Biotin N-hydroxysuccinimide ester (biotin-NHS), DMPA, toluene, heptane and recombinant hCG were purchased from Sigma-Aldrich. Repel Silane (Dimethyldichlorosilane, 2% solution in octamethylcyclotetrasiloxane) was purchased from GE Healthcare. Deionized water was produced by Arium® 611 UV system (Sartorius AG).

4.2.2 Fabrication of gel microstructure chips

4.2.2.1 The chip design

All the gel microstructures were fabricated on the same microscopic glass slides used for the gel pad array chip discussed in **Chapter 3**. The design of the masks was done in AutoCAD software (Autodesk). The design of the mask allows the fabrication of 8 gel microstructure units as shown in **Figure 4.1a**. The distance between two gel microstructure units was set to be 14 mm to leave enough space for the capping of microfluidic modules on each array unit. Three types of microstructure array units

were designed: (1) gel pad array unit, with 17 x 17 square gel pads (20 μm x 20 μm) with 10 μm gap (**Figure 4.1b**); (2) gel well array unit, with 6 x 6 gel wells (60 μm of diameter) with 110 μm distance between two wells (**Figure 4.1c**); (3) mixed structured array with both gel pads and gel wells (**Figure 4.1d**). The designs of different gel microstructures units are for the immobilization of different microparticles which will be discussed in detail in later sections.

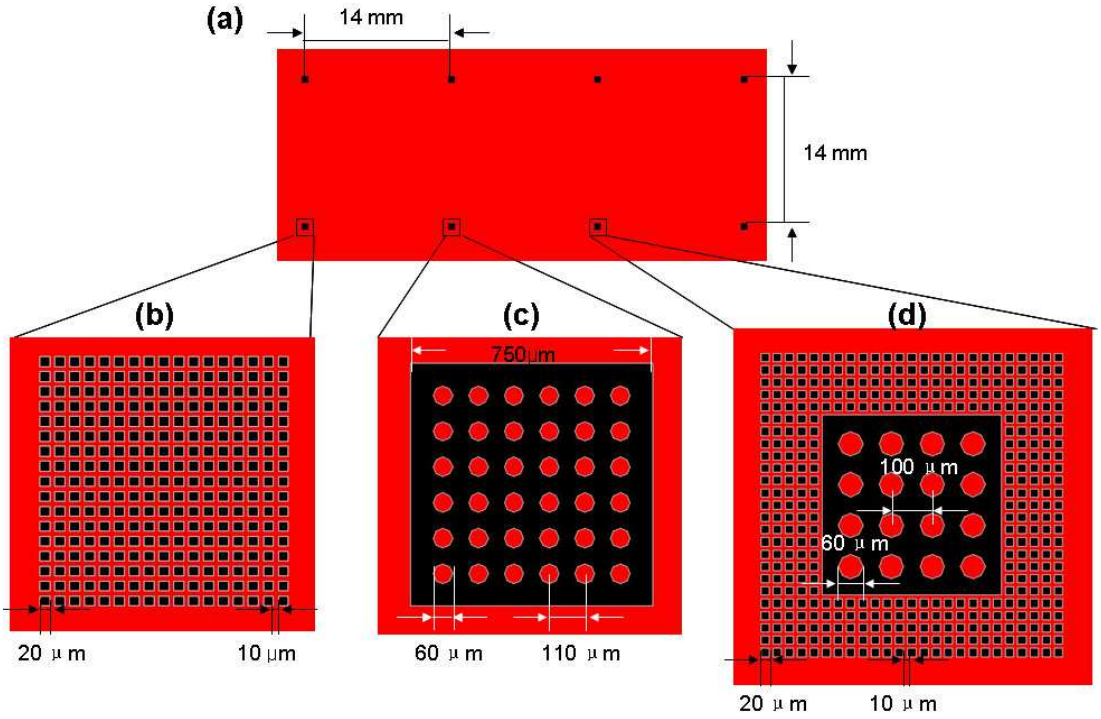

Figure 4.1 The mask design of the gel microstructure chip for microfluidic integration. (a) Microstructure array units. (b) Gel pad array unit. (c) Gel well array unit. (d) Mixed structure array unit.

4.2.2.2 Fabrication process

Polyacrylamide gel-based microstructures were fabricated in the similar way as the fabrication process for gel pad array units as described in **Chapter 3**. Polyacrylamide gel precursor solution was photopolymerized by exposure under UV through the hard

mask and the result microstructures were able to be attached to the TPM treated glass slide. The height of hydrated gel microstructures was defined by a pair of spacers. 12 μm spacers were used for the fabrication of gel pad array unit while 24 μm spacers were used for the fabrication of gel well array unit as well as the mixed microstructure array unit. All the chips with gel microstructure arrays were stored in clean petri-dishes sealed with parafilm. The fabricated gel microstructure chip is shown in **Figure 4.2**.

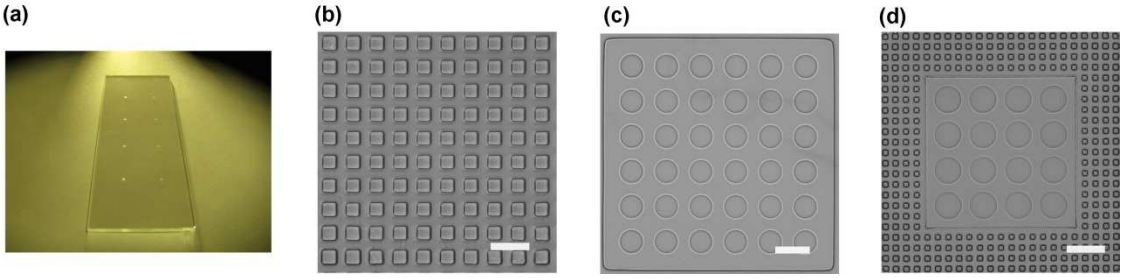

Figure 4.2 Gel microstructure chips. (a) Overview of gel microstructures chip. (b) Gel pad array. (c) Gel well array. (d) Mixed gel microstructure array. The scale bars represent 50 μm for (b), 100 μm for (c) and (d).

4.2.3 Fabrication of PDMS-based microchannels

The design of the microchannel features was done using AutoCAD software. The feature was then printed on a transparency soft mask. The master for soft-lithography was fabricated with standard photolithography process on 4 inch silicon wafers with detailed protocol described in **Table 4.1**.

The PDMS microchannels were fabricated using a standard soft-lithography method [227]. First, the master was treated with trichloro(1*H*,1*H*,2*H*,2*H*-perfluorooctyl) silane to prevent the adhesion with PDMS prepolymer. A 10:1 (w/w) of PDMS base and PDMS curing agent was mixed and degassed for 40 min to remove air bubbles. Next,

the PDMS prepolymer mixture was poured onto the master and cured at 65 °C for 2 h. The replica PDMS microchannels were then peeled off from the master, punched with holes and diced as demanded. Two types of microchannels were fabricated with the channel width of 500 μm and 800 μm respectively. The entire PDMS microchannel fabrication process is summarized in **Scheme 4.1**.

Table 4.1 Photolithography protocol for the fabrication of master for microchannel

Steps	**Procedures**
Spin coat	
	500 rpm for 10 s
	2000 rpm for 45 s
Soft Bake	
	65 ºC for 7 min
	95 ºC for 21 min
	cooling down in air for 2 min
Exposure	
	365 nm UV light source, ~20 mW/cm^2, exposure time 30 s
Post Exposure Bake (PEB)	
	65 ºC for 1 min
	95 ºC for 6 min
	cooling down in air for 2 min
Develop	
	SU8 developer 10 min
Rinsing	
	isopropanol + distilled water
Hard Bake	
	150 ºC for 30 min

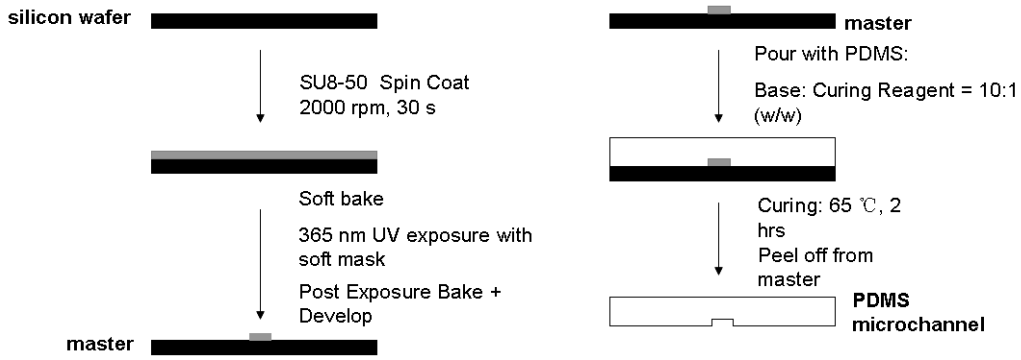

Scheme 4.1 PDMS microchannel fabrication process.

4.2.4 Preparation of biofunctionalized microparticles

4.2.4.1 Preparation of antibody-coated microbeads

The method for the preparation of anti-hCG and anti-PSA microbeads are the same with the method mentioned in **Chapter 3**. Thus, it is omitted here.

4.2.4.2 Preparation of enzyme-containing microparticles

Enzyme-containing microparticles were prepared in a photopolymerization process with PEG-DA as shown in **Scheme 4.2**. Poly (ethylene glycol) diacrylate (PEG-DA, Mw 575 Da) was pre-dissolved with 2% (w/v) 2,2-dimethoxy-2-phenyl acetophenone (DMAP). The PEG-DA solution was then mixed with an equal volume of PBS solution which contained 5 mg/ml GOx and 5 mg/ml HRP. The mixed solution was transferred between a glass photomask and a glass slide and was then illuminated under a spot UV lamp (100 W, UVP) for 5 s. The photopolymerized cylindrical microparticles were around 50 μm in diameter as defined by the features on the mask and a pair of spacers. The height of the microparticles was defined by a pair of 12 μm spacers. Both the glass photomask and the glass slide were pre-treated with Repel

Silane to prevent the attachment of PEG-DA. After exposure, the polymerized PEG microparticles were rinsed out, washed with PBS for five times and stored at 4 °C. The current design of the mask allows simultaneous fabrication of 10000 enzyme-containing microparticles.

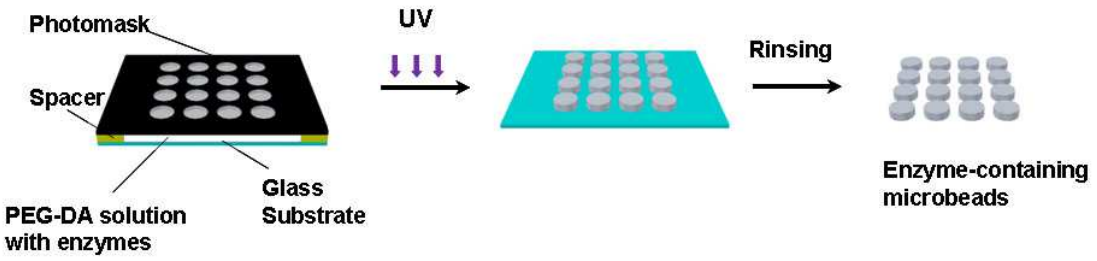

Scheme 4.2 Preparation of enzyme-containing PEG-based microparticles.

4.2.5 Microfluidic biochemical assay

4.2.5.1 Microfluidic setup

The setup for the microfluidic microbead-based biochemical assay is shown in **Figure 4.3**. The gel microstructure chip covered with certain microfluidic channel was placed onto a microscope mount. FEP tubings were used for the connection and reagent delivery. All the reagents were delivered into the microchannel by a syringe pump (Fusion 200, Chemyx Inc.) and an Eppendorf tube was used for waste collection. A 20X magnification lens was used for imaging.

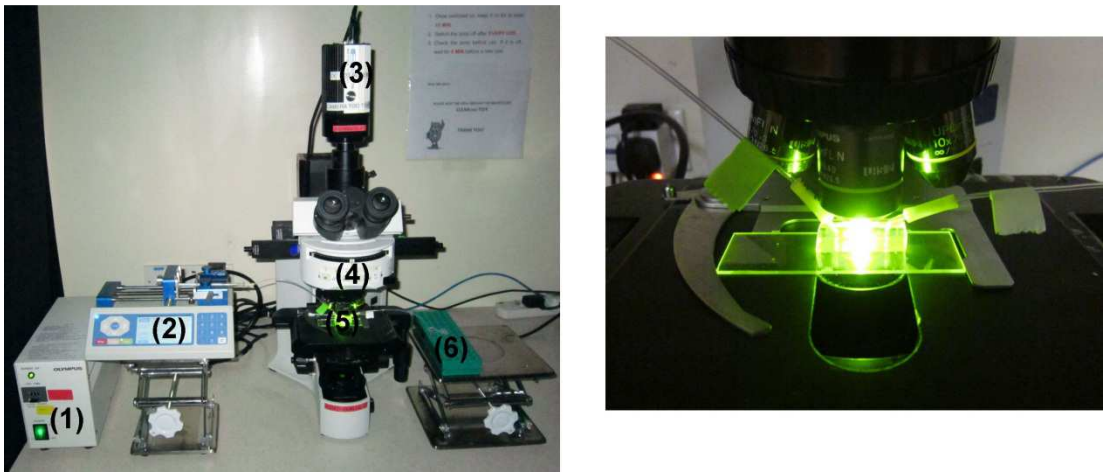

Figure 4.3 Experimental setup for microfluidic biochemical assays. Left: (1) Mercury Arc Power. (2) Syringe Pump. (3) CCD camera. (4) Microscope. (5) The gel microstructure chip. (6) Waste tube. Right: A close view of gel microstructure chip on the microscope mount.

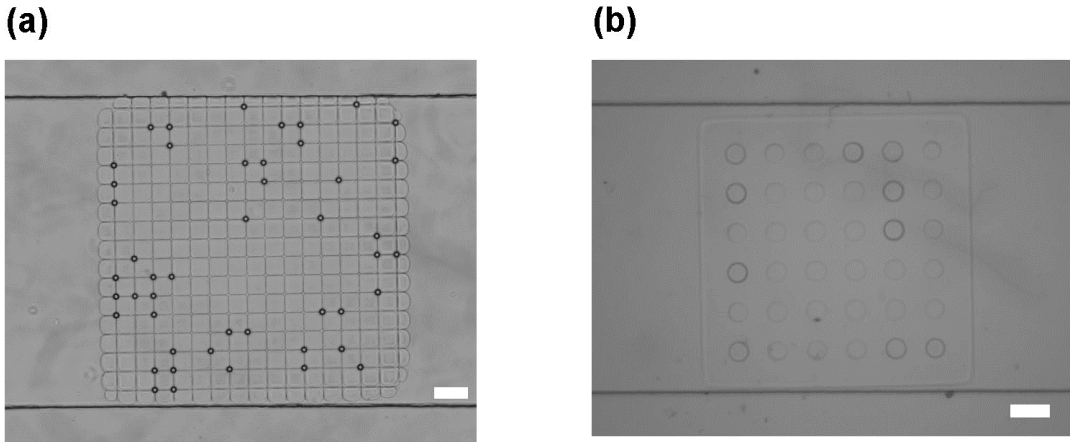

Figure 4.4 Microparticle arrays in microchannels. (a) Alignment of a gel pad array within a microchannel with antibody-coated microbeads deposited. (b) Alignment of a gel well array within a microchannel with enzyme-containing microparticles deposited. Scale bars represent 50 μm for (a) and 100 μm for (b).

4.2.5.2 Microfluidic immunoassay

The gel pad arrays were used to carry out microbead-based immunoassays. For the single-plexed assay for PSA and hCG, each gel pad array unit was first pipetted with 0.1 μl solution of antibody-coated microbeads (~500 beads/μl). The microbeads solution was left to dry at room temperature for 2 min. The gel pad array unit was then

capped reversibly with a 500 μm wide PDMS microchannel (**Figure 4.4a**) which was connected with a syringe pump afterwards. PBS-B-T solution was first introduced at 2 μl/min for 5 min to block the microchannel. FBS spiked with target analytes was then introduced into the microchannel at 2 μl/min for 10 min to allow the analytes to bind to the antibody on the microbeads' surface. After PBS-B-T solution was pumped in at 5 μl/min for 5 min to wash away any unbound analytes, 20 μg/ml of Alexa Fluor 594 labelled detection antibody solution was introduced at 2 μl/min for 10 min. Finally, the microchannel was washed again with PBS-B-T at 5 μl/ min for 5 min to wash away any unbound fluorescent detection antibody. The gel pad array area was then imaged with a fluorescence microscopy.

For the multiplexed immunoassay, the microbeads were diluted to ~100 beads/μl to allow more batches of microbeads to be deposited. After depositing one batch of microbeads onto the gel pads array, a bright field image was taken to record the spatial positions of every single microbead. The deposition and image recording process was repeated to encode different types of microbeads with their spatial addresses. The following microfluidic immunoassay procedure was similar to that of the single-plexed immunoassay despite that both analytes were spiked in FBS and a solution containing detection antibodies for both hCG and PSA was used.

4.2.5.3 Microfluidic enzymatic glucose assay

The gel well arrays were used for microparticle-based enzymatic assays for glucose. Each of the gel well array units was pipetted with 0.1 μl solution of enzyme-containing microparticles (~200 beads/μl). After the solution evaporated out in 2 to 3 min, the

array was rinsed from the side with PBS for 30 s to remove any microparticles which did not sit in the wells. The array was then capped reversibly with an 800 μm wide microchannel (**Figure 4.4b**). The microchannel was placed under a microscope and connected with a syringe pump. The microchannel was then washed with PBS at 5 μl/min for 2 min. Next, PBS or FBS spiked with different concentration of glucose and 20 μM of Ampliflu Red were introduced into the microchannel at 5 μl/min for 2 min. A fluorescence image was taken immediately afterwards.

4.2.5.4 Simultaneous immunoassay and enzymatic glucose assay

The mixed microstructure array was used for the simultaneous assay of proteins and glucose in serum. The enzyme-containing microparticles were first deposited onto the 60 μm microwells through the same method mentioned above. The array was then pipetted with 0.1 μl solution of antibody-coated microbeads. After the solution was evaporated out, the array was gently rinsed from the side by PBS for 30 s. This step is to remove the 10 μm antibody-coated microbeads which could possibly sit on the 50 μm cylindrical microparticles. A second batch of antibody-coated microbeads was then deposited in the same way. The microbeads coated with different antibodies were spatially encoded by comparing the images taken after deposition of each batch of microbeads. The mixed structure array was then capped with a microfluidic channel. After the microchannel was blocked with PBS-B-T, FBS spiked with 100 ng/ml of PSA, 1 μg/ml of hCG, 5 mM of glucose and 20 μM of Ampliflu Red was flowed through at 2 μl/min for 2 min. A fluorescence image was taken immediately to record the signals from the enzyme-containing microbeads. The FBS with analytes was then flowed through the channel for 10 min with the flow speed decreased to 2 μl/min. The following steps were the same for the multiplexing microfluidic immunoassay, which

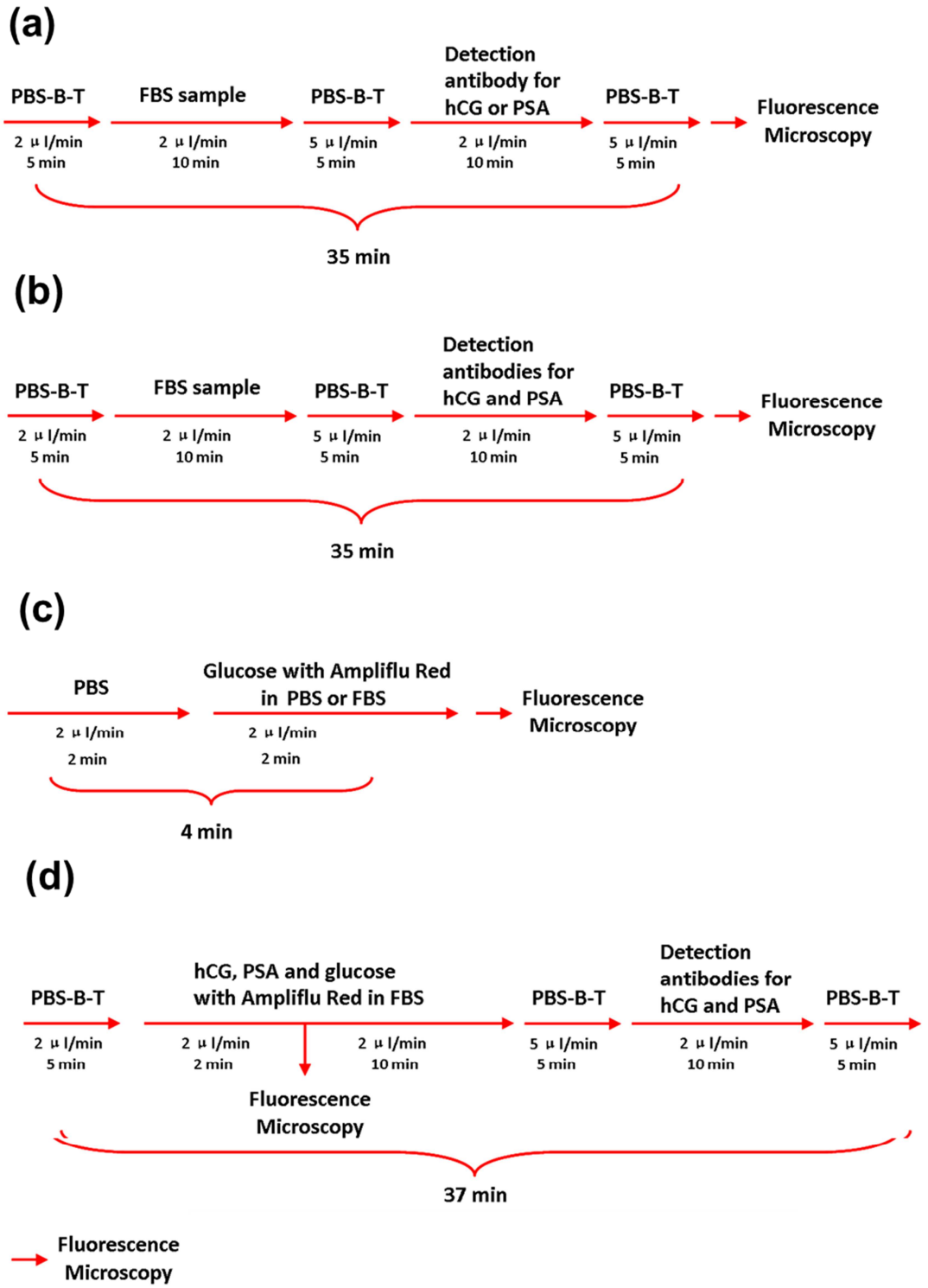

Figure 4.5 Summary of the microfluidic microbead-based biochemical assay procedures. (a) Single-plexed immunoassay. (b) Multiplexed immunoassay. (c) Enzymatic glucose assay. (d) Simultaneous immunoassay and enzymatic glucose assay.

including the first washing step, the introduction of Alexa Fluor labelled detection antibodies and the final washing step. A fluorescence image was taken afterwards to record the signal from the antibody-coated microbeads.

The procedures for different microfluidic microparticle-based biochemical assay are demonstrated in **Figure 4.5**.

4.2.6 Imaging and data analysis

All bright field and fluorescence images were taken by a Retiga 4000R CCD camera (Qimaging) mounted on a BX41 Olympus fluorescence microscope (Olympus) equipped with a Texas Red filter (560 nm excitation, 595 nm dichroic mirror and 630 nm emission, Chroma Technology). The exposure time for immunofluorescence was kept at 4s unless otherwise noted while the exposure time for the glucose assay was 2s but with the excitation light reduced by a 25% intensity grey filter (75% light blocked). The fluorescence intensity was measured by analyzing the pixel values of microparticles with Image J software (National Institutes of Health). The SEM images were recorded with a Supra 40 instrument (Carl Zeiss).

4.3 Results and discussion

4.3.1 Microparticle stability under microfluidic flow

The good stability of microparticles under microfluidic flow conditions is the prerequisite for the microfluidic assays. Thus, the stability of microparticles on our gel-based microstructures was first tested. Protein-coated microbeads immobilized on four gel pad array units and enzyme-containing microparticles immobilized on eight gel well array units were subjected to a flow of 20 μl/min (1 cm/s flow velocity) of PBS for 30 min. As shown in **Table 4.2**, the particle count result shows nearly 100% stability of microparticles after the flow test. These results indicate that the microparticles on the gel-based microstructures should sustain the shear stress in the actual microfluidic bioassays which have much lower flow velocity compared to the test flow velocity. Moreover, the position of microparticles remained unchanged after the flow test (data not shown) which makes it possible to register and encode each batch of microbeads with fixed spatial addresses.

Table 4.2 Numbers of micropaticles before and after microfluidic flow test

Type of microparticles	**No. of microparticles**		
	Before flow	**After flow**	**Stability (%)**
streptavidin coated microbeads	191	191	100
anti-hCG coated microbeads	316	316	100
anti-PSA coated microbeads	339	338	99.7
enzyme-containing microparticles	73	73	100

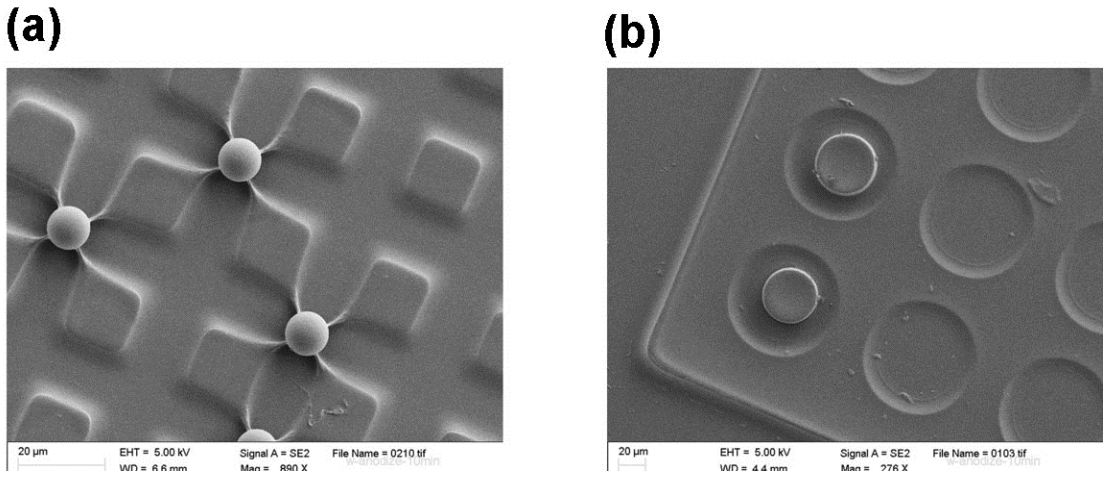

Figure 4.6 SEM images of (a) spherical streptavidin-coated polystyrene microbeads on a gel pad array and (b) cylindrical enzyme-containing PEG microparticles on a gel well array.

While gel-based microstructure provided stable immobilization for both protein-coated polystyrene microbeads and PEG-based microparticles, the immobilization mechanisms could be different. As discussed in **Chapter 3**, the gel pad array holds polystyrene microbeads through not only physical entrapment but also the adhesive force between the gel and the microbeads as indicated by the dried gel pads which were deformed by the polystyrene microbeads (**Figure 4.6a**). The adhesive force could be ascribed to the sticky nature of polyacrylamide gel which was also used as a polymeric labelling adhesive [228]. Nevertheless, the adhesion between PEG-based microparticles and gel wells was not observed (**Figure 4.6b**). This indicated that PEG-based microparticles were immobilized in gel wells merely through physical entrapment. The weak interaction between the PEG and polyacrylamide gel also allows the PEG-based microparticles which do not settle inside the microwells to be easily rinsed off by applying a flow from the side of the array.

4.3.2 Microfluidic microbead-based immunoassay for hCG and PSA

PSA and hCG were chosen as the two target analytes in this study as both of them are important serum tumor markers as described in **Chapter 3**. In our study, all samples were prepared by spiking the analytes in FBS to mimic the conditions in real human serum. Calibration curves were generated with serial dilutions of hCG (0.0625, 0.125, 0.25, 0.5, 1, 2, 4, 8, 16 ng/ml) and PSA (0.125, 0.25, 0.5, 1, 2, 4, 8, 16 ng/ml) (**Figure 4.7**). Each error bar indicates one standard deviation of three individual experiments for samples with the same analyte concentration. In addition, immunoassays with blank FBS were performed. As shown in the calibration curves, for both hCG and PSA, the fluorescence intensity is proportional to the concentration of the analytes. The assay limit of detection (LOD) was determined to be 87 pg/ml (2.4 pM or 0.79 IU/l) for hCG and 114 pg/ml (3.4 pM) for PSA as calculated by adding three standard deviations to the measured mean value of the blank measurements while the assay. Limit of quantitation (LOQ) was determined to be 169 pg/ml (4.6 pM or 1.5 IU/l) for hCG and 253 pg/ml (7.4 pM) for PSA as calculated by adding six standard deviations to the measured mean value the blank measurements. As the commonly used cut-off serum concentration of hCG for testicular cancer diagnosis is 0.5 to 1 ng/ml (15 to 30 pM [188]) and the cut-off concentration of PSA for prostate cancer diagnosis is 4 ng/ml [194], both LODs in our immunoassay are lower than these cut-off concentration levels. Compared with other state-of-the-art microfluidic microbead-based immunoassay [29, 33, 59], our immunoassay has similar or better detection limit while our microbead array are much easier to assemble and are made with materials of lower cost. As the immunoassay was done in less than 40 min using FBS sample, it can be potentially applied to the fast and sensitive analysis of hCG and PSA in real serum samples for cancer diagnostics.

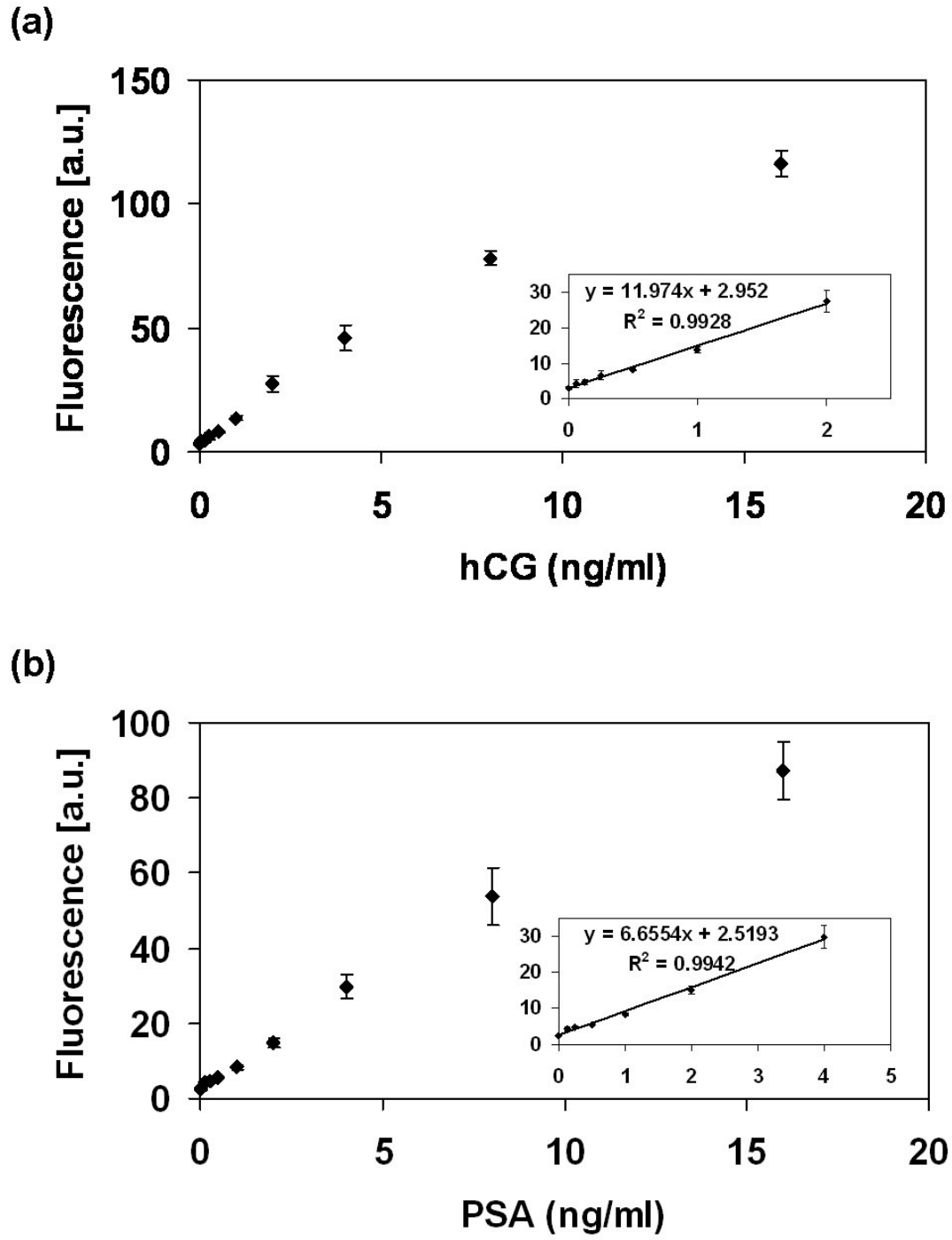

Figure 4.7 Microfluidic microbead-based immunoassay calibration curve for (a) hCG and (b) PSA in FBS.

4.3.3 Multiplexed microfluidic immunoassay for hCG and PSA

We further performed immunoassays for the simultaneous detection of multiple target tumor markers. Two types of antibody-coated microbeads were used for the detection of hCG and PSA while the bare streptavidin-coated microbeads were used as the negative control. These three types of microbeads were sequentially deposited onto the gel pad array with their spatial positions recorded after each deposition by imaging (**Figure 4.8 aI-III**). A microfluidic sandwich immunoassay for serum sample with 100 ng/ml of PSA and 1 μg/ml of hCG was performed. No microbead loss or change of position was observed after the assay (**Figure 4.8aIV**). The anti-hCG and anti-PSA microbeads showed strong fluorescence and the streptavidin microbeads showed very weak fluorescence (**Figure 4.8aV**). Only one reporter dye, Alexa Fluor 594, was used in this experiment, which allowed the detection of multiple analytes with a basic fluorescence microscope equipped with a single fluorescence filter set. This eliminates the need for complicated read-out systems such as flow cytometers or microbarcode readers. The performance of the microbead-based multiplexed immunoassays was also examined by using serum samples spiked with different combinations of two tumor markers in their cut-off concentrations. As shown in **Figure 4.8b**, in the presence of hCG or PSA, only anti-hCG or anti-PSA microbeads showed strong fluorescence, while in the presence of both hCG and PSA, both anti-hCG and anti-PSA microbeads showed strong fluorescence. With no analyte in the sample, both anti-hCG and anti-PSA microbeads showed very weak fluorescence. In all the experiments, the streptavidin-coated microbeads which were used as the negative control showed weak fluorescence signals. These results indicated the high-specificity of the antibodies used in this study which eliminated the cross reaction between antibodies and non-specific analytes.

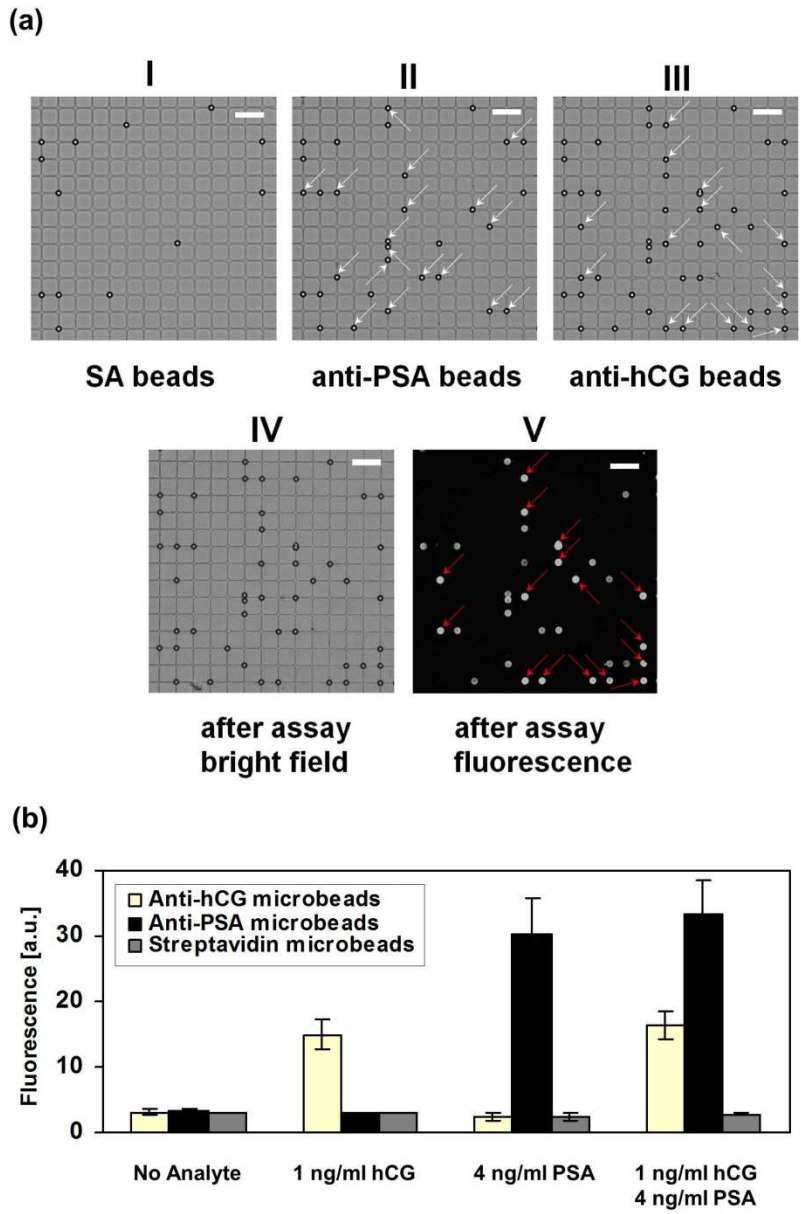

Figure 4.8 Multiplexed microfluidic immunoassay for hCG and PSA. (a) Multiplexed immunoassay using spatially encoded microbeads. (I) to (III) the deposition of three batches of microbeads: streptavidin (I), anti-PSA antibody (II) and anti-hCG antibody coated microbeads (III). The latter two batches of microbeads are arrowed out. (IV) Bright field image after the immunoassay. (V) Fluorescence image after the immunoassay. Anti-hCG microbeads are arrowed. The scale bars represent 50 μm. (b) Multiplexed immunoassay for samples with different combinations of analytes.

Although only three batches of microbeads were shown here, by controlling the density of microbeads in solution, more batches of microbeads can be sequentially

arrayed. In **Chapter 3**, we demonstrated the deposition and spatial encoding of 10 batches of streptavidin-coated microbeads with no microbeads loss or change of position. To test whether the deposition process could influence the biofunctionality of antibody on the microbeads, a microfluidic immunoassay was performed on a gel pad array unit with 10 batches of anti-hCG microbeads pre-immobilized. Serum sample spiked with high concentration of hCG (2 μg/ml) was used to saturate all antibody-binding sites on the microbeads resulting in the maximum signals. As shown in **Figure 4.9**, the signal intensity of batch 1 microbeads was found to be ~85% compared to the signal intensity of batch 10 microbeads which was normalized to 100%. The reduction in signal intensity could result from a loose of antibody biofunctionality e.g. by the drying process during depositions. However, a sufficient high percentage of antibody remains intact to perform successful immunoassays. Thus, with the potential integration of antibody pairs for other tumor markers, our microfluidic microbeads-based immunoassay platform could be promising for the diagnosis of different cancers from a single assay.

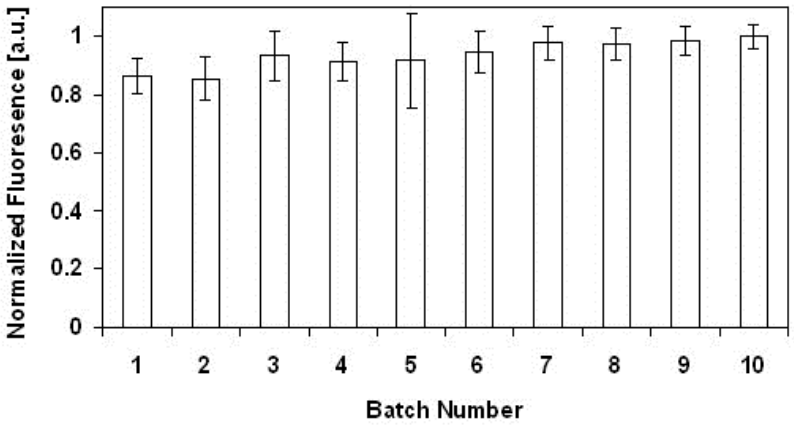

Figure 4.9 Biofunctionality of antibody-coated microbead batches. 10 batches of anti-hCG microbeads were deposited sequentially and fluorescence signals after performing an hCG assay were recorded. Error bars represent the 1X S.D. of the fluorescence intensity of every batch of microbeads. The average fluorescence intensity of batch 10 microbeads is normalized to 1.

4.3.4 Microfluidic microparticle-based enzymatic assay for glucose

PEG based cylindrical microparticles which contain GOx and HRP were used for enzymatic glucose assays. The crosslinked PEG-DA has the appropriate pore size to entrap the big enzyme molecules while allowing small molecules, such as glucose, hydrogen peroxide and Ampliflu Red, to diffuse through [119, 120]. The fabricated microparticles, as shown in **Figure 4.10**, had a good monodispersity with average lateral diameter of 51.8 ±1.7 μm in the PBS buffer. The distribution of the microparticle sizes is shown in **Figure 4.10b**.

The detection of glucose with the microparticles was through a coupled bi-enzymatic reaction previously reported [229]. The principle of the assay is shown in **Figure 4.11**. Once the sample flows through the microparticles, the GOx turns the glucose into gluconolactone and H_2O_2. With the catalysis of HRP, H_2O_2 reacts with the non-fluorescent Ampliflu Red to generate strongly fluorescent resorufin. The resorufin can

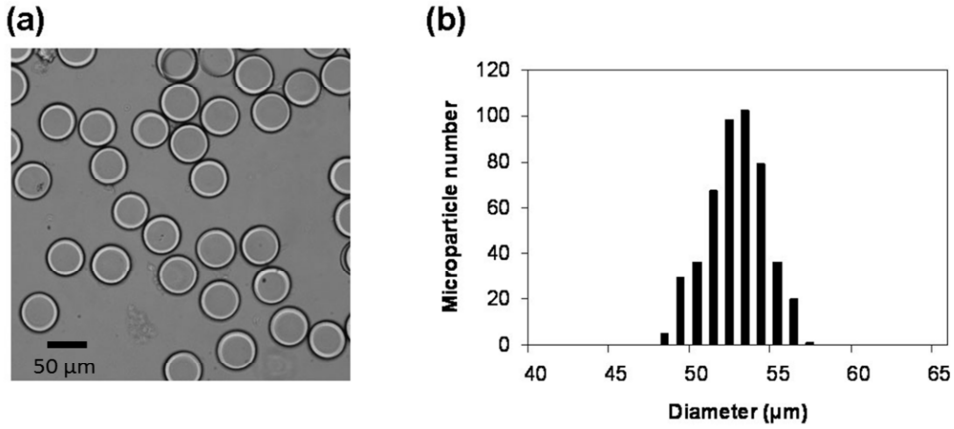

Figure 4.10 Enzyme-containing microparticles. (a) Bright field image of enzyme-containing cylindrical microparticles. (b) Size distribution of microparticles.

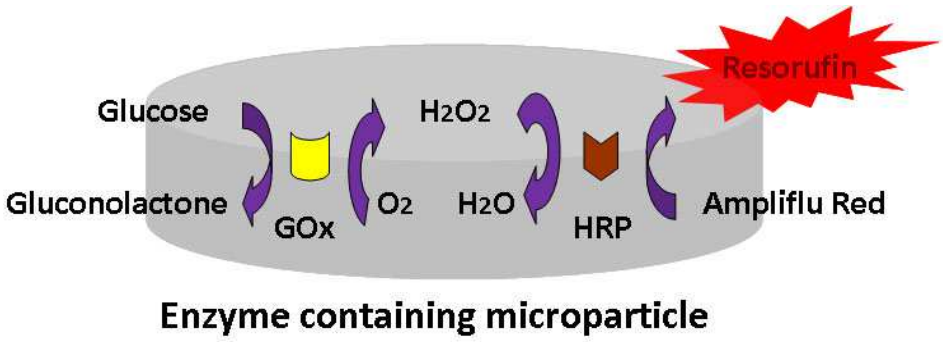

Figure 4.11 Microparticle-based enzymatic glucose assay principle.

then diffuse out of the PEG gel based microparticles. With the continuous feed of the glucose sample in microchannel, equilibrium is reached between the generation of resorufin inside the microparticle and the diffusion of resorufin out of the microparticle. The equilibrium results in a constant fluorescence intensity of the gel microparticles. In principle, this fluorescence intensity should be proportional to the concentration of glucose in the sample.

To develop quantitative microfluidic glucose assay, we first examined the time-dependent fluorescence intensity of microparticles using 5 mM glucose sample in either PBS or FBS. The sample was introduced into the channel at 2 μl/min for 5 min and fluorescence images were taken every 10 s. With both PBS and FBS samples, the fluorescence intensity of microparticles gradually increased until it reached a steady state value after 2 min (**Figure 4.12a**). Therefore, for the quantitative detection of glucose, all the fluorescence images were taken right after 2 min flow through of sample. Microparticle-based enzymatic glucose assay were then performed to analyze a serial dilution of PBS and FBS samples spiked with 1.25, 2.5, 5 and 10 mM of glucose which covers the physiological glucose range (3 to 6 mM). The calibration curve for glucose is shown in **Figure 4.12b**. Each error bar indicates one standard deviation of three individual experiments for samples with the same concentration. We found a proportional relationship between the microparticle fluorescence intensity and the glucose concentration. Interestingly, the fluorescence signals arisen from the FBS samples were significantly lower than the signals arisen from the PBS samples. This could be attributed to the antioxidant species (uric acid and ascorbic acid etc.) in the FBS which consume the H_2O_2 generated by the first enzymatic reaction and thus reducing the amount of resorufin generated in the second enzymatic reaction. Compared with previous reported works which employed packed enzyme-containing microparticles for microfluidic assay of glucose spiked in buffer [49, 219], we used spatially separated microparticles which minimized the crossed contamination of resorufin diffused from one particle into another. As the cut-off concentration of fasting plasma glucose is 7.0 mM [230], our microparticle array could be potentially used for the diagnosis of *diabetes mellitus* using real human plasma sample.

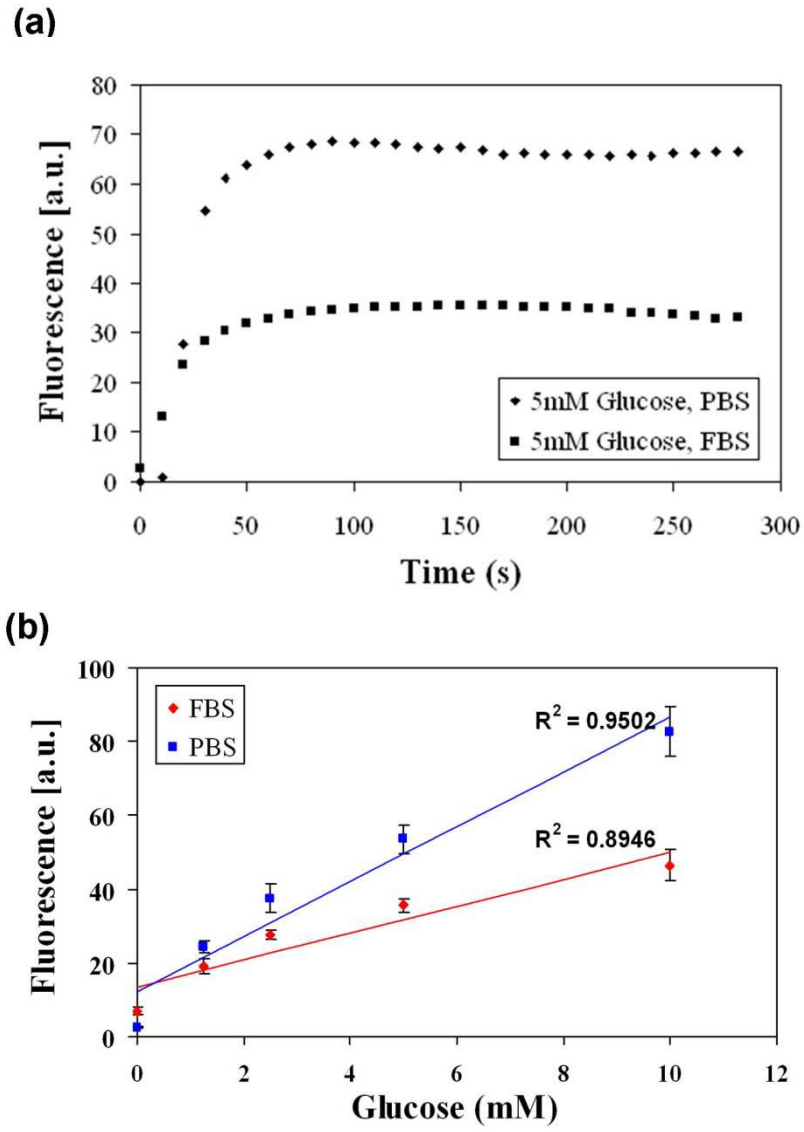

Figure 4.12 Microfluidic microparticle-based enzymatic glucose assay. (a) Time dependent fluorescence of enzyme containing microparticles in the presence of 5 mM of glucose in either PBS or FBS. (b) Calibration curve for glucose in either PBS or FBS.

Similar to the reuse of gel pad array as discussed in **Chapter 3**, the gel well array can also be reused by removing PEG-based microparticles. As shown in **Figure 4.13**, PEG microparticles can be removed from the gel wells array after 15 min sonication in pure ethanol. The re-deposited new batch of PEG microparticle (**Figure 4.13c**) can sustain the microfluidic flow after the 30 min flow test (**Figure 4.13d**) with no loss of microparticles. Furthermore, if desired, the PDMS microchannel can also be reused

after sonication in PBS-T (1X PBS, 0.05% w/v Tween 20) for 30 min and subsequent sonication in 100% ethanol for 30 min.

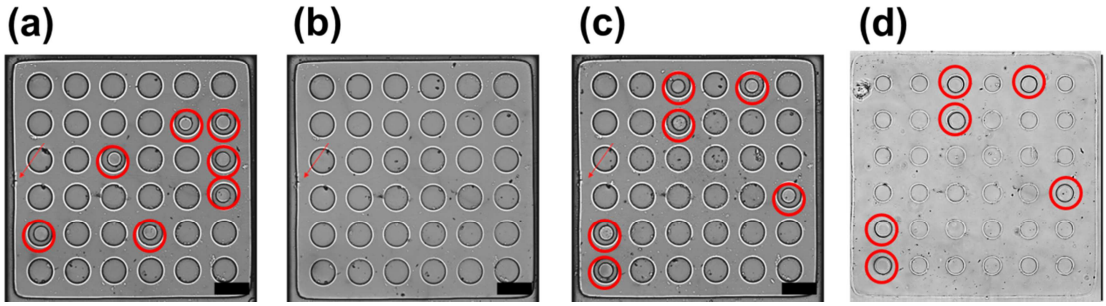

Figure 4.13 Reuse of gel well array unit. (a) Deposited with microparticles; (b) Subsequent sonication in 100% ethanol for 15 min to remove microparticles; (c) Deposited with a new batch of microparticles; (d) Subjected to fluid flows (PBS at 20 µl/min for 30 min). The microparticles are circled out. Gel-based microstructures with small defects (red arrowed) were intentionally used to demonstrate that the same arrays were employed. Scale bars represent 50 µm.

4.3.5 Simultaneous detection of proteins and glucose in serum

The mixed gel structure array which contains both 60 µm microwells and 20 µm micropads was used for the sequential immobilization of enzyme-containing cylindrical microparticles and antibody-coated spherical microbeads. The enzyme-containing microparticles were deposited first (**Figure 4.14a**) as the smaller spherical microbeads can also sit in the microwells thus impeding the settlement of bigger cylindrical microparticles. The antibody-coated microbeads were then deposited and encoded by their spatial positions with bright field microscopic images (**Figure 4.14b** and **c**). A microfluidic bioassay was then performed to analyze a FBS sample spiked with 5 mM glucose, 100 ng/ml of PSA and 1 µg/ml of hCG. After the sample was flowed through for 2 min, the enzyme-containing microparticles showed strong fluorescence while all antibody-coated microbeads remained non-fluorescent (**Figure 4.14d**). This result indicated that there was no non-specific absorption of the resorufin,

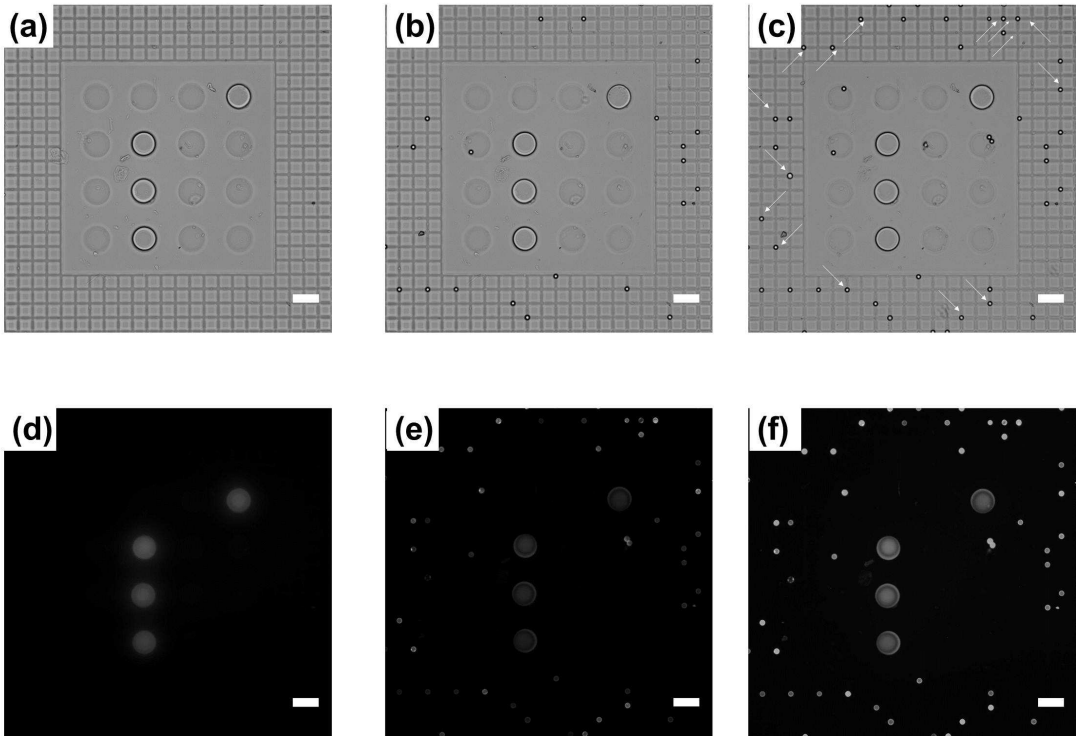

Figure 4.14 Simultaneous immunoassay and enzymatic assay for the detection of proteins and glucose. (a) Deposition of enzyme-containing microparticles. (b) Deposition of anti-PSA antibody-coated microbeads. (C) Deposition of anti-hCG antibody-coated microbeads which are arrowed out. (D) Fluorescence image taken with a 25% excitation light intensity filter after the enzymatic glucose assay. (E) Fluorescence image taken with a 25% excitation light intensity filter after the immunoassay. (F) Fluorescence image taken with no excitation light filtered after the immunoassay. Anti-hCG microbeads were arrowed out. The scale bars represent 50 μm in all the figures.

which diffused out of the enzyme-containing microparticles, onto the antibody-coated microbeads. After completion of the immunoassay, while the antibody-coated microbead became fluorescent, the fluorescence from the enzyme-containing microparticles was reduced as the majority of resorufin was washed away during the washing steps for the immunoassay (**Figure 4.14e**). A clearer image of the fluorescence from the antibody-coated microbeads is shown in **Figure 4.14f** which was taken through higher intensity of excitation light. Thus, the signals from the enzymatic assay and the signals from the immunoassay can be analyzed using the two images taken after 2 min of sample introduction (**Figure 4.14d**) and taken after the

completed immunoassay (**Figure 4.14f**). Notably, the fluorescence from the enzymatic assay (resorufin) and from the immunoassay (Alexa Fluor 594) was also detected by the same Texas Red filter set. Compared to the recently reported work for simultaneous immuno- and enzymatic assays using hydrogel-patterned nanofiber [231], our microfluidic assay based on microparticle array chip requires shorter assay time, has additional capability for simultaneous analysis of multiple antigens and is reusable. Thus, our microfluidic microparticle array platform could be potentially used for the fast and low-cost diagnosis of diabetes as well as testicular cancer and prostate cancer in a single bioassay. As immunoassay and enzymatic glucose assay represent two important types of biochemical assays, binding kinetic based assay and reaction kinetic based assay, the application of our microparticle array could be extended for the multiplexed detection of other categories of biomolecules, for example, DNAs (through binding kinetic based hybridization assay) [232] and other small metabolites, such as alcohol [39], choline [229] and uric acid (through reaction kinetic based enzymatic assays).

4.4 Conclusion

In this chapter, we integrated the gel based microstructure chip into a microfluidic platform for the microparticle-based bioassays. The integrated microfluidic platform was utilized for the quantitative fluorescence sandwich immunoassay for hCG and PSA in serum samples with LODs determined to be 87 pg/ml and 117 pg/ml respectively, which are one order lower than the cut-off concentration for cancer diagnosis. Enzymatic glucose assays were also performed using enzyme-containing PEG microparticles which were immobilized on novel gel well array. The glucose

assay had a dynamic response range from 0 – 10 mM which covers not only the physiological serum glucose level but also the threshold concentration for the diagnosis of *diabetes mellitus*.

The multiplexing capability of our microfluidic microparticle array platform was first validated by the multiplexed immunoassay for hCG and PSA using spatially encoded microbeads. We also demonstrated simultaneous detection of hCG, PSA and glucose using microparticles immobilized on novel mixed microstructure array. A single wavelength fluorescent readout (Texas Red) with a common microscope was used to distinguish spatially encoded microparticles thus eliminating the need for complicated read-out systems. To the best of our knowledge, this is the first microfluidic microparticle array platform which enables the simultaneous immunoassay and enzymatic assay for the detection of different categories of biomolecules. This low cost, versatile and reusable microfluidic microparticle array platform could be promising for the rapid clinical diagnosis of multiple diseases which are related to either protein markers and/or metabolites through the analysis of real serum samples or other biofluidic samples.

Chapter 5

Integrated microbead array in PEG-based capillary system for immunoassay

Chapter 5 - Integrated microbead array in PEG-based capillary system for immunoassay

5.1 Introduction

Point-of-care biomedical tests play an important role in the clinical diagnostics as they provide reliable results with less time, less sample volume, less assay steps, more simplified equipment and much lower cost as compared to the conventional biomedical assays performed in a specialized lab [233]. One example is the lateral flow test strip which integrates immunosensing elements into a simple membrane sheet and allows the qualitative or semi-quantitative detection of proteins in tens of microliters of blood or urine in 10 - 20 min without the requirement of any complicated equipment [162]. Microfluidic biochemical assay, with its fast reaction kinetics as well as the minute sample volume required, is a promising candidate to be applied to point-of-care diagnostics, especially for sensitive and quantitative determination of biomolecules in biofluids [234]. In conventional microfluidic biochemical assays, the samples and reagents are delivered by external pumping elements such as peristaltic pumps, syringe pumps and centrifugation devices. However, these external pumping elements usually consist of bulky operation units as well as external power source, thus making the microfluidic system not ideal for point-of-care applications. It is thus demanded to develop passive pumping techniques which integrate pumping element inside a microfluidic system to substitute external pumps for point-of-care microfluidic assays.

As reviewed in **Chapter 2**, a most frequently used passive pumping method is the capillary pressure (surface tension) driven pumping which employs wettable microstructures inside microfluidic networks to draw the fluid and to form a "microfluidic capillary system" for the application in external pump free microfluidic biochemical assays [36]. In such a microfluidic capillary system, the flow rate of the samples and reagents can be "programmed" by alternating the geometry of the microstructures [147] and the surface wettability (capillary pressure) of these microstructures [235]. The major biomedical application so far for microfluidic capillary systems is in the fast and sensitive quantitative immunoassays which are not applicable for lateral flow test strips [148]. Juncker et al. [36] pioneered the utilization of silicon based capillary systems for on-chip immunoassays. Reagents were delivered to the detection zone by simple sequential pipetting to the inlet and the tedious washing steps involved in conventional ELISA was totally avoided. Meanwhile, with this capillary system, detection limit for target protein in the picomolar concentration level was achieved [163] which is comparable to the ELISA method. Hereafter, an one-step immunoassay was developed on this capillary system as the user only needs to fill the inlet with one droplet of blood and wait for the final result to come out [149]. Moreover, a multiplexed immunoassay was also integrated into the capillary system as recently reported by Wang et al. [161] with a glass-polymer hybrid chip.

For most immunoassays performed in capillary systems, the antibody which serves to capture the target protein from the sample is patterned on a planar substrate such as a PDMS surface [150] or a glass surface [155]. As discussed in **Chapter 3**, three dimensional surfaces on microbeads enable more antibody molecules to be immobilized per unit of area and faster reaction kinetics as compared to planar substrate surface. However, in contrast to antibodies immobilized on planar surfaces,

the integration of antibody conjugated microbeads into a capillary system was rarely reported. Kim et al. [159] reported the introduction of packed microbeads in a polymer based capillary system for immunoassays. Total fluorescence signals from packed microbeads were correlated to the goat IgG concentration for quantitative analysis. However, this capillary system is less likely to be compatible with multiplexing protein analysis as encoding different microbeads from a packed cluster is very challenging. So far, there is still no report for multiplexed microbead-based immunoassay in a capillary system.

In this chapter, a microfluidic chip is developed which, for the first time, integrates a microbead array into a capillary system for multiplexed immunoassays. The chip is based on a novel PEG-based capillary system for liquid delivery and a polyacrylamide gel pad array for microbead array assembly. Photopolymerization reactions are utilized for the fabrication of both capillary system and gel pad array with no cleanroom work involved during the fabrication. The filling time and flow rate of different fluids in the PEG-based capillary system can be altered by simple modification with different concentration of surfactant solution. On-chip sandwich immunoassays for PSA and hCG in serum samples are performed to validate the performance of the chip. Finally, the multiplexed immunoassays for PSA and hCG are demonstrated on the chip to verify its capability for multiplexed protein analysis. This microfluidic chip could be promising for the detection of multiple protein markers in real human serum sample for point-of-care diagnostics.

5.2 Materials and Methods

5.2.1 Materials and reagents

Microscopic glass slides were purchased from Corning. Polydimethylsiloxane (PDMS) prepolymer (Sylgard 184) was purchased from Dow Corning. Sodalime hard masks were purchased from Infinite Graphic (Singapore). Streptavidin-coated polystyrene microbeads (~10 μm in diameter) were purchased from Bangs Laboratory. Repel silane (Dimethyldichlorosilane, 2% solution in octamethylcyclotetrasiloxane) was purchased from GE healthcare. Acrylamide/Bis-acrylamide solution (40%, 19:1), Poly(ethylene glycol) diacrylate (PEG-DA, Mw 575 Da), bovine serum albumin (BSA), N,N,N',N'-Tetramethylethylenediamine (TEMED), 3-(Trichlorosilyl)propyl methacrylate (TPM), Tween® 20, (+)-Biotin N-hydroxysuccinimide ester (biotin-NHS), DMPA, heptane and recombinant hCG were purchased from Sigma-Aldrich. Ethanol was purchased from Fisher Chemicals. PBS was purchased from 1st Base. Alexa Fluor 594 NHS ester and fetal bovine serum (FBS) were purchased from Invitrogen. PSA, monoclonal anti-PSA clone 5 antibody, monoclonal anti-PSA clone 7 antibody, monoclonal anti-β-hCG clone 1 antibody and polyclonal goat anti-whole hCG antibody were purchased from Arista Biologicals. Deionized water was produced by Arium® 611 UV system (Sartorius AG).

5.2.2 The fabrication of the chip with capillary system and gel pad array

5.2.2.1 The chip design

The chips with capillary system and gel pad array were fabricated on microscopic glass slides with the dimension of 75 mm (L) x 25 mm (W) x 1 mm (H). The design

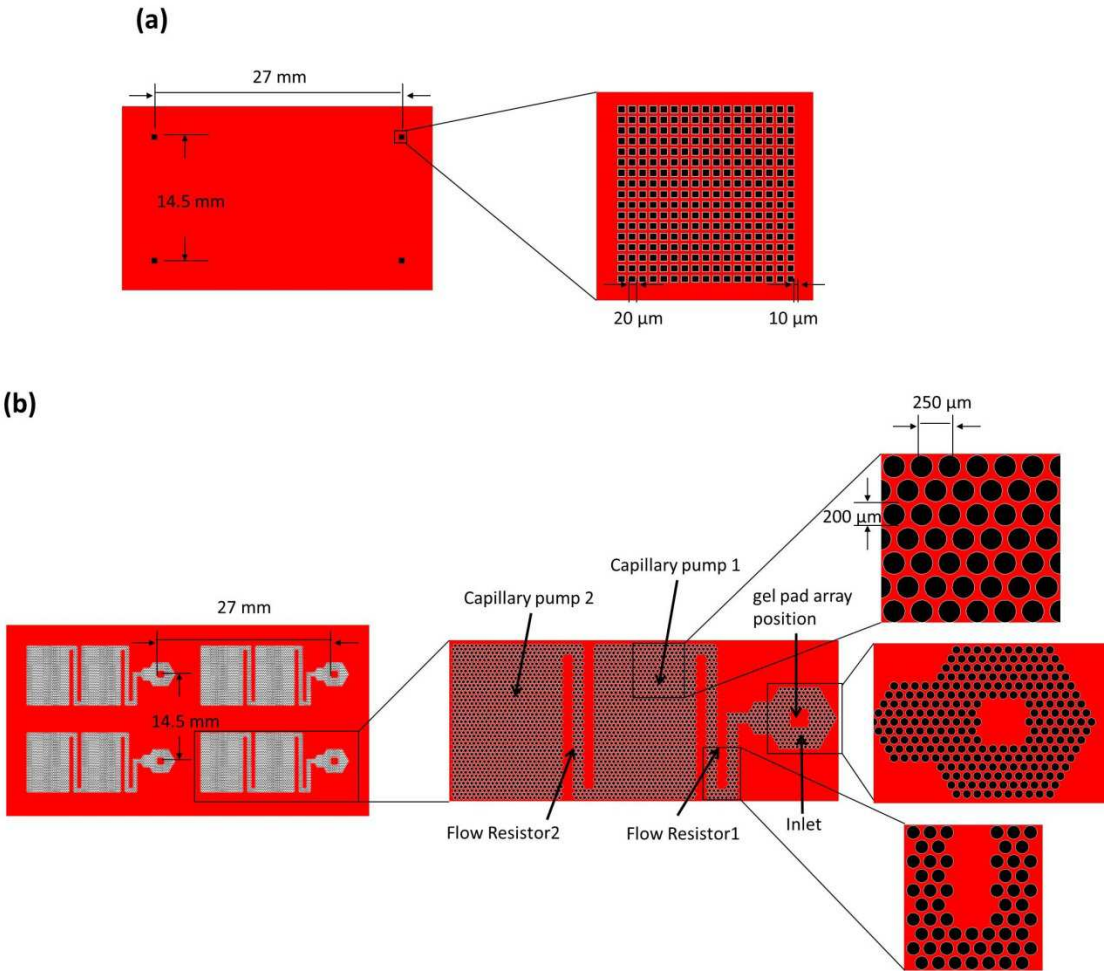

Figure 5.1 The mask design for chip. Red area is chrome coated and black area is kept clear. (a) The design for polyacrylamide gel pad array units. Left: design of four gel pad array units on chip; Right: a single gel pad array unit; (b) The design for PEG-based capillary system. Left: design of four capillary systems on chip; Middle: a single capillary system; Right: design of the components of a capillary pump.

of the masks was done in AutoCAD software (Autodesk). The design of the masks allowed the fabrication of four polyacrylamide gel pad array units (**Figure 5.1a**) to be integrated into four PEG-based micropillar-rings (**Figure 5.1b**). Feature for each gel pad array unit remained the same as the feature in **Chapter 3** and **4**, which contains 17 x 17 square gel pads (20 µm x 20 µm) with 10 µm gap (**Figure 5.1a**). The design of the capillary system contains one inlet for the integration of the gel pad array unit, two flow resistor areas and two capillary pump areas (**Figure 5.1b**). All these components consist of 200 µm diameter circles with 50 µm gap between each other (**Figure 5.1b**).

The entire features on the mask design cover an area of approximately 50 mm x 23 mm which fits well onto a microscopic glass.

5.2.2.2 Fabrication process

The fabrication process for the chip consists of three steps:

(1) Surface modification of the glass slides.

The glass slides were sequentially cleaned with ethanol, detergent and deionized water. They were then treated with 30% H_2O_2 for 30 min. These glass slides were subsequently treated with 5 mM TPM solution (4:1 heptane and chloroform [120]). The silanized glass slides were cleaned with ethanol and deionized water before being stored in a clean microscopic slide storage box.

(2) Fabrication of polyacrylamide gel pad units through photopolymerization.

The mask with features of gel pad array units was pre-treated with Repel Silane for 15 min to prevent the attachment of polyacrylamide gel. Next, a 10% acrylamide/bisacrylamide precursor solution doped with 0.02% (w/v) DMPA and 1.2% (v/v) TEMED was transferred into the gap between the photomask and a TPM treated glass slides through capillary action. The height of the gap is defined by a pair of 12 μm spacers. The solution was then UV exposed under a fluorescence microscope equipped with a mercury lamp, a 4X magnification lens and a DAPI filter (350 nm excitation). The power of the UV light was ~150 mW/cm^2. Each gel pad array unit was exposed for 1 min which made the total fabrication time of 4 min. The glass slide with four patterned gel pad array units was then detached from the mask and washed with ethanol and deionized water.

(3) Fabrication of PEG capillary system through photopolymerization.

The hard mask with features of capillary systems was spin coated with a thin layer of PDMS at the speed of 4000 rpm and was subsequently baked at 65 °C on a hotplate for 1 hour to cure the PDMS. This step is to prevent the adhesion between the PEG-DA and the mask which ensures that polymerized PEG microstructures are not detached from the glass slide [236]. The PDMS modified hard mask was then manually aligned with the gel pad arrays on the glass slide to make sure each array unit was in the center of the inlet of the capillary system. A pair of 150 μm spacers was used to define the height of the gap between mask and the glass slide. The mask-spacers-slide apparatus was then clamped from the side to prevent movement. Subsequently, pure PEG-DA pre-dissolved with 5% (w/v) DMPA was transferred into the gap. The apparatus was then put into the center of the chamber in a UV crosslinker (365 nm excitation; power of ~4 mW/cm^2) and exposed with appropriate dose of UV. The chip with both gel pad array and PEG capillary system was then detached from the mask and washed with ethanol. Next, the chip was immersed into pure ethanol and stripped at 60 rpm on a rotator for 5 min to completely remove the unpolymerized PEG-DA residues and was then rinsed with deionized water to remove the ethanol. Finally, the chip was completely dried at 60 °C in an incubation oven for 10 min and then put in a clean petri dish and stored in a dry cabinet. The fabricated capillary system has approximately 15 μl of volume. It is also noted that the assembly of the mask and the glass slides is done in a laminar flow cabinet to minimize the particle contamination and the PDMS coated mask can be cleaned with ethanol and reused for at least 50 times without the need for a new coating.

The fabrication process is shown in **Scheme 5.1** while the fabricated chip was shown in **Figure 5.2**.

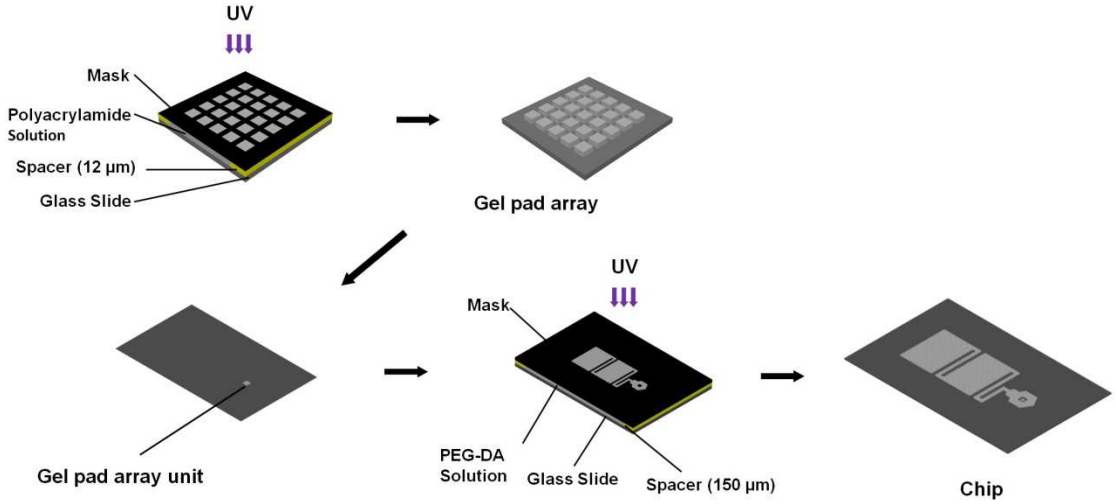

Scheme 5.1 Fabrication process of the chip.

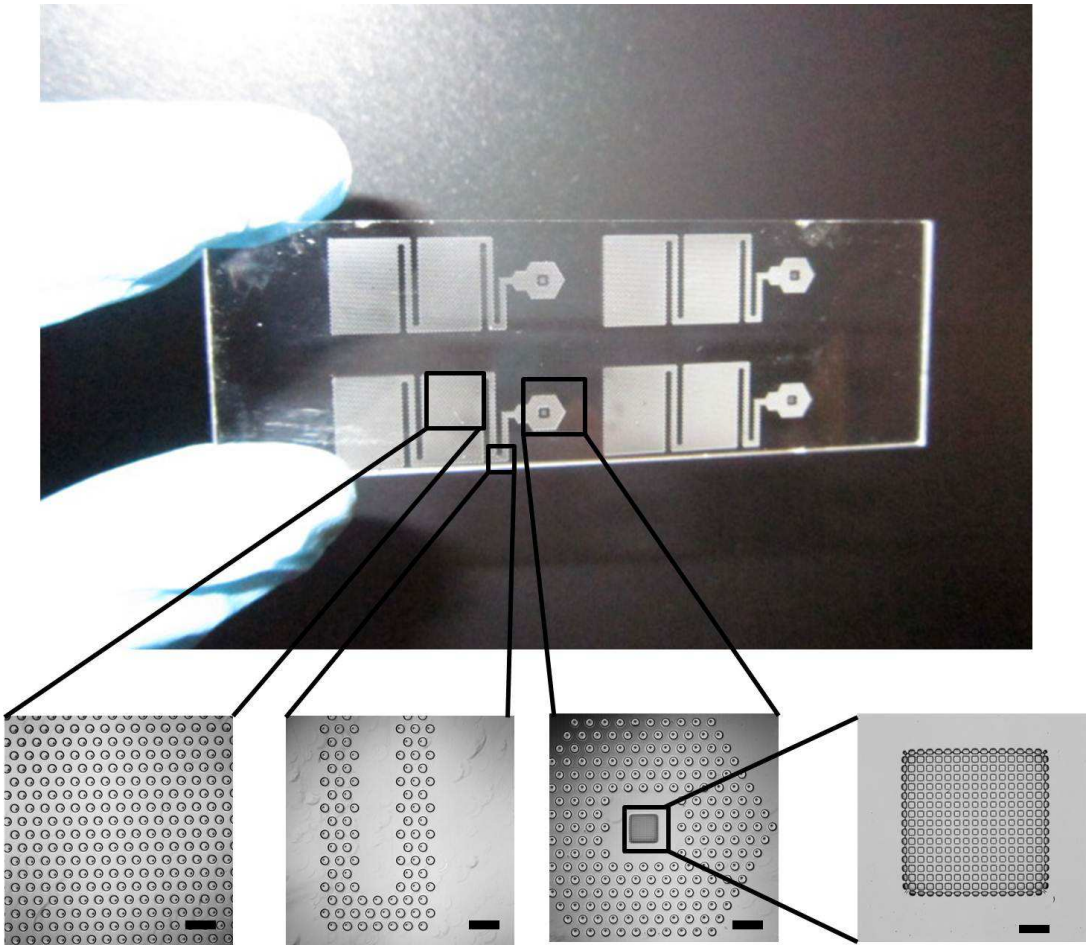

Figure 5.2 The capillary system chip integrated with gel pad arrays. Top: the chip with capillary system and four gel pad array units. Bottom from left to right: capillary pump region; flow resistor area; inlet; gel pad array unit. Scale bars represent 500 µm in images except the bottom rightmost image in which, the scale bar represent 50 µm.

5.2.2.3 Surface modification of the capillary system

The surface modification of the capillary system was done with a simple two-step procedure (**Scheme 5.2**). 20 µl of Tween® 20 solution was first pipetted onto the downstream 2nd capillary pump area on the chip. The chip was then immediately placed into a homemade wet chamber (100% humidity) to prevent evaporation. The solution autonomously filled the entire capillary system through capillary action. As polymerized PEG (contact angle of ~40°) has more hydrophilic surface than a TPM treated glass slide (contact angle of ~70°), the solution was trapped inside the PEG capillary system. Subsequently, the chip was immediately dried in an oven at 60 °C for 10 min to evaporate out all the solution and let Tween® 20 to adsorb onto the surface of the capillary system. The modified chip was stored in the dry cabinet.

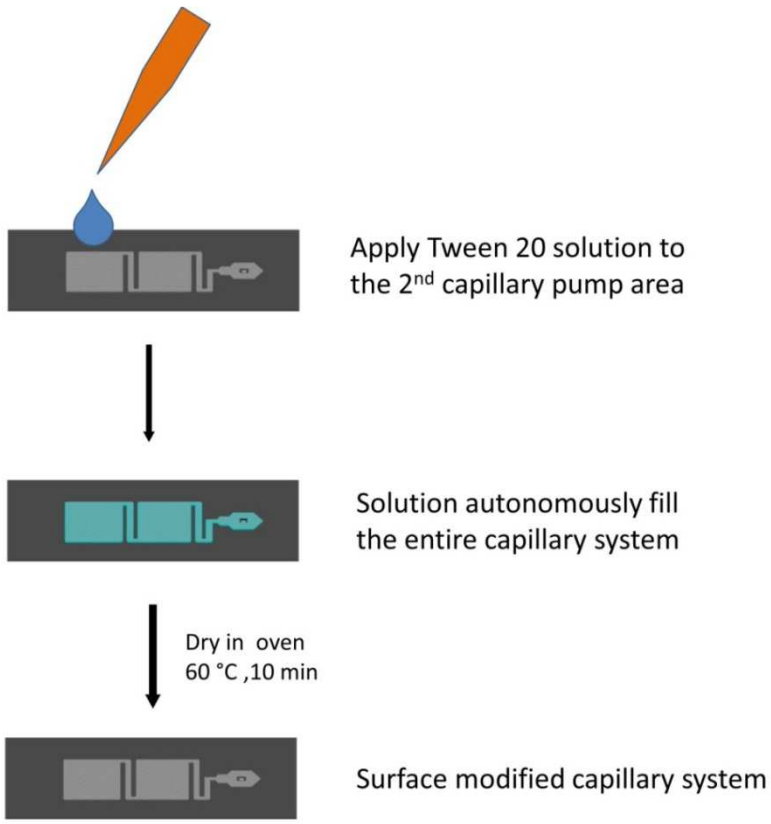

Scheme 5.2 Method for surface modification of PEG capillary system.

5.2.3 Flow test of the capillary system

Flow tests were done on chips with the PEG capillary systems in a homemade wet chamber at RT (~22 °C). All the tests were done within 48 hrs after the surface modification of the capillary system. Three kinds of liquid, FBS, PBS-B-T solution (1X PBS, 1% BSA and 0.05% Tween® 20) and deionized water, were tested on the capillary system modified with different concentration of Tween® 20 solution (0.005, 0.01, 0.02, 0.05% v/v). The liquid was pipetted onto the inlet in three consecutive steps with a volume of 5 μl for each pipetting step and a total volume of 15 μl. After each step, the fluid was allowed to autonomously flow into the capillary system, and the filling time was recorded from the pipetting of fluid to the stop of the fluid front. Right after the stop of the fluid front, the next pipetting was conducted. The total flow time was calculated by adding the filling time for three pipetting steps together.

5.2.4 Preparation of antibody-coated microbeads

The methods for the preparation of anti-hCG and anti-PSA microbeads are the same with the methods mentioned in **Chapter 3**. Thus, it is omitted here.

5.2.5 On-chip immunoassay protocol

For single-plexed immunoassays of hCG and PSA, 0.1 μl solution of antibody-coated microbeads (~500 beads/μl) was first pipetted onto a gel pad array unit. These microbeads settled down and were immobilized onto the gel pad array after the solution was evaporated out in ~2 min. The chip was then placed into a homemade wet chamber (100% relative humidity). The subsequent on-chip immunoassay was done in

three steps. First, 5 μl of FBS spiked with hCG or PSA was applied to the gel pad array and was allowed to autonomously fill the capillary system. Next, immediately after all the sample flow into the capillary system, 5 μl of FBS with 2 μg/ml of fluorescence detection antibody was pipetted onto the gel pad array. Finally, after the detection antibody was flowed through, 8 μl of PBS-B-T solution was applied to the inlet to wash out the unbound target analyte as well as the excess detection antibody. The total volume of liquid added is a little more than the volume of the capillary system to ensure that a layer of liquid was on the gel pad array which was to be imaged in hydrated conditions. A fluorescent image of the microbeads on the gel pad array was then taken with a microscope.

For multiplexed immunoassays, two batches of microbeads, anti-hCG microbeads and anti-PSA microbeads, were sequentially deposited onto the gel pad array employing the same deposition procedure for single-plexed assay. After each deposition process, 0.1 μl of PBS was added to the array region and an image was immediately taken to record the spatial address for every microbeads on hydrated gel pad array. The following immunoassay procedures were similar to the single-plexed immunoassay except that FBS samples were spiked with both analytes (PSA and hCG) and FBS with detection antibody for both analytes was used.

5.2.6 Imaging and data analysis

All bright field and fluorescence images were taken by a CCD camera (Retiga 4000R, Qimaging) mounted on a BX41 Olympus fluorescence microscope (Olympus) equipped with a Texas Red filter (560 nm excitation, 595 nm dichroic mirror and 630

nm emission, Chroma Technology) and a mercury arc excitation source. The exposure time for immunofluorescence imaging was kept at 4 s unless otherwise noted. The fluorescence intensity was measured by analyzing the pixel values of microparticles with Image J software (National Institutes of Health).

5.3 Results and discussion

5.3.1 Optimization of fabrication of PEG microstructures

Microstructures in a microfluidic capillary system can be fabricated with conventional microfabrication methods such as photolithography and etching [36], injection molding [152], hot embossing [153], soft-lithography [154, 155] and replica molding [159, 160]. Photolithography and etching method for silicon based substrate, which usually requires multi-step process in cleanroom with expensive equipment, is relatively tedious and uneconomical. Other methods, which are usually utilized to fabricated microstructures on polymer based substrate, are with less fabrication steps and with much lower material cost. Nevertheless, these methods all require certain micromolds with its fabrication still involving multi-step process in cleanrooms.

In this study, we utilized the photopolymerization method to fabricated PEG micropillars on the glass slides. PEG-DA was chosen as the material not only because it is photo-curable but also due to the protein-repellent property of polymerized PEG which is suitable for immunoassay applications [184]. The fabrication method requires no pre-fabricated micromolds, no fabrication work in cleanroom and no expensive equipment. The fabrication time is ~20 min which includes all post-exposure steps. To optimize the fabrication process, the effect of UV exposure dose on the resulting PEG

microstructures was first examined. As shown in **Figure 5.3a**, cone-like structures were formed with low dose of UV exposure (18 mJ/cm^2). These cones are unstable as the dimension of the bottom is much smaller than the top, and therefore these microstructures collapsed upon the detachment of the glass slide from the hard mask. The formation of these cones indicates the undercure of deeper layer of the prepolymer which could be attributed to the absorption of UV light by the surface layer which reduced the penetration of incident light to the lower layer [237]. By increasing the exposure dose to 26 mJ/cm^2, more UV light is allowed to penetrate the surface layer and thus cylindrical PEG micropillars can be formed as shown in **Figure 5.3b**. However, when exposure dose further increased to 34 mJ/cm^2, the PEG micropillars crosslinked with each other in the bottom as shown in **Figure 5.3c**. As the exposure time was elongated, the crosslinked structures could arise from the increase of free radicals which diffuse out and react with the peripheral monomers or from the diffraction effect of the UV light. The effect of the exposure dose with the dimension of the PEG micropillars is demonstrated in **Figure 5.3d**. The diameter of the micropillars increases with the increase of the exposure time. Moreover, when the exposure dose rises to 30 mJ/cm^2, the crosslinking between the micropillars emerges. These crosslinked micropillars are not desired as its effect on the flow behavior of liquid in the capillary system is unpredictable. Thus, for later fabrication of PEG micropillars for capillary system, exposure dose of 26 mJ/cm^2 was employed to prevent the formation of either cone-like microstructures or crosslinked micropillars.

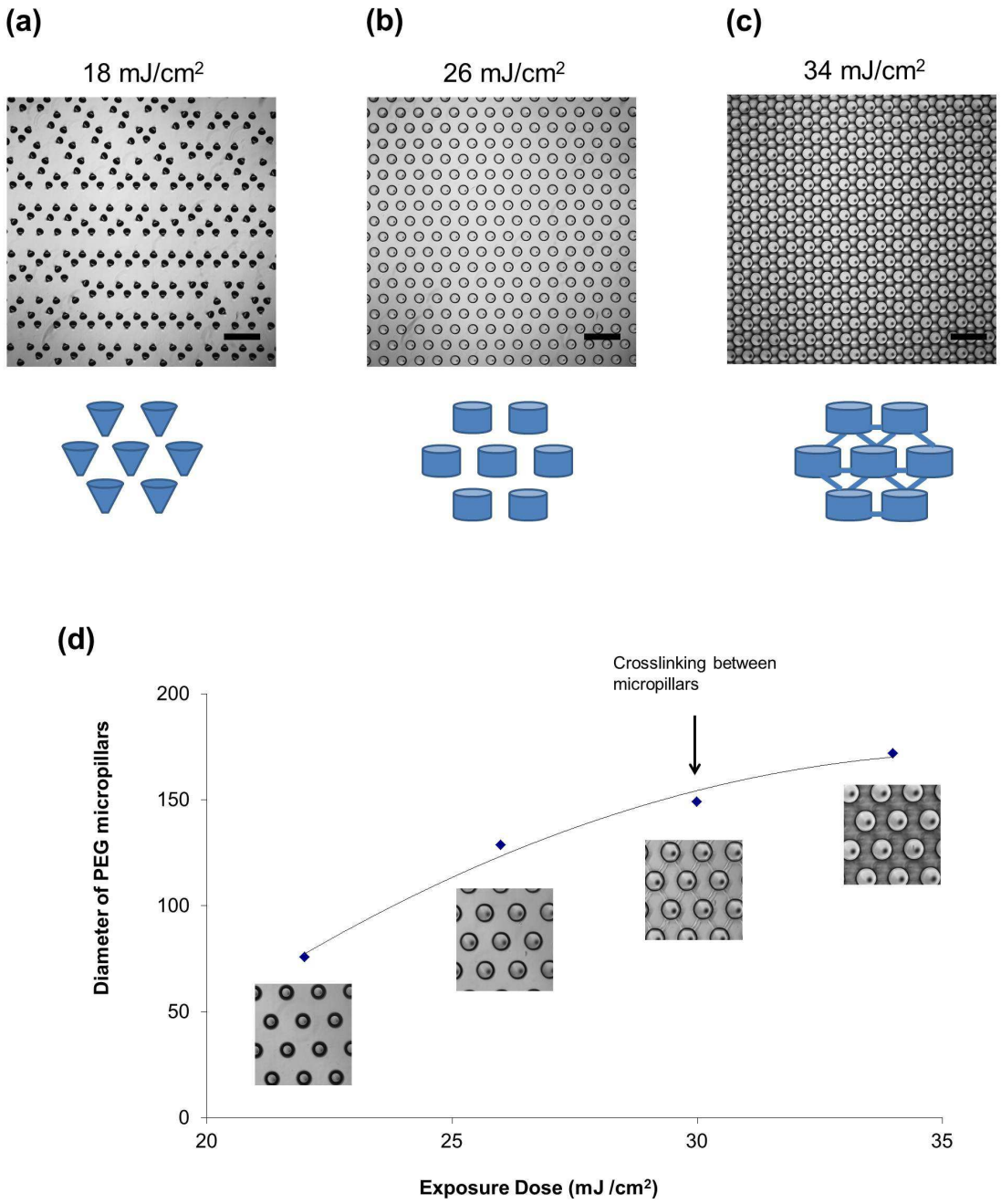

Figure 5.3 Effect of exposure dose to the PEG-based microstructures. The microscopic picture of PEG-based microstructures with the exposure dose of (a) 18 mJ/cm^2; (b) 26 mJ/cm^2; (c) 34 mJ/cm^2. (d) Relationship of the exposure dose to the diameter of the PEG micropillars. Each diameter value is the average of diameters of 30 micropillars. All scale bars represent 500 μm.

The dimension of the microstructures determines the flow rate in a capillary system [147] and thus should be kept with reproducible consistence during the fabrication process. The consistence of the dimension of the PEG micropillars was examined with

20 capillary systems fabricated on five chips. As shown in **Figure 5.4**, the average diameter of dried PEG micropillars with 26 mJ/cm^2 is ~130 μm. The inter-chip CV of PEG micropillar diameter is 2.3% and intra-chip CV of PEG micropillar range from 2.9% to 3.3%. These variances could result from the non-collimated UV light source and the energy fluctuation of the UV light in the UV crosslinker. The variance could be potentially reduced by using a collimated UV source for exposure, although, in this case, the equipment will cost much more than the current setup.

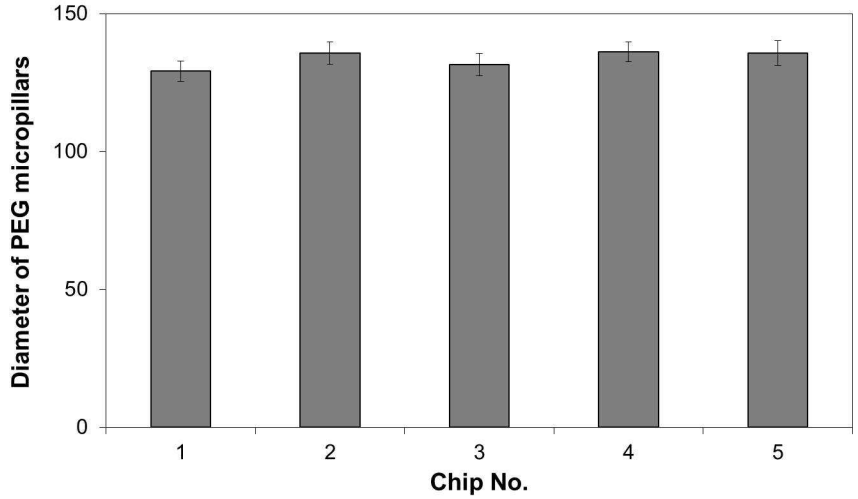

Figure 5.4 Variance of the diameter of PEG micropillars. Exposure dose is 26 mJ/cm^2. Each error bar indicates one standard deviation of the diameter of 120 micropillars on each chip (30 micropillars each capillary system).

5.3.2 Flow test on PEG-based capillary system

Flow test on PEG-based capillary system was done with three kinds of liquid: deionized water, PBS-B-T buffer and FBS. PBS-B-T buffer is the washing buffer, while FBS is the matrix for the sample and for the detection antibody in the immunoassay. The flow test was first conducted on unmodified PEG capillary systems. As shown in **Figure 5.5a** and **5.5b**, although both PEG and TPM treated glass surfaces are hydrophilic, both deionized water and FBS cannot flow through the first resistance.

In contrast, PBS-B-T can easily flow into the capillary system autonomously (**Figure 5.5c**). This can be attributed to the higher wettability of PBS-B-T buffer as the surfactant Tween® 20 reduced the surface energy. In theory, in order to make capillary pump fillable with FBS and water, two strategies could be taken: (1) to dissolve FBS or water with surfactants to lower the surface tension of these liquids; (2) to modify the capillary system to increase the hydrophilicity of the surface. However, the accurate spiking of surfactant into certain volume of sample is only feasible in a professional lab and is not practical for point-of-care applications for users. Thus, rather than adding surfactant to the sample, we tried to make the surface of capillary system more hydrophilic by surface modification.

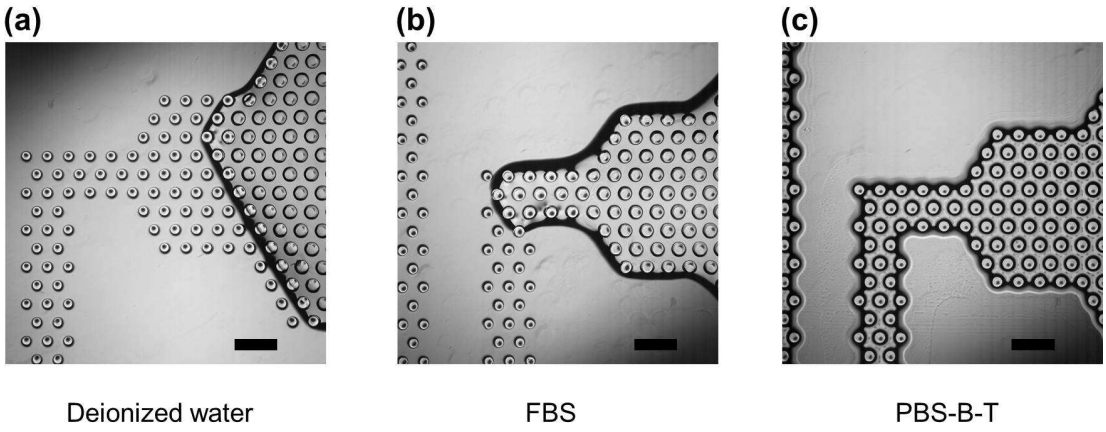

Figure 5.5 Flow behavior of different liquid on the unmodified PEG capillary system. (a) Deionized water; (b) FBS; (c) PBS-B-T. All images were taken after the stop of the front of flow with pipetting of 5 µl of liquid. Scale bars represent 500 µm.

.

The surface modification of capillary systems was done by adsorbing Tween® 20 onto the surfaces of PEG micropillars and glass slides. Solutions with different concentrations of Tween® 20 (0.005, 0.01, 0.02, 0.05%, v/v) was utilized to autonomously fill the capillary system. As expected, the solution filling time decreases with increasing concentration of Tween® 20 (decreasing of surface tension) as shown

in **Table 5.1**. Tween® 20 was later adsorbed onto the capillary system after drying out the water.

Table 5.1 Filling time of solution with different concentrations of Tween® 20

	Concentration of Tween® 20 (v/v)			
	0.005%	**0.01%**	**0.02%**	**0.05%**
Filling Time* (s)	646 ± 60**	277 ± 29	158 ± 26	49 ± 8

***** Filling time is counted from the introduction of the solution onto the chip to the complete filling of the inlet.

****** One standard deviation of filling time from four capillary systems.

Flow test on modified capillary systems was through three consecutive pipetting steps, with 5 μl of liquid applied onto the inlet in each step. The second and third 5 μl of liquid were pipetted onto the inlet immediately after the liquid pipetted in the previous step was entirely flow into the capillary system. As shown in **Figure 5.6**, the fronts of the liquid after each step are (1) passing the first flow resistor and into the first capillary pump; (2) pass the second flow resistor and into the second capillary pump; (3) filling the entire second capillary pump. Each 5 μl represents one step in the immunoassay, with first 5 μl of sample introduction, second 5 μl of detection antibody introduction, and third 5 μl of washing. In contrast to the inability to flow into unmodified capillary system, both FBS and deionized water were able to autonomously flow into the Tween® 20 modified capillary systems. The change of the flow behaviour could be due to two reasons: (1) the increase of hydrophilicity (wettability) of the PEG micropillar and glass slide surface by Tween® 20; (2) the decrease of the surface tension of the liquid in the flow front by dissolving the Tween® 20 on the capillary system surfaces.

Figure 5.6 Fluid front after introduction of liquid. (a) after 5 μl; (b) after 10 μl; (c) after 15 μl. Fluid used was PBS-B-T with red food color.

The filling time of different kinds of liquid in different filling steps is demonstrated in **Table 5.2** and the total filling time is demonstrated in **Table 5.3**. As expected, PBS-B-T, which has lower surface energy, took less time to fill the capillary system as compared to water and FBS, especially on the capillary system modified with lower concentration of Tween® 20. Moreover, filling time of the liquid becomes shorter on the capillary system modified with higher concentration of Tween® 20. This could be due to the more increased wettability of the capillary system surfaces with more Tween® 20 adsorbed and the more reduced surface tension of the liquid with more Tween® 20 dissolved. The average flow rate of liquid in different filling steps, as calculated from the filling time data in **Table 5.2**, is shown in **Figure 5.7**. The average flow rate increases on the capillary system modified with increased concentration of Tween® 20. This proves that the flow rate can be altered by simply modifying the capillary system with different concentration of Tween® 20 without changing the microstructure design. In other recently reported capillary systems, the flow rates of liquid were mainly altered by changing the design of either flow resistor or capillary pump [147, 150] or by patterning different region in the capillary system with different hydrophilicity [235]. Our approach could thus provide a new and effective method to alternate flow rate in a capillary system.

Table 5.2 Filling time of each step introduction of liquid on Tween® 20 modified capillary system

Liquid Type	**Filling time* (s)**				
	Concentration of Tween 20				
	0%**	**0.005%**	**0.01%**	**0.02%**	**0.05%**
1st 5 µl					
PBS-B-T	79 ±4***	68 ±5	45 ±8	29 ±1	23 ±2
Water	N/A****	170 ±44	48 ±7	23 ±3	21 ±4
FBS	N/A	206 ±33	114 ±4	54 ±4	42 ±7
2st 5 µl					
PBS-B-T	66 ±7	74 ±9	66 ±5	39 ±4	29 ±3
Water	N/A	128 ±7	110 ±17	65 ±7	43 ±5
FBS	N/A	189 ±29	150 ±11	57 ±6	39 ±10
3rd 5 µl					
PBS-B-T	60 ±4	65 ±6	67 ±14	54 ±8	38 ±3
Water	N/A	70 ±3	70 ±12	63 ±5	48 ±6
FBS	N/A	130 ±25	147 ±19	92 ±5	74 ±7

***** Filling time is counted from the introduction of the solution onto the chip to the stop of the liquid front.

****** Unmodified capillary system.

******* One standard deviation of filling time from three capillary systems on three different chips.

******** Liquid cannot flow through.

Table 5.3 Total filling time of liquid on Tween® 20 modified capillary system

Liquid Type	**Total Filling time* (s)**				
	Concentration of Tween® 20				
	0%**	**0.005%**	**0.01%**	**0.02%**	**0.05%**
PBS-B-T	206 ±8***	207 ±1	178 ±15	123 ±9	91 ±5
Water	N/A****	361 ±43	228 ±33	151 ±8	112 ±15
FBS	N/A	525 ±87	412 ±8	203 ±8	155 ±18

***** Total filling time is calculated by summing up the filling time of three steps liquid introduction.

****** Unmodified capillary system.

******* One standard deviation of total filling time from three capillary systems on three different chips.

******** Liquid cannot flow through.

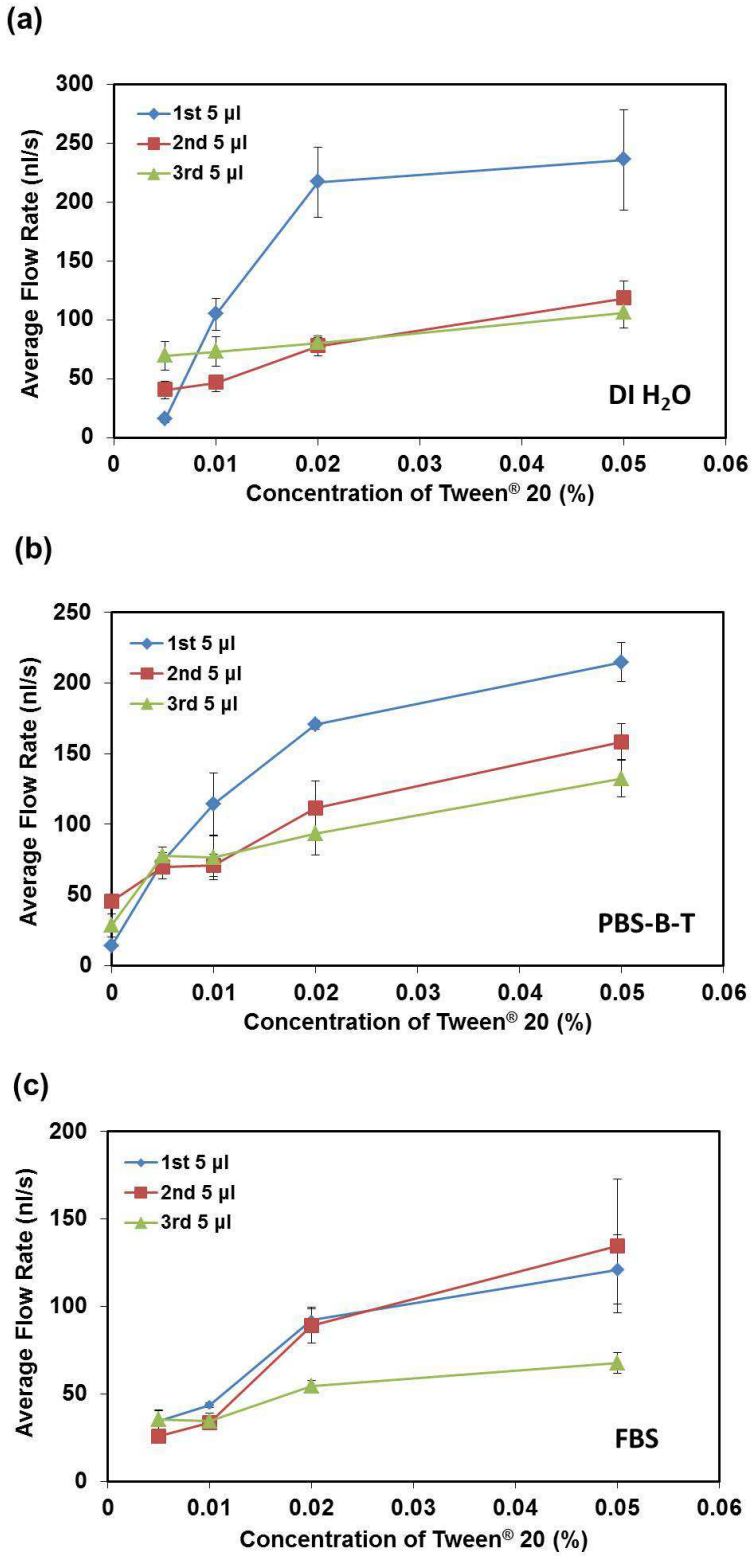

Figure 5.7 Average flow rate of liquid of each filling step on capillary system modified with different concentration of Tween® 20. (1) Deionized water; (2) PBS-B-T; (3) FBS. The average flow rate is calculated as (filling volume/average filling time). Each error bar represents one S.D. from three capillary systems on three different chips.

Another interesting finding is that, water has less filling time (higher average flow rate) than the FBS in the capillary system. It is known that proteins in serum, such as albumins and immunoglobulins and fibrinogens, act as surfactants which result in the lower surface tension of serum than the pure water [238]. On the other hand, serum (human serum viscosity of 1.5 -1.9 centipoise [239]) has higher viscosity than pure water (~1.0 centipoise at 20 °C). According to **Equation 2.1** and **2.2** described in **Chapter 2**, in a capillary system, lower surface tension results in higher flow rate and shorter filling time while higher viscosity results in the lower flow rate and longer filling time. From our results, as FBS has longer filling time than water, it can be concluded that serum's high viscosity has more dominated effect than its low surface tension on the flow rate and filling time in our capillary system.

5.3.3 On-chip microbead-based immunoassay for PSA and hCG

The detection for PSA and hCG was performed to validate the performance of on-chip microbead-based immunoassay. FBS was used as the sample to mimic the condition in real human serum. The immunoassay was done in three pipetting steps with the first step pipetting of FBS sample spiked with PSA or hCG, second step pipetting of detection antibody diluted in FBS and third step pipetting of PBS-B-T for washing. Capillary systems modified with 0.005% of Tween® 20, which enabled the longest filling time of liquid for the first and second pipetting of FBS (**Table 5.2**), were used for the immunoassay to provide enough incubation time for the binding between analytes with capture antibodies and between the detection antibodies with the analytes. The total immunoassay time is ~10 minutes. Serial dilutions of PSA (2 ng, 10 ng, 50 ng, 250 ng/ml) and hCG (1 ng, 5 ng, 25 ng, 125 ng/ml) were tested on chip. Blank FBS

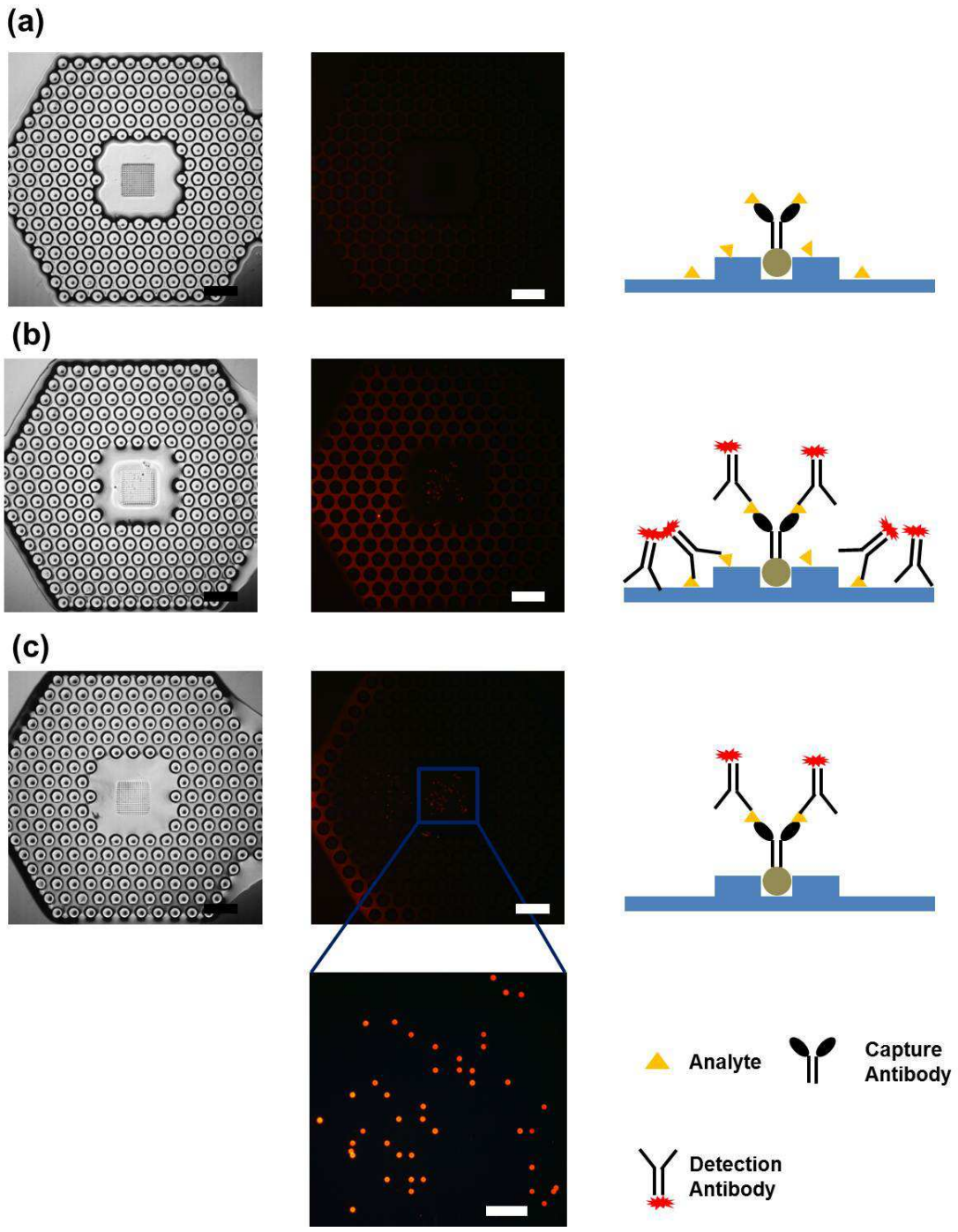

Figure 5.8 Bright field (left) and fluorescence (middle) images of the inlet and the array during the immunoassay. (a) After sample introduction. (b) After detection antibody introduction. (c) After adding washing buffer. The enlarged fluorescence image of microbeads array after the assay for 250 ng/ml PSA is shown in the bottom. Scale bars represent 500 μm except for the bottom image in which the scale bar represents 100 μm.

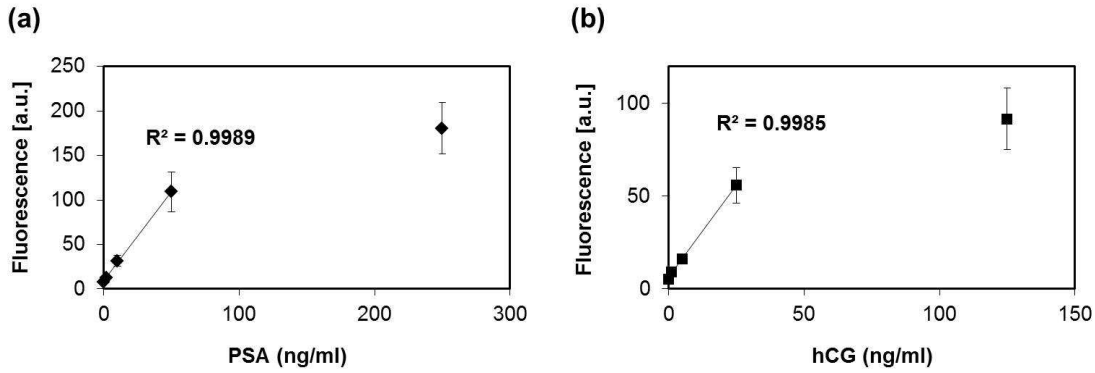

Figure 5.9 Calibration curves for on-chip immunoassay. (a) Calibration curve of PSA; (b) Calibration curve of hCG. Each error bar represents one standard deviation of fluorescence signals of all the microbeads on one gel pad array.

was used as 0 ng/ml sample. The images of the inlet and the array during the three-step immunoassay process are shown in **Figure 5.8**. After introduction of FBS sample, there is very weak fluorescence in the inlet while no fluorescence is shown in the gel pad array region (**Figure 5.8a**). After the subsequent introduction of fluorescence detection antibody, there is strong fluorescence from the microbeads as well as from the other inlet region (**Figure 5.8b**). Notably, only the peripheral of the PEG micropillars shows strong fluorescence which indicates that the detection antibody cannot diffuse into the PEG matrix [119]. Finally, after the washing buffer is added, non-binding analytes and excess detection antibody are washed out, resulting in the low background noise around the inlet and the gel pad array (**Figure 5.8c**). The calibration curves for PSA and hCG are shown in **Figure 5.9**. The fluorescence signal is proportional to the concentration of analytes and the linear range is 0 – 50 ng/ml for PSA and 0 – 25 ng/ml for hCG. The calculated limits of detection (LODs) based on the 3 S.D. rule are 0.31 ng/ml for PSA and 0.73 ng/ml for hCG. The LOD for PSA is lower than the commonly used serum cut-off value (4 ng/ml [194]) for prostate cancer screening and the serum cut-off value (2 ng/ml [188]) for the monitoring of prostate cancer recurrence after radiotherapy while the LOD for hCG is lower than the cut-off

value (10 U/l or 1.0 ng/ml [188]) for testicular cancer screening. The LODs could be potentially improved by enabling longer incubation time which can be achieved by either increasing the area of capillary system to accommodate bigger sample volume or elongating the flow resistor region to reduce the average flow rate. Thus, our chip could be potentially used for rapid and sensitive point-of-care cancer diagnostics. Most of the previous immunoassays performed on capillary system employed antibodies which were patterned on planar surfaces with microfabricated microstamps or microchannels [149, 155, 161]. In this case, redundancy of the data points was enabled by patterning multi-lines of antibodies. In this work, the utilization of randomly arrayed microbeads not only allows more antibody to be immobilized per unit of area but also simplifies the process to introduce antibody into the capillary system while microbeads also enables the redundancy of data points.

5.3.4 Multiplexed on-chip immunoassay

Simultaneous detection of both PSA and hCG was also achievable on our chip using the spatial encoding method mentioned in **Chapter 3** and **Chapter 4**. As shown in **Figure 5.10a** and **5.10b**, anti-PSA microbeads and anti-hCG microbeads were sequentially deposited onto gel pad array and their spatial positions were recorded in images. After the assay, the fluorescence signals from both kinds of microbeads can be obtained with single fluorescence filter set on a single image (**Figure 5.10c**) and the fluorescence intensity can then be analyzed. FBS samples spiked with different concentration of two analytes (1, 5, 25, 125 ng/ml hCG with 2, 10, 50, 250 ng/ml PSA)

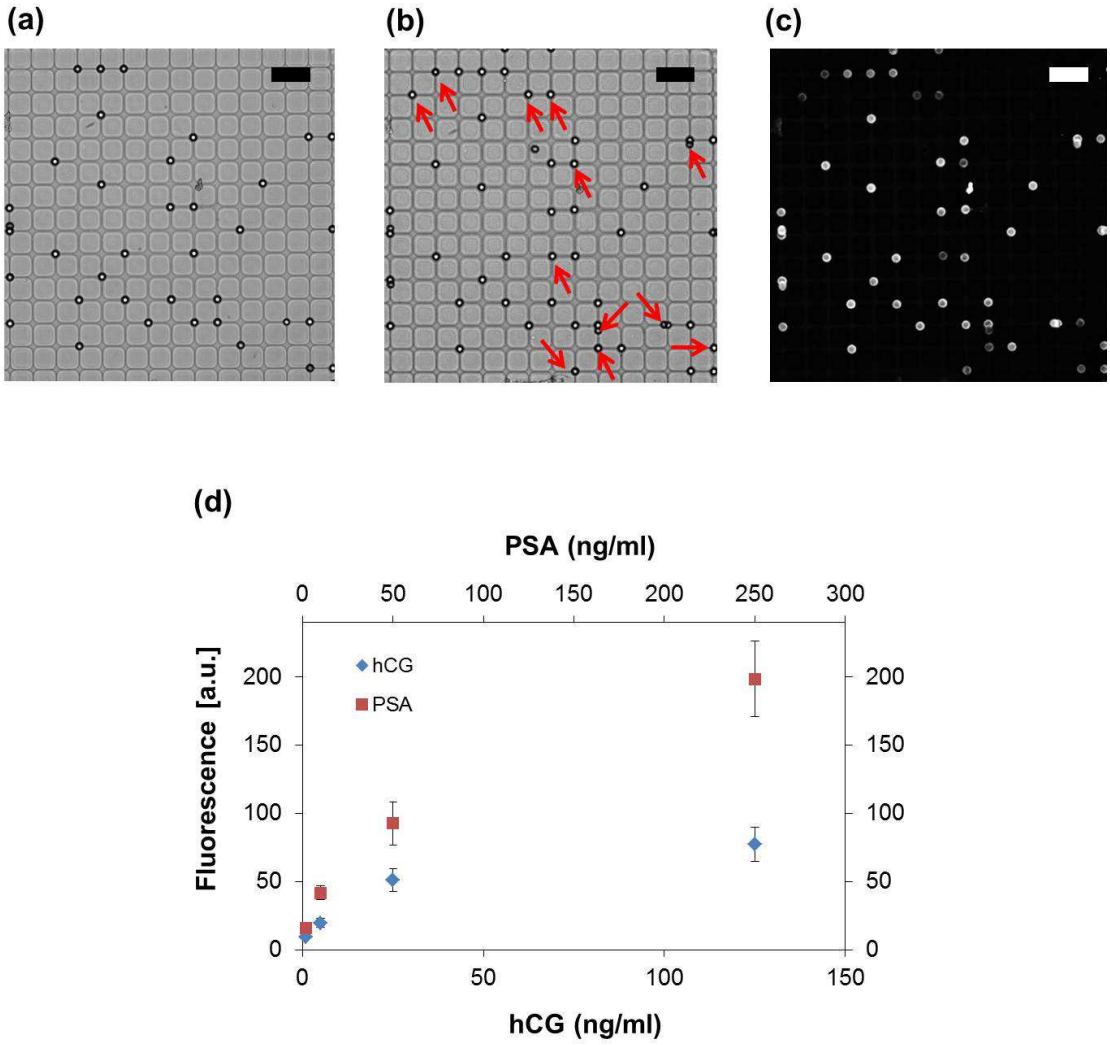

Figure 5.10 On-chip multiplexed immunoassay using spatially encoded microbead array. (a) Deposition of anti-PSA microbeads; (b) Deposition of anti-hCG microbeads; (3) Fluorescence image after the immunoassay with FBS sample spiked with 50 ng/ml PSA and 20 ng/ml hCG. Scale bars represent 50 μm. (d) Microbead fluorescence signal as a function of analyte concentration in multiplexed immunoassay. Each error bar represents one standard deviation of fluorescence signals of one type of microbeads on one gel pad array.

were tested on chip. As demonstrated in **Figure 5.10d**, fluorescence signals are proportional to the signal intensities and the function accords well with the calibration curve obtained in the single-plexed assay. With other available antibody pairs, the number of analytes which can be simultaneously analyzed could be increased simply by encoding more batches of microbeads as discussed in **Chapter 3**. Previously, Wang et al. [161] developed immunoassay in a capillary system wherein the

multiplexing capability was achieved by hybridization of oligonucleotide conjugated antibodies with site-specifically patterned complementary oligonucleotides. However, the antibody immobilization process is time-consuming as the patterning of oligonucleotide probes took more than 4 hrs and the subsequent hybridization step also required ~1 hr [164]. In this work, the antibody coated microbeads is simply pipetted onto the gel pad array and each deposition and encoding step takes ~3 minutes. Thus, our method could be a more flexible and more rapid one to achieve multiplexing capability for immunoassay in a capillary system.

5.4 Conclusion

In this work, we successfully employ PEG to be a new candidate material for the fabrication of microstructures in a capillary system. The fabrication process of PEG-based capillary system is fast, simple and reproducible while no mold, no cleanroom facilities and expensive equipment is required during the process. The modification of the surface of the capillary system by different concentration of Tween® 20 enables the filling time and average flow rate to be changed without the need to change the microstructure design. A microfluidic chip, which integrates the gel pad array into the capillary system, is fabricated and the chip allows the microbead-based immunoassay to be performed within 10 min. The quantitative detection of two serum tumor markers, PSA and hCG, is done with the LODs below the cut-off value for cancer diagnosis. Moreover, with spatially encoded microbead array, quantitative and multiplexing protein detection is also achieved on chip. In the future, this chip will be optimized toward the one-step and multiplexed protein detection in blood samples to contribute to the low-cost, multi-targets and rapid serum/blood based point-of-care tests for clinical diagnostics.

Chapter 6

Conclusion & Future Works

Chapter 6 - Conclusion & Future Works

6.1 Conclusion

In this PhD work, a novel microparticle array platform has been developed based on the assembly of microparticles on polyacrylamide gel microstructures. These gel microstructures have been fabricated on inexpensive microscopic glass slides with photopolymerization reaction through a mask. The fabrication protocol has been optimized to enable much lower autofluorescence from the gel as compared to the high autofluorescence from previous reported gel-based microstructures [5], thus making these new generation gel-based microstructures suitable for sensitive and quantitative microparticle-based biochemical assays rather than for only semi-quantitative DNA hybridization assays with the previous gel pad array platform [5,139]. The fabrication process is rapid (1 min/per microstructure unit) with very low material cost and, without the need for a cleanroom and expensive equipment. Besides the simplicity for fabrication, gel microstructures enable stable immobilization and effective assembly of microparticles with different surface bioprobes. In this work, three types of gel microstructure chips with different designs have been fabricated for various applications in multiplexed biochemical assays.

The first type of gel microstructure chip (**Chapter 3**) consists of 40 gel pad array units with distances between each two gel pad array units fitting for the multi-channel micropipette for simple on-chip liquid handling. PEG micropillar rings have been introduced onto the chip to serve as hydrophilic barriers around each array unit to trap the liquids and thus 40 different microbead-based biochemical assays can be

simultaneously performed on chip. Quantitative fluorescence immunoassays for human chorionic gonadotropin (hCG) and prostate specific antigen (PSA) have been successfully done on chip with limits of detections at least one order lower than the cut-off concentrations of these two tumor markers for cancer diagnosis. Moreover, as most of microbeads (> 99%) remain in their initial position after the assay, multiplexed immunoassay for hCG and PSA is enabled by encoding batchwise deposited microbeads with their spatial addresses on the array. The spatial encoded microbead array eliminates the need for color encoding or barcode encoding as well as the corresponding complicated decoding process. In addition, the chip can be reused by simply dissolving polystyrene based microbeads with toluene and subsequent depositing of new microbeads. The reusability is further validated in immunoassays for hCG and there is no compromise of the stability of microbeads as well as the sensitivity of the immunoassay with the reused chip. Lastly, in a preliminary study, the on-chip simultaneous detection of DNA and protein has also been achieved with arrays of oligonucleotide and antibody coated microbeads. In sum, this low cost gel pad array chip allows sensitive and high throughput immunoassay to be performed with merely 1 μl of serum sample for each multiplexed assay and thus could have good potential to be employed for clinical diagnostics.

The second type of gel microstructure chips (**Chapter 4**) is designed to be integrated into a microfluidic system. Three different gel microstructures, gel pad array, gel well array and mixed microstructure array, have been fabricated for the assembly of antibody coated microbeads, enzyme containing microparticle and the both types of microparticles, respectively. With microbead arrays assembled on gel pad arrays, microfluidic quantitative immunoassays for hCG and PSA in serum have been

demonstrated with LODs lower than their cut-off concentration for cancer diagnosis. Multiplexed immunoassay for hCG and PSA has also been achieved with spatially encoded microbeads. Meanwhile, with microparticle array assembled on gel well array, microfluidic quantitative enzymatic glucose assays have also been demonstrated with the dynamic response range covers not only the physiological serum glucose level but also the threshold concentration for the diagnosis of *diabetes mellitus*. Furthermore, antibody coated microbeads and enzyme containing micropaticles have been assembled on the mixed microstructure array for the simultaneous immunoassays and enzymatic glucose assays. This is the first time the integration of a binding kinetic based assay (immunoassay) with a reaction kinetic based assay (enzymatic glucose) into one microparticle microarray platform. This versatile microfluidic microparticle array platform could be promising to be applied to the simultaneous detection of protein markers and metabolite for disease diagnostics.

The third type of gel microstructure chip (**Chapter 5**) is designed to be integrated into a passing pumping system, PEG-based capillary system. The PEG-based capillary system consists of PEG micropillars fabricated by photopolymerization reaction with no mold and without the need for cleanroom facilities, which is much more simplified than any other existing capillary systems fabricated with either silicon/glass or polymeric materials. These PEG micropillars have been fabricated on glass slides with reproducible dimension by controlling the UV exposure dose. With the intrinsic protein repellent property of PEG, pre-blocking steps, which is required for all the other existing capillary systems for immunoassays, is eliminated and thus further adding to the simplicity of this system. The filling time and average flow rate of liquid on the capillary system can be simply altered by modification with different concentration of Tween® 20 surfactant. After the integration of the gel pad array into

with PEG capillary system, the chip is tested by microbead-based immunoassays for PSA and hCG. The on-chip quantitative immunoassays require only three filling steps and 10 min assay time and the LODs of two serum tumor markers are lower than the cut-off concentrations for cancer diagnosis. Moreover, on-chip multiplexing immunoassay has also been achieved simply by using spatially encoded microbead array. This is, to the best of our knowledge, the first bioanalytical microbead array to be integrated into an autonomous capillary system for multiplexing biochemical assays.

The characteristics for these three types of gel microstructure chips are summarized in **Table 6.1**.

In sum, this thesis work developed an easy-fabricated, easy-integrated, low cost, flexible and versatile platform for the assembly of microparticle arrays for various kinds of biochemical assays. This novel platform could be a useful and more accessible research tool for common biolabs to customize their own microparticle arrays for multiplexed and quantitative bioanalysis.

Table 6.1 Comparison of three types of gel microstructure chips in this work

	Gel pad array chip	**Gel microstructure array chip**	**Capillary system & gel pad array chip**
Sample Volume	1 µl	20 µl (immunoassay); 4 µl (glucose assay)	5 µl
Assay Time	< 1.5 hrs (immunoassay)	40 min (immunoassay); 5 min (glucose assay)	< 10 min (immunoassay)
Performance	LODs: 42 pg/ml for hCG; 136 pg/ml for PSA	LODs: 87 pg/ml for hCG; 114 pg/ml for PSA Range for glucose: 1 - 10 mM	LODs: 0.31 ng/ml for PSA; 0.73 ng/ml for hCG
Multiplexing	Yes (also for protein and DNA)	Yes (also for protein and glucose)	Yes
Particle Encoding	Spatial	Spatial + Size	Spatial
Microfluidics	No	Yes	Yes
Fabrication time	< 1 hr	10 min	< 30 min
Cleanroom work	No	No	No
Reusability	Yes	Yes	No
Assays per chip	8	40	4
Trained User	Yes	Yes	No

6.2 Future Works

- In this PhD work, polyacrylamide gel has been used for the fabrication of microstructures. Polyacrylamide gel shows strong adhesion with antibody and oligonucleotide coated polystyrene microbeads. It is necessary to investigate the actual mechanism behind the adhesion and the stability of microbeads with other surface chemistry could also be tested on the gel microstructures.

Furthermore, gels with other polymeric materials may also be utilized and tested for the assembly of microparticle-based microarray.

- The 2-plex immunoassay and 3-plex detection of proteins and glucose were demonstrated in this thesis with the current microparticle array platform. However, the multiplexing power of our platform, which is theoretically infinite, has not been fully explored. In practice, there are several potential challenges to apply our microparticle array to high-multiplexing bioanalysis. First, the likelihood of the cross-reactivity between the antibodies or other bioprobes will increase when more types of analyte exist in the same sample. This may cause false positive signals. Second, with increasing batches of microparticles deposited, new batches of microparticles will get less chance to settle on the gel microstructure array given the less available immobilization sites (cross-points for gel pad array, wells for gel well array.). This may cause decreasing number of microparticles to be immobilized in later batches and in the extreme case, there could be no microparticles in certain batch which is deposited. In this case, the adjustment of microparticle density in the solution should be important to ensure that enough number of microparticles can be immobilized for every later batch. Finally, the manual imaging of each array after each deposition step for spatial encoding could be tedious if large number of batches of microparticles is to be immobilized. Thus, to achieve high multiplexing capability, certain automation and integration is needed for the deposition process which includes the deposition, imaging and microparticle pattern recognition. All these challenges need to be conquered in the future work.

- Fetal bovine serum (FBS) has been used as the medium for samples throughout this work. As FBS shares similarity in constitution with real human serum, the use of the gel microstructure chip for the analysis of multiplexed protein markers in human serum sample could be achievable and promising for the clinical diagnostics.

- The readout of the fluorescence signals from the microparticle array is currently through fluorescence microscopy and the analysis of the signals is a manual process. In the future work, the gel microstructure chip may be designed to be compatible with microscanners and with automated imaging analysis software to provide faster assay as well as faster data analysis.

- The gel pad array chip (**Chapter 3**) enables the microparticle-based biochemical assays to be performed with only 1 μl of sample volume. Thus, the chip could have other bioanalysis applications wherein the collection of big amount of samples is difficult and challenging. These applications include the biomarker detection in fetal blood/serum, the bioanalysis of the cell lysate, the bioanalysis of extract from tissue biopsy and the hybridization assay for DNA samples amplified from on-chip μPCR or from 384 or 1536 wells microplate PCR. In addition, by reducing the distance between the two gel pad array units and by decreasing the size of the PEG micropillar ring, the current throughput of the chip (40 samples) can be further increased to simultaneously deal with more samples.

- The capability of the mixed microstructure chip (**Chapter 4**) to allow simultaneous immunoassay and enzymatic assay to be performed could be further used in real disease diagnostics. As mentioned in **Chapter 1**, the diagnostics of insulinoma requires the quantitation of serum glucose and insulin which usually requires two separated assays. With microbeads coated with anti-insulin antibody and with the enzyme containing microparticle for glucose, a one-assay diagnosis of insulinoma could be achieved which may greatly reduce the diagnosis time and may enable fast treatment.

- The crosslinked PEG has been shown in **Chapter 4** to trap big molecules while letting small molecules to diffuse freely. It may be interesting to further investigate the cut-off molecular weight for different concentrations of polymerized PEG under different conditions such as ionic strength and pH. These cut-off molecular weight values may be helpful for the design of novel microparticle-based biosensors.

- In **Chapter 5**, flow test has been done on PEG-based capillary systems with one particular design. PEG-based capillary systems with other designs could also be fabricated and tested. For example, the length of the flow resistor, the dimension of the PEG micropillar or the area of the capillary pump can all be altered to give different filling times. With these alternations, the capillary system could be optimized to improve the performance of on-chip microbead-based immunoassay. The capillary system may be further designed to fit for the one-step lateral flow multiplexed immunoassay based on the microbead array. A potential design for blood samples is shown in **Figure 6.1**. With this design, the challenge could lie in (1) the fabrication of much smaller PEG-based

microstructures at the inlet for blood filtering and in the region for microbead array assembly for microbead physical confinement; (2) the need for a robust reproducible method to pre-immobilize antibodies onto the chip; (3) the proper mixing between the sample and the detection antibody in the mixer. Thus, solutions should be found to overcome these challenges.

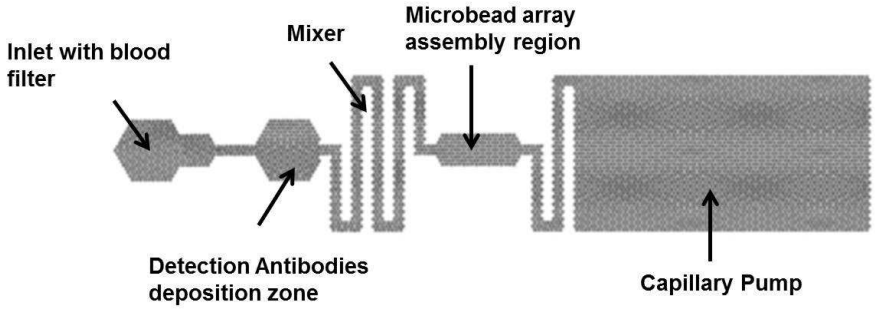

Figure 6.1 A potential design for the PEG capillary system for one-step multiplexed lateral flow immunoassay.

References

References

1. Barbulovic-Nad, I., et al., *Bio-microarray fabrication techniques - A review.* Critical Reviews in Biotechnology, 2006. **26**(4): p. 237-259.
2. Schena, M., et al., *Quantitative Monitoring of Gene Expression Patterns with a Complementary DNA Microarray.* Science, 1995. **270**(5235): p. 467-470.
3. Singer, J.M. and C.M. Plotz, *The latex fixation test: I. Application to the serologic diagnosis of rheumatoid arthritis.* The American Journal of Medicine, 1956. **21**(6): p. 888-892.
4. Verpoorte, E., *Beads and chips: new recipes for analysis.* Lab on a chip, 2003. **3**: p. 60N–68N.
5. Ng, J.K., E.S. Selamat, and W.T. Liu, *A spatially addressable bead-based biosensor for simple and rapid DNA detection.* Biosensors and Bioelectronics, 2008. **23**(6): p. 803-810.
6. Gunderson, K.L., et al., *A genome-wide scalable SNP genotyping assay using microarray technology.* Nature Genetics, 2005. **37**(5): p. 549-554.
7. Steemers, F.J. and K.L. Gunderson, *Whole genome genotyping technologies on the BeadArray™ platform.* Biotechnology Journal, 2007. **2**(1): p. 41-49.
8. Shen, R., et al., *High-throughput SNP genotyping on universal bead arrays.* Mutation Research , 2005. **573**(1-2): p. 70-82.
9. Ali, M.F., et al., *DNA hybridization and discrimination of single-nucleotide mismatches using chip-based microbead arrays.* Analytical Chemistry, 2003. **75**(18): p. 4732-4739.
10. Blicharz, T.M., et al., *Fiber-Optic Microsphere-Based Antibody Array for the Analysis of Inflammatory Cytokines in Saliva.* Analytical Chemistry, 2009. **81**(6): p. 2106-2114.
11. Li, H., R.F. Leulmi, and D. Juncker, *Hydrogel droplet microarrays with trapped antibody-functionalized beads for multiplexed protein analysis.* Lab on a Chip, 2011. **11**(3): p. 528-534.
12. Zhou, L., et al., *Quantitative intracellular molecular profiling using a one-dimensional flow system.* Analytical Chemistry, 2006. **78**(17): p. 6246-6251.
13. Wilson, D.H., et al., *Fifth-generation digital immunoassay for prostate-specific antigen by single molecule array technology.* Clinical Chemistry, 2011. **57**(12): p. 1712-1721.
14. Xie, C. and G. Wang, *Development of Simultaneous Detection of Total Prostate-Specific Antigen (tPSA) and Free PSA With Rapid Bead-Based Immunoassay.* Journal of Clinical Laboratory Analysis, 2011. **25**(1): p. 37-42.
15. Walt, D.R., *Bead-based fiber-optic arrays.* Science, 2000. **287**(5452): p. 451-452.
16. Xia, Y., et al., *Template-Assisted Self-Assembly of Spherical Colloids into Complex and Controllable Structures.* Advanced Functional Materials, 2003. **13**(12): p. 907-918.
17. Lim, C.T. and Y. Zhang, *Novel Dome-Shaped Structures for High-Efficiency Patterning of Individual Microbeads in a Microfluidic Device.* Small, 2007. **3**(4): p. 573-579.
18. Smistrup, K., et al., *On-chip magnetic bead microarray using hydrodynamic focusing in a passive magnetic separator.* Lab on a Chip, 2005. **5**(11): p. 1315-1319.
19. Xu, W. and J. Ketterson, *Assembly of ordered magnetic microsphere arrays.* Journal of Applied Physics, 2008. **104**(4): 044701.
20. Barbee, K.D. and X. Huang, *Magnetic assembly of high-density DNA arrays for genomic analyses.* Analytical Chemistry, 2008. **80**(6): p. 2149-2154.
21. Barbee, K.D., et al., *Electric field directed assembly of high-density microbead arrays.* Lab on a chip, 2009. **9**(22): p. 3268-3274.

22. Winkleman, A., et al., *Directed self-assembly of spherical particles on patterned electrodes by an applied electric field.* Advanced Materials, 2005. **17**(12): p. 1507-1511.
23. Aizenberg, J., P.V. Braun, and P. Wiltzius, *Patterned Colloidal Deposition Controlled by Electrostatic and Capillary Forces.* Physical Review Letters, 2000. **84**(13): p. 2997-3000.
24. Sivagnanam, V., et al., *Micropatterning of protein-functionalized magnetic beads on glass using electrostatic self-assembly.* Sensors and Actuators B: Chemical, 2008. **132**(2): p. 361-367.
25. Kim, Y.H., et al., *Selective assembly of colloidal particles on a nanostructured template coated with polyelectrolyte multilayers.* Advanced Materials, 2007. **19**(24): p. 4426-4430.
26. Goodey, A., et al., *Development of Multianalyte Sensor Arrays Composed of Chemically Derivatized Polymeric Microspheres Localized in Micromachined Cavities.* Journal of the American Chemical Society, 2001. **123**(11): p. 2559-2570.
27. Sato, K., et al., *Integration of an immunosorbent assay system: Analysis of secretory human immunoglobulin A on polystyrene beads in a microchip.* Analytical Chemistry, 2000. **72**(6): p. 1144-1147.
28. Jason, A.T., et al., *Polymeric microbead arrays for microfluidic applications.* Journal of Micromechanics and Microengineering, 2010. **20**(11): p. 115017.
29. Du, N., et al., *A disposable bio-nano-chip using agarose beads for high performance immunoassays.* Biosensors and Bioelectronics, 2011. **28**(1): p. 251-256.
30. Filipponi, L., et al., *Microbeads on microposts: An inverted architecture for bead microarrays.* Biosensors and Bioelectronics, 2009. **24**(7): p. 1850-1857.
31. Lim, C.T. and Y. Zhang, *Bead-based microfluidic immunoassays: The next generation.* Biosensors and Bioelectronics, 2007. **22**(7): p. 1197-1204.
32. Zhang, H., et al., *A microfluidic device with microbead array for sensitive virus detection and genotyping using quantum dots as fluorescence labels.* Biosensors and Bioelectronics, 2010. **25**(11): p. 2402-2407.
33. Sivagnanam, V., et al., *On-Chip Immunoassay Using Electrostatic Assembly of Streptavidin-Coated Bead Micropatterns.* Analytical Chemistry, 2009. **81**(15): p. 6509-6515.
34. Wen, J., et al., *One-dimensional microfluidic beads array for multiple mRNAs expression detection.* Biosensors and Bioelectronics, 2007. **22**(11): p. 2759-2762.
35. Dimov, I.K., et al., *Stand-alone self-powered integrated microfluidic blood analysis system (SIMBAS).* Lab on a chip, 2011. **11**(5): p. 845-850.
36. Juncker, D., et al., *Autonomous microfluidic capillary system.* Analytical Chemistry, 2002. **74**(24): p. 6139-6144.
37. Qin, L., et al., *Self-powered microfluidic chips for multiplexed protein assays from whole blood.* Lab on a chip, 2009. **9**(14): p. 2016-2020.
38. Dunbar, S.A., *Applications of Luminex® xMAP™ technology for rapid, high-throughput multiplexed nucleic acid detection.* Clinica Chimica Acta, 2006. **363**(1-2): p. 71-82.
39. Jang, E. and W.-G. Koh, *Multiplexed enzyme-based bioassay within microfluidic devices using shape-coded hydrogel microparticles.* Sensors and Actuators B: Chemical, 2010. **143**(2): p. 681-688.
40. Vaidakis, D., et al., *Pancreatic insulinoma: Current issues and trends.* Hepatobiliary and Pancreatic Diseases International, 2010. **9**(3): p. 234-241.
41. Flamini, E., et al., *Free DNA and carcinoembryonic antigen serum levels: An important combination for diagnosis of colorectal cancer.* Clinical Cancer Research, 2006. **12**(23): p. 6985-6988.
42. Yap, F.L. and Y. Zhang, *Protein and cell micropatterning and its integration with micro/nanoparticles assembly.* Biosensors and Bioelectronics, 2007. **22**(6): p. 775-788.
43. Kawaguchi, H., *Functional polymer microspheres.* Progress in Polymer Science, 2000. **25**(8): p. 1171-1210.

44. Derveaux, S., et al., *Synergism between particle-based multiplexing and microfluidics technologies may bring diagnostics closer to the patient.* Analytical and Bioanalytical Chemistry, 2008. **391**(7): p. 2453-2467.
45. Drummond, J.E., et al., *Design and optimization of a multiplex anti-influenza peptide immunoassay.* Journal of Immunological Methods, 2008. **334**(1-2): p. 11-20.
46. Rissin, D.M., et al., *Simultaneous Detection of Single Molecules and Singulated Ensembles of Molecules Enables Immunoassays with Broad Dynamic Range.* Analytical Chemistry, 2011: p. 2279-2285.
47. Theilacker, N., et al., *Multiplexed protein analysis using encoded antibody-conjugated microbeads.* Journal of The Royal Society Interface, 2011. **8**(61): p. 1104-1113.
48. Russom, A., et al., *Genotyping by dynamic heating of monolayered beads on a microheated surface.* Electrophoresis, 2004. **25**(21-22): p. 3712-3719.
49. Lee, W., et al., *Suspension arrays of hydrogel microparticles prepared by photopatterning for multiplexed protein-based bioassays.* Biomedical Microdevices, 2008. **10**(6): p. 813-822.
50. Fulton, R.J., et al., *Advanced multiplexed analysis with the FlowMetrix(TM) system.* Clinical Chemistry, 1997. **43**(9): p. 1749-1756.
51. Vignali, D.A.A., *Multiplexed particle-based flow cytometric assays.* Journal of Immunological Methods, 2000. **243**(1-2): p. 243-255.
52. Guesdon, J.-L. and S. Avrameas, *Magnetic solid phase enzyme-immunoassay.* Immunochemistry, 1977. **14**(6): p. 443-447.
53. Gijs, M.A.M., F. Lacharme, and U. Lehmann, *Microfluidic applications of magnetic particles for biological analysis and catalysis.* Chemical Reviews, 2010. **110**(3): p. 1518-1563.
54. Fan, Z.H., et al., *Dynamic DNA hybridization on a chip using paramagnetic beads.* Analytical Chemistry, 1999. **71**(21): p. 4851-4859.
55. Choi, J.-W., et al., *A new magnetic bead-based, filterless bio-separator with planar electromagnet surfaces for integrated bio-detection systems.* Sensors and Actuators B: Chemical, 2000. **68**(1-3): p. 34-39.
56. Trau, M., D.A. Seville, and I.A. Aksay, *Field-induced layering of colloidal crystals.* Science, 1996. **272**(5262): p. 706-709.
57. Yeh, S.R., M. Seul, and B.I. Shraiman, *Assembly of ordered colloidal aggregates by electric-field-induced fluid flow.* Nature, 1997. **386**(6620): p. 57-59.
58. Miller, M.S., G.J.E. Davidson, and T.B. Carmichael, *Templated self-assembly of glass microspheres into ordered two-dimensional arrays under dry conditions.* Langmuir, 2010. **26**(7): p. 5286-5290.
59. Barbee, K.D., et al., *Multiplexed protein detection using antibody-conjugated microbead arrays in a microfabricated electrophoretic device.* Lab on a chip, 2010. **10**(22): p. 3084-3093.
60. Zheng, H., et al., *Two component particle arrays on patterned polyelectrolyte multilayer templates.* Advanced Materials, 2002. **14**(8): p. 569-572.
61. Lyles, B.F., et al., *Directed Patterned Adsorption of Magnetic Beads on Polyelectrolyte Multilayers on Glass.* Langmuir, 2004. **20**(8): p. 3028-3031.
62. Sivagnanam, V., A. Sayah, and M.A.M. Gijs, *Bead-based single protein micro-array realized through electrostatic self-assembly of carboxylated beads.* Microelectronic Engineering, 2008. **85**(5-6): p. 1355-1358.
63. Ashkin, A., *Acceleration and Trapping of Particles by Radiation Pressure.* Physical Review Letters, 1970. **24**(4): p. 156-159.
64. Ashkin, A., et al., *Observation of a single-beam gradient force optical trap for dielectric particles.* Optics Letters, 1986. **11**(5): p. 288-290.
65. Ashkin, A., J.M. Dziedzic, and T. Yamane, *Optical trapping and manipulation of single cells using infrared laser beams.* Nature, 1987. **330**(6150): p. 769-771.
66. Chu, S., et al., *Experimental observation of optically trapped atoms.* Physical Review Letters, 1986. **57**(3): p. 314-317.

67. Tam, J.M., I. Biran, and D.R. Walt, *An imaging fiber-based optical tweezer array for microparticle array assembly.* Applied Physics Letters, 2004. **84**(21): p. 4289-4291.
68. Merenda, F., et al., *Miniaturized high-NA focusing-mirror multiple optical tweezers.* Optics Express, 2007. **15**(10): p. 6075-6086.
69. Faustov, A.R., M.R. Webb, and D.R. Walt, *Note: Toward multiple addressable optical trapping.* Review of Scientific Instruments, 2010. **81**(2).
70. Michael, K.L., et al., *Randomly Ordered Addressable High-Density Optical Sensor Arrays.* Analytical Chemistry, 1998. **70**(7): p. 1242-1246.
71. Pantano, P. and D.R. Walt, *Ordered nanowell arrays.* Chemistry of Materials, 1996. **8**(12): p. 2832-2835.
72. Christodoulides, N., et al., *A microchip-based multianalyte assay system for the assessment of cardiac risk.* Analytical Chemistry, 2002. **74**(13): p. 3030-3036.
73. Szurdoki, F., K.L. Michael, and D.R. Walt, *A duplexed microsphere-based fluorescent immunoassay.* Analytical Biochemistry, 2001. **291**(2): p. 219-228.
74. Steemers, F.J., J.A. Ferguson, and D.R. Walt, *Screening unlabeled DNA targets with randomly ordered fiber-optic gene arrays.* Nature Biotechnology, 2000. **18**(1): p. 91-94.
75. Lee, M. and D.R. Walt, *A Fiber-Optic Microarray Biosensor Using Aptamers as Receptors.* Analytical Biochemistry, 2000. **282**(1): p. 142-146.
76. Walt, D.R., *Bead-based optical fiber arrays for artificial olfaction.* Current Opinion in Chemical Biology, 2010. **14**(6): p. 767-770.
77. *www.illumina.com*.
78. Li, S., et al., *Disposable polydimethylsiloxane/silicon hybrid chips for protein detection.* Biosensors and Bioelectronics, 2005. **21**(4): p. 574-580.
79. Kirby, R., et al., *Aptamer-based sensor arrays for the detection and quantitation of proteins.* Analytical Chemistry, 2004. **76**(14): p. 4066-4075.
80. Christodoulides, N., et al., *Application of microchip assay system for the measurement of C-reactive protein in human saliva.* Lab on a chip, 2005. **5**(3): p. 261-269.
81. Curey, T.E., et al., *Characterization of Multicomponent Monosaccharide Solutions Using an Enzyme-Based Sensor Array.* Analytical Biochemistry, 2001. **293**(2): p. 178-184.
82. Wen, J., et al., *Telomerase catalyzed fluorescent probes for sensitive protein profiling based on one-dimensional microfluidic beads array.* Biosensors and Bioelectronics, 2008. **23**(12): p. 1788-1792.
83. Zhang, H., et al., *On-chip oligonucleotide ligation assay using one-dimensional microfluidic beads array for the detection of low-abundant DNA point mutations.* Biosensors and Bioelectronics, 2008. **23**(7): p. 945-951.
84. Bunz, U.H.F., *Breath figures as a dynamic templating method for polymers and nanomaterials.* Advanced Materials, 2006. **18**(8): p. 973-989.
85. Lu, M.H. and Y. Zhang, *Microbead patterning on porous films with ordered arrays of pores.* Advanced Materials, 2006. **18**(23): p. 3094-3098.
86. Thompson, J.A. and H.H. Bau, *Microfluidic, bead-based assay: Theory and experiments.* Journal of Chromatography B, 2010. **878**(2): p. 228-236.
87. Lee, J., et al., *Simple fabrication of a smart microarray of polystyrene microbeads for immunoassay.* Colloids and Surfaces B: Biointerfaces, 2009. **72**(2): p. 173-180.
88. Yan, X., et al., *Microcontact printing of colloidal crystals.* Journal of the American Chemical Society, 2004. **126**(34): p. 10510-10511.
89. Yan, X., et al., *Fabrication of non-close-packed arrays of colloidal spheres by soft lithography.* Journal of the American Chemical Society, 2005. **127**(21): p. 7688-7689.
90. Li, X., et al., *Modulating two-dimensional non-close-packed colloidal crystal arrays by deformable soft lithography.* Langmuir, 2010. **26**(4): p. 2930-2936.
91. Lilliehorn, T., et al., *Trapping of microparticles in the near field of an ultrasonic transducer.* Ultrasonics, 2005. **43**(5): p. 293-303.
92. Lilliehorn, T., et al., *Dynamic arraying of microbeads for bioassays in microfluidic channels.* Sensors and Actuators, B: Chemical, 2005. **106**(2): p. 851-858.

93. Palla-Papavlu, A., et al., *Microfabrication of polystyrene microbead arrays by laser induced forward transfer*. Journal of Applied Physics, 2010. **108**(3): 033111.
94. Czarnik, A.W., *Encoding methods for combinatorial chemistry.* Current Opinion in Chemical Biology, 1997. **1**(1): p. 60-66.
95. Braeckmans, K., et al., *Encoding microcarriers: Present and future technologies.* Nature Reviews Drug Discovery, 2002. **1**(6): p. 447-456.
96. Mulvaney, S.P., H.M. Mattoussi, and L.J. Whitman, *Incorporating fluorescent dyes and quantum dots into magnetic microbeads for immunoassays.* Biotechniques, 2004. **36**(4): p. 602-609.
97. Battersby, B.J., et al., *Toward larger chemical libraries: Encoding with fluorescent colloids in combinatorial chemistry.* Journal of the American Chemical Society, 2000. **122**(9): p. 2138-2139.
98. Egner, B.J., et al., *Tagging in combinatorial chemistry: The use of coloured and fluorescent beads.* Chemical Communications, 1997(8): p. 735-736.
99. Han, M., et al., *Quantum-dot-tagged microbeads for multiplexed optical coding of biomolecules.* Nature Biotechnology, 2001. **19**(7): p. 631-635.
100. Zhao, Y., et al., *Encoded silica colloidal crystal beads as supports for potential multiplex immunoassay.* Analytical Chemistry, 2008. **80**(5): p. 1598-1605.
101. Medintz, I.L., et al., *Quantum dot bioconjugates for imaging, labelling and sensing.* Nature Materials, 2005. **4**(6): p. 435-446.
102. Zhao, Y., X. Zhao, and Z. Gu, *Photonic crystals in bioassays.* Advanced Functional Materials, 2010. **20**(18): p. 2970-2988.
103. Cunin, F., et al., *Biomolecular screening with encoded porous-silicon photonic crystals.* Nature Materials, 2002. **1**(1): p. 39-41.
104. Tang, B., et al., *Binary optical encoding strategy for multiplex assay.* Langmuir, 2011. **27**(18): p. 11722-11728.
105. Finkel, N.H., et al., *Barcoding the microworld.* Analytical Chemistry, 2004. **76**(19): p. 353A-359A.
106. Nicewarner-Peña, S.R., et al., *Submicrometer metallic barcodes.* Science, 2001. **294**(5540): p. 137-141.
107. Dejneka, M.J., et al., *Rare earth-doped glass microbarcodes.* Proceedings of the National Academy of Sciences of the United States of America, 2003. **100**(2): p. 389-393.
108. Yuen, P.K., et al., *Microbarcode sorting device.* Lab on a chip, 2003. **3**(3): p. 198-201.
109. Martin, B.R., et al., *Orthogonal self-assembly on colloidal gold-platinum nanorods.* Advanced Materials, 1999. **11**(12): p. 1021-1025.
110. Dames, A., J. England, and E. Colby, *Bio-assay technique*, 2000. WO/2000/016893.
111. Demierre, N. and S. Gamper, *Method for producing microparticles*, 2011. WO/2011/044708.
112. Evans, M., C. Sewter, and E. Hill, *An encoded particle array tool for multiplex bioassays.* Assay and Drug Development Technologies, 2003. **1**(1 Pt 2): p. 199-207.
113. Broder, G.R., et al., *Diffractive micro bar codes for encoding of biomolecules in multiplexed assays.* Analytical Chemistry, 2008. **80**(6): p. 1902-1909.
114. Cavalli, G., et al., *Multistep synthesis on SU-8: Combining microfabrication and solid-phase chemistry on a single material.* Journal of Combinatorial Chemistry, 2007. **9**(3): p. 462-472.
115. Braeckmans, K., et al., *Encoding microcarriers by spatial selective photobleaching.* Nature Materials, 2003. **2**(3): p. 169-174.
116. Dendukuri, D., et al., *Continuous-flow lithography for high-throughput microparticle synthesis.* Nature Materials, 2006. **5**(5): p. 365-369.
117. Pregibon, D.C., M. Toner, and P.S. Doyle, *Multifunctional encoded particles for high-throughput biomolecule analysis.* Science, 2007. **315**(5817): p. 1393-1396.
118. Chapin, S.C., D.C. Pregibon, and P.S. Doyle, *High-throughput flow alignment of barcoded hydrogel microparticles.* Lab on a Chip, 2009. **9**(21): p. 3100-3109.

119. Russell, R.J., et al., *Mass transfer in rapidly photopolymerized poly(ethylene glycol) hydrogels used for chemical sensing*. Polymer, 2001. **42**(11): p. 4893-4901.
120. Zhan, W., G.H. Seong, and R.M. Crooks, *Hydrogel-based microreactors as a functional component of microfluidic systems.* Analytical Chemistry, 2002. **74**(18): p. 4647-4652.
121. Pregibon, D.C. and P.S. Doyle, *Optimization of encoded hydrogel particles for nucleic acid quantification.* Analytical Chemistry, 2009. **81**(12): p. 4873-4881.
122. Zhu, H., et al., *Global Analysis of Protein Activities Using Proteome Chips.* Science, 2001. **293**(5537): p. 2101-2105.
123. Benecky, M.J., et al., *Detection of hepatitis B surface antigen in whole blood by coupled particle light scattering (Copalis (TM)).* Clinical Chemistry, 1997. **43**(9): p. 1764-1770.
124. Kastl, K.F., C.R. Lowe, and C.E. Norman, *Encoded and Multiplexed Surface Plasmon Resonance Sensor Platform.* Analytical Chemistry, 2008. **80**(20): p. 7862-7869.
125. Kastl, K.F., C.R. Lowe, and C.E. Norman, *Label-free genetic and proteomic marker detection within a single flowcell assay.* Biosensors and Bioelectronics, 2010. **26**(4): p. 1719-1722.
126. Gunderson, K.L., et al., *Decoding randomly ordered DNA arrays.* Genome Research, 2004. **14**(5): p. 870-877.
127. Peterson, D.S., *Solid supports for micro analytical systems.* Lab on a chip, 2005. **5**: p. 132-139.
128. Uhlen, M., *Magnetic separation of DNA.* Nature, 1989. **340**(6236): p. 733-734.
129. Hultman, T., et al., *Direct solid phase sequencing of genomic and plasmid DNA using magnetic beads as solid support.* Nucleic Acids Research, 1989. **17**(13): p. 4937-4946.
130. Yang, L., D.K. Tran, and X. Wang, *BADGE, BeadsArray for the Detection of Gene Expression, a high-throughput diagnostic bioassay.* Genome Research, 2001. **11**(11): p. 1888-1898.
131. DeRisi, J., et al., *Use of a cDNA microarray to analyse gene expression patterns in human cancer.* Nature Genetics, 1996. **14**(4): p. 457-460.
132. Chen, J., et al., *A microsphere-based assay for multiplexed single nucleotide polymorphism analysis using single base chain extension.* Genome Research, 2000. **10**(4): p. 549-557.
133. Johnson, S.C., et al., *Multiplexed genetic analysis using an expanded genetic alphabet.* Clinical Chemistry, 2004. **50**(11): p. 2019-2027.
134. Smith, P.L., et al., *A rapid, sensitive, multiplexed assay for detection of viral nucleic acids using the FlowMetrix system.* Clinical Chemistry, 1998. **44**(9): p. 2054-2056.
135. Fan, J.B., et al., *A versatile assay for high-throughput gene expression profiling on universisal array matrices.* Genome Research, 2004. **14**(5): p. 878-885.
136. Bibikova, M., et al., *High-throughput DNA methylation profiling using universal bead arrays.* Genome Research, 2006. **16**(3): p. 383-393.
137. Zhang, H., et al., *Detection of single-base mutations using 1-D microfluidic beads array.* Electrophoresis, 2007. **28**(24): p. 4668-4678.
138. Yang, X., et al., *Nucleic acids detection using cationic fluorescent polymer based on one-dimensional microfluidic beads array.* Talanta, 2009. **77**(3): p. 1027-1031.
139. Ng, J.K.K., et al., *Spatially addressable bead-based biosensor for rapid detection of beta-thalassemia mutations.* Analytica Chimica Acta, 2010. **658**(2): p. 193-196.
140. Carson, R.T. and D.A.A. Vignali, *Simultaneous quantitation of 15 cytokines using a multiplexed flow cytometric assay.* Journal of Immunological Methods, 1999. **227**(1-2): p. 41-52.
141. Bellisario, R., R.J. Colinas, and K.A. Pass, *Simultaneous measurement of antibodies to three HIV-1 antigens in newborn dried blood-spot specimens using a multiplexed microsphere-based immunoassay.* Early Human Development, 2001. **64**(1): p. 21-25.
142. Anderson, G.P., J.D. Lamar, and P.T. Charles, *Development of a Luminex Based Competitive Immunoassay for 2,4,6-Trinitrotoluene (TNT).* Environmental Science and Technology, 2007. **41**(8): p. 2888-2893.

143. Ikami, M., et al., *Immuno-pillar chip: A new platform for rapid and easy-to-use immunoassay.* Lab on a Chip, 2010. **10**(24): p. 3335-3340.
144. Rissin, D.M. and D.R. Walt, *Digital concentration readout of single enzyme molecules using femtoliter arrays and poisson statistics.* Nano Letters, 2006. **6**(3): p. 520-523.
145. Kan, C.W., et al., *Isolation and detection of single molecules on paramagnetic beads using sequential fluid flows in microfabricated polymer array assemblies.* Lab on a Chip, 2012. **12**(5): p. 977-985.
146. Hosokawa, K., et al., *Power-free sequential injection for microchip immunoassay toward point-of-care testing.* Lab on a chip, 2006. **6**(2): p. 236-241.
147. Zimmermann, M., et al., *Capillary pumps for autonomous capillary systems.* Lab on a Chip, 2007. **7**(1): p. 119-125.
148. Delamarche, E., D. Juncker, and H. Schmid, *Microfluidics for processing surfaces and miniaturizing biological assays.* Advanced Materials, 2005. **17**(24): p. 2911-2933.
149. Gervais, L. and E. Delamarche, *Toward one-step point-of-care immunodiagnostics using capillary-driven microfluidics and PDMS substrates.* Lab on a chip, 2009. **9**(23): p. 3330-3337.
150. Gervais, L., M. Hitzbleck, and E. Delamarche, *Capillary-driven multiparametric microfluidic chips for one-step immunoassays.* Biosensors and Bioelectronics, 2011. **27**(1): p. 64-70.
151. Zimmermann, M., P. Hunziker, and E. Delamarche, *Autonomous capillary system for one-step immunoassays.* Biomedical Microdevices, 2009. **11**(1): p. 1-8.
152. Jönsson, C., et al., *Silane-dextran chemistry on lateral flow polymer chips for immunoassays.* Lab on a Chip, 2008. **8**(7): p. 1191-1197.
153. Dudek, M.M., T.L. Lindahl, and A.J. Killard, *Development of a Point of Care Lateral Flow Device for Measuring Human Plasma Fibrinogen.* Analytical Chemistry, 2010. **82**(5): p. 2029-2035.
154. Lillehoj, P.B., F. Wei, and C.M. Ho, *A self-pumping lab-on-a-chip for rapid detection of botulinum toxin.* Lab on a Chip, 2010. **10**(17): p. 2265-2270.
155. Li, C., et al., *A power-free deposited microbead plug-based microfluidic chip for whole-blood immunoassay.* Microfluidics and Nanofluidics, 2012. **12**(5): p. 829-834.
156. Thorslund, S., et al., *A PDMS-based disposable microfluidic sensor for CD4+ lymphocyte counting.* Biomedical Microdevices, 2008. **10**(6): p. 851-857.
157. Morra, M., et al., *On the aging of oxygen plasma-treated polydimethylsiloxane surfaces.* Journal of Colloid And Interface Science, 1990. **137**(1): p. 11-24.
158. Thorslund, S., et al., *Bioactive heparin immobilized onto microfluidic channels in poly(dimethylsiloxane) results in hydrophilic surface properties.* Colloids and Surfaces B: Biointerfaces, 2005. **46**(4): p. 240-247.
159. Kim, H., et al., *Simple route to hydrophilic microfluidic chip fabrication using an Ultraviolet (UV)-cured polymer.* Advanced Functional Materials, 2007. **17**(17): p. 3493-3498.
160. Dupont, E.P., R. Luisier, and M.A.M. Gijs, *NOA 63 as a UV-curable material for fabrication of microfluidic channels with native hydrophilicity.* Microelectronic Engineering, 2010. **87**(5-8): p. 1253-1255.
161. Wang, J., et al., *A self-powered, one-step chip for rapid, quantitative and multiplexed detection of proteins from pinpricks of whole blood.* Lab on a Chip, 2010. **10**(22): p. 3157-3162.
162. Posthuma-Trumpie, G.A., J. Korf, and A. Van Amerongen, *Lateral flow (immuno)assay: Its strengths, weaknesses, opportunities and threats. A literature survey.* Analytical and Bioanalytical Chemistry, 2009. **393**(2): p. 569-582.
163. Sandro Cesaro-Tadic, G.D., David Juncker, Gerrit Buurman, and B.M. Harald Kropshofer, Christof Fattinger and Emmanuel Delamarche, *High-sensitivity miniaturized immunoassays for tumor necrosis factor a using microfluidic systems.* Lab on a chip, 2004. **4**: p. 563-569.
164. Fan, R., et al., *Integrated barcode chips for rapid, multiplexed analysis of proteins in microliter quantities of blood.* Nature Biotechnology, 2008. **26**(12): p. 1373-1378.

165. Hitzbleck, M., et al., *Capillary soft valves for microfluidics.* Lab on a Chip, 2012. **12**(11): p. 1972-1978.
166. Zhang, H., et al., *Multienzyme-nanoparticles amplification for sensitive virus genotyping in microfluidic microbeads array using Au nanoparticle probes and quantum dots as labels.* Biosensors and Bioelectronics, 2011. **29**(1): p. 89-96.
167. Rissin, D.M., et al., *Single-molecule enzyme-linked immunosorbent assay detects serum proteins at subfemtomolar concentrations.* Nature Biotechnology, 2010. **28**(6): p. 595-599.
168. Zhang, F., et al., *Cytometric Microsphere Array for Subtyping Avian Influenza Virus.* Viral Immunology, 2011. **24**(5): p. 403-407.
169. Leach, K.M., J.M. Stroot, and D.V. Lim, *Same-Day Detection of Escherichia coli O157:H7 from Spinach by Using Electrochemiluminescent and Cytometric Bead Array Biosensors.* Applied and Environmental Microbiology, 2010. **76**(24): p. 8044-8052.
170. Andersson, H., et al., *Micromachined flow-through filter-chamber for chemical reactions on beads.* Sensors and Actuators, B: Chemical, 2000. **67**(1): p. 203-208.
171. Guschin, D., et al., *Manual Manufacturing of Oligonucleotide, DNA, and Protein Microchips.* Analytical Biochemistry, 1997. **250**(2): p. 203-211.
172. Lyubimova, T., et al., *Photopolymerization of polyacrylamide gels with methylene blue.* Electrophoresis, 1993. **14**(1-2): p. 40-50.
173. Hermanson, G.T., *Bioconjugate techniques*, 1996, Academic Press.
174. Liu, L. and W. Yang, *Photoinitiated, inverse emulsion polymerization of acrylamide: Some mechanistic and kinetic aspects.* Journal of Polymer Science Part A: Polymer Chemistry, 2004. **42**(4): p. 846-852.
175. Wen, J., et al., *Microfluidic Preparative Free-Flow Isoelectric Focusing: System Optimization for Protein Complex Separation.* Analytical Chemistry, 2010. **82**(4): p. 1253-1260.
176. Gehring, A., et al., *An antibody microarray, in multiwell plate format, for multiplex screening of foodborne pathogenic bacteria and biomolecules.* Analytical and Bioanalytical Chemistry, 2008. **391**(2): p. 497-506.
177. Li, C., et al., *A multiplexed bead assay for profiling glycosylation patterns on serum protein biomarkers of pancreatic cancer.* Electrophoresis, 2011. **32**(15): p. 2028-2035.
178. Desmet, C., et al., *Multiplexed immunoassay for the rapid detection of anti-tumor-associated antigens antibodies.* Analyst, 2011. **136**(14): p. 2918-2924.
179. Lee, M., et al., *Fabrication of a hydrophobic/hydrophilic hybrid-patterned microarray chip and its application to a cancer marker immunoassay.* BioChip Journal, 2012. **6**(1): p. 10-16.
180. Jung, J.-W., et al., *Label-free and quantitative analysis of C-reactive protein in human sera by tagged-internal standard assay on antibody arrays.* Biosensors and Bioelectronics, 2009. **24**(5): p. 1469-1473.
181. Forrester, S., et al., *Low-volume, high-throughput sandwich immunoassays for profiling plasma proteins in mice: Identification of early-stage systemic inflammation in a mouse model of intestinal cancer.* Molecular Oncology, 2007. **1**(2): p. 216-225.
182. Revzin, A., et al., *Fabrication of Poly(ethylene glycol) Hydrogel Microstructures Using Photolithography.* Langmuir, 2001. **17**(18): p. 5440-5447.
183. Liu, J., et al., *Surface-Modified Poly(methyl methacrylate) Capillary Electrophoresis Microchips for Protein and Peptide Analysis.* Analytical Chemistry, 2004. **76**(23): p. 6948-6955.
184. Bi, H., et al., *Deposition of PEG onto PMMA microchannel surface to minimize nonspecific adsorption.* Lab on a chip, 2006. **6**(6): p. 769-775.
185. Sturgeon, C., *Practice guidelines for tumor marker use in the clinic.* Clinical Chemistry, 2002. **48**(8): p. 1151-1159.
186. Lapthorn, A.J., et al., *Crystal structure of human chorionic gonadotropin.* Nature, 1994. **369**(6480): p. 455-461.

187. Stenman, U.-H., H. Alfthan, and K. Hotakainen, *Human chorionic gonadotropin in cancer*. Clinical Biochemistry, 2004. **37**(7): p. 549-561.
188. Sturgeon, C.M., et al., *National Academy of Clinical Biochemistry Laboratory Medicine Practice Guidelines for use of tumor markers in testicular, prostate, colorectal, breast, and ovarian cancers.* Clinical Chemistry, 2008. **54**(12): p. e11-e79.
189. Butler, S.A., L.A. Cole, and S.A. Khanlian, *Detection of early pregnancy forms of human chorionic gonadotropin by home pregnancy test devices.* Clinical Chemistry, 2001. **47**(12): p. 2131-2136.
190. Cole, L.A., *Immunoassay of human chorionic gonadotropin, its free subunits, and metabolites.* Clinical Chemistry, 1997. **43**(12): p. 2233-2243.
191. Lilja, H., *Biology of prostate-specific antigen.* Urology, 2003. **62**(5, Supplement 1): p. 27-33.
192. Balk, S.P., Y.-J. Ko, and G.J. Bubley, *Biology of Prostate-Specific Antigen.* Journal of Clinical Oncology, 2003. **21**(2): p. 383-391.
193. Stamey, T.A., et al., *Prostate-Specific Antigen as a Serum Marker for Adenocarcinoma of the Prostate.* New England Journal of Medicine, 1987. **317**(15): p. 909-916.
194. Catalona, W.J., et al., *Measurement of prostate-specific antigen in serum as a screening test for prostate cancer*. New England Journal of Medicine, 1991. **324**(17): p. 1156-1161.
195. Catalona, W.J., et al., *Comparison of digital rectal examination and serum prostate specific antigen in the early detection of prostate cancer: results of a multicenter clinical trial of 6,630 men.* The Journal of urology, 1994. **151**(5): p. 1283-90.
196. Acevedo, B., et al., *Development and validation of a quantitative ELISA for the measurement of PSA concentration.* Clinica Chimica Acta, 2002. **317**(1–2): p. 55-63.
197. Basu, A., T.G. Shrivastav, and S.K. Maitra, *Development of Isotopic and Non-Isotopic Microwell Based Immunoassays for hCG Using 125I and Biotin Labeled hCG.* Journal of Immunoassay and Immunochemistry, 2005. **26**(4): p. 313-324.
198. Basu, A., S.K. Maitra, and T.G. Shrivastav, *Development of dual-enzyme-based simultaneous immunoassay for measurement of progesterone and human chorionic gonadotropin.* Analytical Biochemistry, 2007. **366**(2): p. 175-181.
199. Wu, J.T. and L.W. Wilson, *Development of a microplate elisa for free psa and psa–act complex in serum.* Journal of Clinical Laboratory Analysis, 1995. **9**(4): p. 252-260.
200. Wu, T.-L., et al., *Establishment of ELISA on 384-well microplate for AFP, CEA, CA 19-9, CA 15-3, CA 125, and PSA-ACT: Higher sensitivity and lower reagent cost.* Journal of Clinical Laboratory Analysis, 2003. **17**(6): p. 241-246.
201. Ghosh, S., A. Schmidt, and D. Trau, *Fast bead detection and inexact microarray pattern matching for in-situ encoded bead-based array.* VISAPP 2012 - Proceedings of the International Conference on Computer Vision Theory and Applications 2012. **2**: p. 5-14.
202. Kong, D.-H., et al., *Normalization using a tagged-internal standard assay for analysis of antibody arrays and the evaluation of serological biomarkers for liver disease.* Analytica Chimica Acta, 2012. **718**(0): p. 92-98.
203. Zong, C., et al., *Chemiluminescence Imaging Immunoassay of Multiple Tumor Markers for Cancer Screening.* Analytical Chemistry, 2012. **84**(5): p. 2410-2415.
204. Taton, T.A., C.A. Mirkin, and R.L. Letsinger, *Scanometric DNA Array Detection with Nanoparticle Probes.* Science, 2000. **289**(5485): p. 1757-1760.
205. Cai, H., et al., *Carbon nanotube-enhanced electrochemical DNA biosensor for DNA hybridization detection.* Analytical and Bioanalytical Chemistry, 2003. **375**(2): p. 287-293.
206. Liu, D., et al., *Immobilization of DNA onto Poly(dimethylsiloxane) Surfaces and Application to a Microelectrochemical Enzyme-Amplified DNA Hybridization Assay.* Langmuir, 2004. **20**(14): p. 5905-5910.
207. Le Goff, G.C., et al., *Impact of immobilization support on colorimetric microarrays performances.* Biosensors and Bioelectronics, 2012. **35**(1): p. 94-100.

208. Ng, L.F.P., et al., *Detection of Severe Acute Respiratory Syndrome Coronavirus in Blood of Infected Patients.* Journal of clinical microbiology, 2004. **42**(1): p. 347-350.
209. Wingren, C., et al., *Microarrays based on affinity-tagged single-chain Fv antibodies: Sensitive detection of analyte in complex proteomes.* Proteomics, 2005. **5**(5): p. 1281-1291.
210. Bilitewski, U., et al., *Biochemical analysis with microfluidic systems.* Analytical and Bioanalytical Chemistry, 2003. **377**(3): p. 556-569.
211. Sia, S.K. and G.M. Whitesides, *Microfluidic devices fabricated in Poly(dimethylsiloxane) for biological studies.* Electrophoresis, 2003. **24**(21): p. 3563-3576.
212. Henares, T.G., F. Mizutani, and H. Hisamoto, *Current development in microfluidic immunosensing chip.* Analytica Chimica Acta, 2008. **611**(1): p. 17-30.
213. Beebe, D.J., G.A. Mensing, and G.M. Walker, *Physics and applications of microfluidics in biology.* Annual Review of Biomedical Engineering, 2002. **4**(1): p. 261-286.
214. Whitesides, G.M., *The origins and the future of microfluidics.* Nature, 2006. **442**(7101): p. 368-373.
215. Wang, L., et al., *Fungal pathogenic nucleic acid detection achieved with a microfluidic microarray device.* Analytica Chimica Acta, 2008. **610**(1): p. 97-104.
216. Yu, L., et al., *Flow-through functionalized PDMS microfluidic channels with dextran derivative for ELISAs.* Lab on a chip, 2009. **9**(9): p. 1243-1247.
217. Uchiyama, Y., et al., *Combinable poly(dimethyl siloxane) capillary sensor array for single-step and multiple enzyme inhibitor assays.* Lab on a chip, 2012.
218. Ng, J.K.-K., H. Feng, and W.-T. Liu, *Rapid discrimination of single-nucleotide mismatches using a microfluidic device with monolayered beads.* Analytica Chimica Acta, 2007. **582**(2): p. 295-303.
219. Choi, D., et al., *Development of microfluidic devices incorporating non-spherical hydrogel microparticles for protein-based bioassay.* Microfluidics and Nanofluidics, 2008. **5**(5): p. 703-710.
220. Ziegler, J., et al., *High-performance immunoassays based on through-stencil patterned antibodies and capillary systems.* Analytical Chemistry, 2008. **80**(5): p. 1763-1769.
221. Diercks, A.H., et al., *A microfluidic device for multiplexed protein detection in nano-liter volumes.* Analytical Biochemistry, 2009. **386**(1): p. 30-35.
222. Lee, Y.-F., et al., *An integrated microfluidic system for rapid diagnosis of dengue virus infection.* Biosensors and Bioelectronics, 2009. **25**(4): p. 745-752.
223. Ko, Y.J., et al., *Microchip-based multiplex electro-immunosensing system for the detection of cancer biomarkers.* Electrophoresis, 2008. **29**(16 SPEC. ISS.): p. 3466-3476.
224. Russom, A., et al., *Single-nucleotide polymorphism analysis by allele-specific extension of fluorescently labeled nucleotides in a microfluidic flow-through device.* Electrophoresis, 2003. **24**(1-2): p. 158-161.
225. Sato, K., et al., *Microbead-based rolling circle amplification in a microchip for sensitive DNA detection.* Lab on a chip, 2010. **10**(10): p. 1262-1266.
226. Kim, D.N., Y. Lee, and W.-G. Koh, *Fabrication of microfluidic devices incorporating bead-based reaction and microarray-based detection system for enzymatic assay.* Sensors and Actuators B: Chemical, 2009. **137**(1): p. 305-312.
227. Xia, Y. and G.M. Whitesides, *Soft Lithography.* Angewandte Chemie International Edition, 1998. **37**(5): p. 550-575.
228. Krul', L.P., et al., *Water-Soluble Polymers of Acrylamide as Labeling Adhesives.* Russian Journal of Applied Chemistry, 2005. **78**(5): p. 839-842.
229. Heo, J. and R.M. Crooks, *Microfluidic Biosensor Based on an Array of Hydrogel-Entrapped Enzymes.* Analytical Chemistry, 2005. **77**(21): p. 6843-6851.
230. Sacks, D.B., et al., *Guidelines and Recommendations for Laboratory Analysis in the Diagnosis and Management of Diabetes Mellitus.* Clinical Chemistry, 2011. **57**(6): p. e1-e47.

231. Lee, Y., et al., *Fabrication of hydrogel-micropatterned nanofibers for highly sensitive microarray-based immunosensors having additional enzyme-based sensing capability.* Journal of Materials Chemistry, 2011. **21**(12): p. 4476-4483.
232. Zhu, Q., and Trau, D., *Simultaneous detection of protein and DNA in a microfluidic device using spatial addressable microbeads on a gel pad array,* in The 14th International Conference on Miniaturized Systems for Chemistry and Life Sciences, μTAS 2010, 2010: Groningen, The Netherlands. p. 455-457.
233. Gubala, V., et al., *Point of care diagnostics: Status and future.* Analytical Chemistry, 2012. **84**(2): p. 487-515.
234. Gervais, L., N. De Rooij, and E. Delamarche, *Microfluidic chips for point-of-care immunodiagnostics.* Advanced Materials, 2011. **23**(24): p. H151-H176.
235. Kim, S.J., et al., *Passive microfluidic control of two merging streams by capillarity and relative flow resistance.* Analytical Chemistry, 2005. **77**(19): p. 6494-6499.
236. Lee, W., Choi, D., Kim, J., Koh, W., *Suspension arrays of hydrogel microparticles prepared by photopatterning for multiplexed protein-based bioassays.* Biomedical Microdevices, 2008. **10**(6): 813-822.
237. Gruber, H.F., *Photoinitiators for free radical polymerization.* Progress in Polymer Science, 1992. **17**(6): p. 953-1044.
238. Rosina, J., et al., *Temperature dependence of blood surface tension.* Physiological Research, 2007. **56**(SUPPL. 1): p. S93-S98.
239. Dalakas, M.C., *High-dose intravenous immunoglobulin and serum viscosity: Risk of precipitating thromboembolic events.* Neurology, 1994. **44**(2): p. 223-226.

List of Publications & Awards

Journal Publications:

Kantak, C., **Zhu, Q.,** Beyer, S.,Bansal, T., Trau, D., *Utilizing microfluidics to synthesize polyethylene glycol microbeads for Förster resonance energy transfer based glucose sensing***.** Biomicrofluidics, 2012. **6**: 022006.

Zhu, Q., Trau, D., *Multiplexed Detection Platform for Tumor Markers and Glucose in Serum based on a Microfluidic Microparticle Array*. Analytica Chimica Acta, 2012. **751**:146-154.

Zhu, Q., Trau, D., *Low volume microbead array chip for high throughput and multiplexed immunoassays.* In preparation.

Zhu, Q., Trau, D., *Microbead array in an autonomous capillary system for sensitive immunoassays for serum samples.* In preparation.

International Conferences

Trau, D., Ng, K. J., **Zhu, Q**., Liu, W-T., Simultaneous Hybridization and Immune Assays on a Bead Based Microarray with Novel Encoding Technology. *Biosensor 2008, The Tenth World Congress on Biosensors*, Shanghai, China, 2008, Poster Presentation.

Trau, D., and **Zhu, Q**., Simultaneous Hybridization and immunoassays on a bead based microarray with novel in-situ encoding technology. *World Congress on Bioengineering 2009*, Hong Kong, China, 2009, Oral Presentation.

Zhu, Q. and Trau, D., Simultaneous Detection of protein and DNA in a microfluidic device using spatial addressable microbeads on a gel pad array. *μTAS 2010, The 14th International Conference on Miniaturized Systems for Chemistry and Life Sciences*, Groningen, The Netherlands, 2010, Poster Presentation.

Workshops

Zhu, Q. and Trau, D., Novel gel pad array for microbead based hybridization assay and immunoassay. *The Fourth East Asian Pacific Student Workshop on Nano-Biomedical Engineering*, Singapore, 2010, Oral Presentation.

Zhu, Q. and Trau, D., Microfluidic Bioassays using microbeads patterned on gel-based structures. *The Fifth East Asian Pacific Student Workshop on Nano-Biomedical Engineering*, Singapore, 2011, Oral Presentation.

Awards

Student travel grant award, *μTAS 2010, The 14th International Conference on Miniaturized Systems for Chemistry and Life Sciences*.

Oral Presentation Award, *The Fifth East Asian Pacific Student Workshop on Nano-Biomedical Engineering*.